Co-activation of selective nicotinic acetylcholine receptor subtypes is required for neuroprotection in Alzheimer's disease

Co-activation of nicotinic receptors protects AD

Rahmi Lee, Gayeon Kim, Ellison R. Black, Seonil Kim

Department of Biomedical Sciences, Colorado State University, Fort Collins, CO 80523, USA

*Corresponding author: Seonil Kim

Email: seonil.kim@colostate.edu

Abstract (150 words)

Alzheimer's disease (AD) is characterized by hippocampal hyperexcitability and cognitive impairment, in part due to β-amyloid (Aβ)–induced suppression of GABAergic interneuron activity. Enhancing hippocampal inhibition is therefore considered protective, but inhibitory interneurons are highly diverse and not uniformly affected by Aβ. We previously showed that Aβ selectively inhibits α7- and α4β2-nicotinic acetylcholine receptors (nAChRs), but not α3β4-nAChRs, on hippocampal inhibitory interneurons, leading to excitatory neuron hyperactivity, and that co-activation of α7- and α4β2-nAChRs reverses these effects. Here, we demonstrate that α7- and α4β2-nAChRs predominantly regulate cholinergic synaptic activity in parvalbumin-positive (PV+) and somatostatin-positive (SST+) interneurons, respectively. Systemic co-stimulation of these receptors is required to reverse hippocampal hyperexcitability, fear learning-related oscillatory dysfunction, and fear memory loss, and reduce Aβ pathology in AD model mice, indicating that coordinated activation of PV+ and SST+ interneurons via co-activation of α7- and α4β2-nAChRs is required for optimal therapeutic benefit.

Teaser (125 characters including space)

Co-activation of selective cholinergic receptors is required to protect Alzheimer's disease.

Introduction

About 5.8 million Americans currently have Alzheimer's disease (AD); that figure is projected to reach 14 million people by 2050 (*1*). In 2020, the direct costs to American society of caring for those with AD and related dementias are a total of an estimated $305 billion, which makes AD the most expensive disease in America (*1*). However, there is no known cause and cure for AD (*2*). Therefore, understanding the neural mechanisms of AD pathogenesis is of the utmost importance for better diagnostic and therapeutic development.

Both preclinical and clinical studies have shown that cortical and hippocampal hyperactivity is found in the early stages of AD (*3*). Increased neuronal activity enhances the release of both beta-amyloid peptide (Aβ) (*4, 5*) and tau (*6, 7*), which contributes to AD pathology. Additionally, in patients, hyperexcitability is strongly linked to cognitive decline (*8-10*). Studies show that reducing hippocampal hyperactivity with the antiepileptic drug improves cognition in AD model mice (*11-13*) and individuals with mild cognitive impairment (*14, 15*). Hyperactivity in the brain is thus most likely a driver of AD pathology and cognitive impairment. Hence, it could be a potential target for both symptomatic and disease-modifying therapies. However, there is still much to learn about hyperexcitability in AD, including the neuronal circuits that are affected in AD, as well as their composite cell types, and the mechanistic link between hyperactivity, pathology, and cognitive impairment.

A key role of toxic Aβ in AD (*16-18*) is supported by the success of recent clinical studies on anti-Aβ treatments resulting in the U.S. Food and Drug Administration (FDA) approval (*19, 20*). However, their limited efficacy and significant side effects (*21-26*), along with Aβ's known physiological roles (*23*), suggest that targeting downstream effects of Aβ toxicity may be a safer and more effective strategy. Aβ is one of the main components of amyloid plaques in the brain of AD patients (*27*). Increased neuronal excitability is observed in the vicinity of Aβ plaques (*28, 29*). Studies have also shown that neuronal hyperactivity can promote Aβ accumulation in mice (*4, 5*). Besides, reducing neuronal excitability decreases Aβ deposition in mice (*5, 8*). This suggests that Aβ is a major trigger of hyperexcitability, which in turn establishes a vicious cycle of AD progress. However, the mechanisms of how Aβ could participate in hyperexcitability are still not fully understood.

The hippocampal memory system is particularly vulnerable to AD-related cellular pathology (*30*). Importantly, maintaining proper inhibition within the hippocampus is essential to ensure normal cognition.

Notably, distinct subtypes of GABAergic inhibitory interneurons differentially regulate hippocampal activity at the cellular, circuit, and network levels (*31, 32*). In the hippocampus, Aβ is shown to decrease the activity of inhibitory cells to increase excitation in pyramidal cells (*33*). This likely results in hippocampal hyperexcitability and network dysfunction, leading to cognitive decline in AD (*3, 33, 34*). This suggests that the reduction of hippocampal inhibition by Aβ is a crucial trigger for hyperexcitability-induced cognitive impairment in AD. Hence, enhancing hippocampal inhibition is thought to be protective against AD (*35*). However, Aβ unlikely affects all subtypes of hippocampal interneurons equally (*36-38*). Therefore, identifying the affected interneuron subtypes in AD to enhance hippocampal inhibition optimally is conceptually and technically challenging.

Cholinergic regulation of GABAergic inhibitory network is generally stronger than direct actions on excitatory neurons in the hippocampus since nicotinic acetylcholine receptors (nAChRs) are more densely expressed in inhibitory interneurons than excitatory cells (*39-44*). The loss of cholinergic neurons and nAChR expression in the hippocampus is a prominent AD pathology (*45-52*). This suggests that cholinergic dysfunction is likely a primary cause for hippocampal inhibition deficits in AD. Although nAChRs are high-affinity targets for Aβ (*53*), contradictory results have been reported describing effects of Aβ on nAChRs (*54-57*). For example, Aβ appears to bind to nAChRs producing functional inhibitory effects or receptor activation, depending on Aβ concentration, type of preparation (i.e., monomers, soluble oligomers or fibrils), and incubation times (*54-56*). Moreover, 17 subtypes of neuronal nAChRs have been reported (*58*). In fact, FDA-approved current drugs for AD mostly attempt to delay the general breakdown of acetylcholine, which potentially stimulates all types of acetylcholine receptors. Thus, it is not surprising that these non-selective activators suffer from modest efficacy (*47, 59, 60*). This suggests, in turn, that distinct nAChR subtypes are differentially affected in AD. Thus, it is challenging to comprehend how Aβ impacts nAChR functions in AD. Furthermore, the important question of how Aβ-induced subtype-specific disruptions in hippocampal interneuron functions are linked to distinct nAChR subtypes remains unanswered.

The three major nAChR subtypes in the hippocampus are composed of α7, α4β2, and α3β4 subunit combinations (*61-63*). Importantly, our previous work using Ca^{2+} imaging in cultured hippocampal neurons has shown that Aβ selectively inhibits α7- and α4β2-nAChRs together, but not α3β4-nAChRs, which reduces overall neuronal activity in interneurons, resulting in neuronal hyperexcitation in excitatory cells (*64, 65*).

Additionally, our published data using co-immunoprecipitation have shown that Aβ can specifically bind to α7- and α4-containing nAChRs, but not α3-containing receptors (*65*). We have also identified two amino acids that are critical for the interaction of Aβ with α7 and α4 subunits, but not the α3 subunit, providing the molecular mechanism underlying the selective interaction of Aβ with specific nAChRs (*65*). In line with these findings, considerable evidence suggests that Aβ is shown to exert subtype-specific inhibition of α7- and/or α4β2-nAChR function without affecting α3β4-nAChRs (*53-56, 64, 66-69*). α7 and α4 subtypes are also more significantly reduced in the brains of AD patients compared to α3-type receptors (*70*). This supports the idea that Aβ predominantly reduces neuronal activity in inhibitory interneurons via selective inhibition of α7- and α4β2-nAChRs, but not α3β4-nAChRs (*64*). We have further revealed that co-activation of α7- and α4β2-nAChRs is required to reverse the Aβ-induced adverse effects in hippocampal excitatory and inhibitory cells (*64, 65*). Moreover, non-selective stimulation of acetylcholine receptors exacerbates Aβ effects on cultured neurons (*64, 65*). Therefore, our published works have shown that selective co-activation of α7- and α4β2-nAChRs is required to reverse the Aβ effects on the activity of inhibitory interneurons in AD. Nonetheless, it is still unknown how the Aβ effects on distinct nAChR subtypes differentially affect inhibitory interneurons to disrupt hippocampal activity at the local circuits and network, resulting in amyloid pathology and cognitive decline in AD.

Parvalbumin-positive (PV+) and somatostatin-positive (SST+) cells, two major subtypes of inhibitory interneurons in the hippocampus, mainly provide somatic and dendritic inhibition onto pyramidal cells, respectively, to differentially regulate hippocampal network activity and cognitive processes (*32*). Here, we reveal that α7-, α4β2-, and α3β4-nAChRs regulate the cholinergic activity mainly in PV+, SST+, and excitatory cells, respectively. As PV+ and SST+ cells differentially provide inhibition onto excitatory neurons in the hippocampus, co-activation of these cells by stimulating α7- and α4β2-nAChRs together has significant impacts on hippocampal inhibition at the circuit levels. Indeed, we find that systemic co-stimulation of α7- and α4β2-nAChRs is required to reverse hippocampal hyperexcitability, dysfunction of fear learning-associated hippocampal oscillatory activity, and fear memory loss and reduce Aβ pathology in a widely used amyloid pathology mouse model, 5XFAD mice (*71*). This suggests that co-stimulation of PV+ and SST+ cells via activation of α7- and α4β2-nAChRs together is required to enhance hippocampal inhibition optimally, which reverses hippocampal dysfunction, reduces amyloid pathology, and ultimately prevents memory loss in AD.

Results

Nicotinic cholinergic regulation of cultured hippocampal PV+ and SST+ interneurons is mainly mediated by α7- and α4β2-nAChRs, respectively.

To determine whether nicotinic cholinergic regulation was stronger in GABAergic inhibitory cells than in excitatory neurons, we first compared nicotinic cholinergic activity between excitatory cells (EX) and inhibitory interneurons (IN) using Ca^{2+} imaging with nicotine uncaging in 12-14 days *in vitro* (DIV) cultured mouse hippocampal neurons as neuronal nAChRs are ligand-gated ion channels, and when activated, they induce membrane depolarization and increase somatic Ca^{2+} levels (*72*). We found that nicotinic cholinergic activity measured by Ca^{2+} transients in inhibitory interneurons was significantly higher than in excitatory neurons (EX, 1.000 ± 0.879 $\Delta F/F_0$ and IN, 1.575 ± 1.208 $\Delta F/F_0$, $p = 0.0109$) (**Fig. 1a and Table S1**). This finding is consistent with the previous reports that cholinergic regulation of inhibitory cells is stronger than excitatory neurons in the hippocampus (*39-44*).

Figure 1. Nicotinic cholinergic regulation of cultured hippocampal PV+ and SST+ interneurons is mainly mediated by α7- and α4β2-nAChRs, respectively.

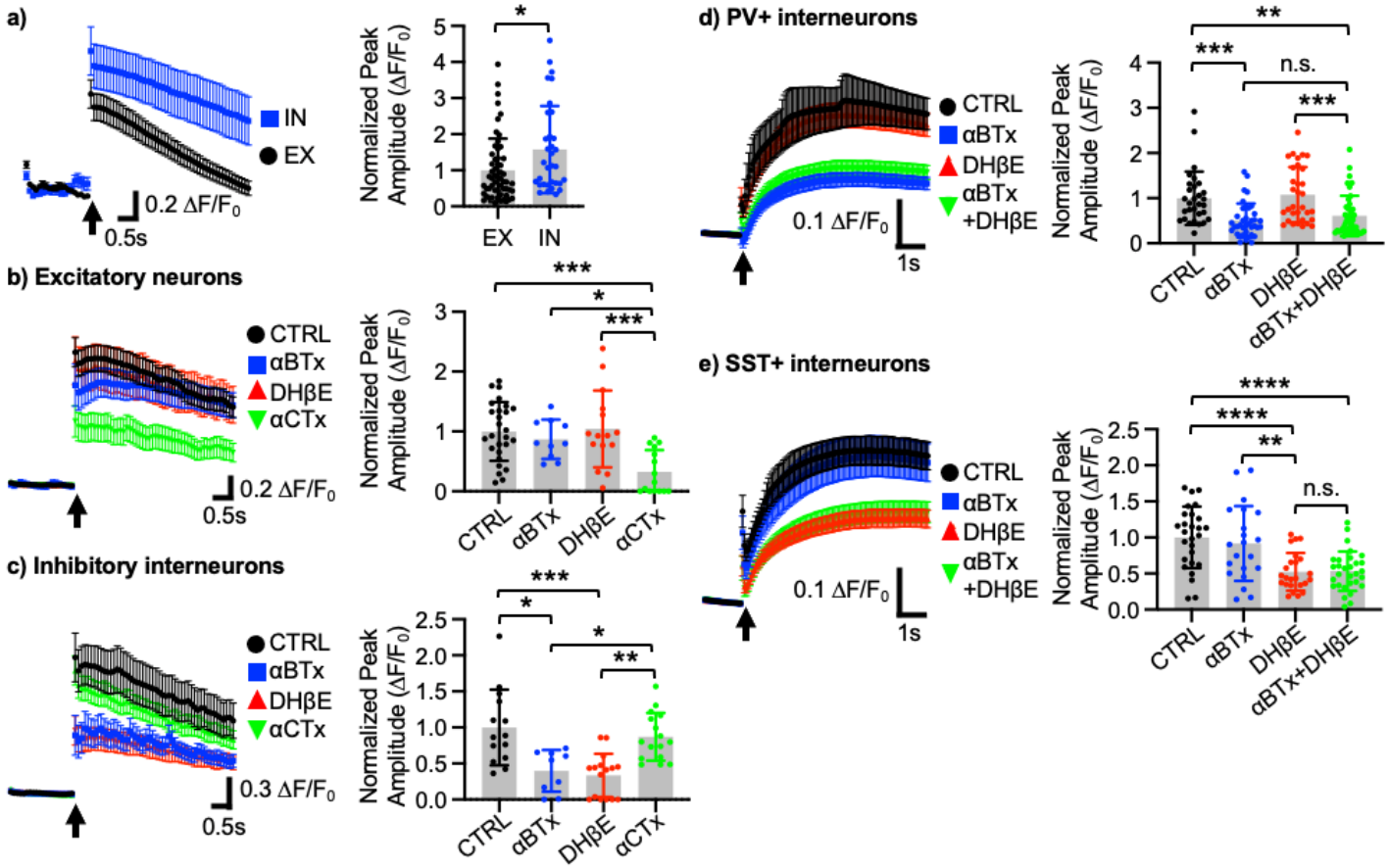

a) Average traces of GCaMP6f signals in excitatory (EX) and inhibitory (IN) cells and summary data of normalized peak amplitude in each condition (n = number of cells excitatory cells = 57 and inhibitory cells = 33 from 4 pups in 2 independent cultures). *$p < 0.05$, unpaired two-tailed student's t-test. Average traces of

GCaMP6f signals and summary graphs of normalized peak amplitude in each condition in **b)** excitatory neurons (n = number of cells, CTRL = 27, αBTx = 10, DhβE = 15, and αCTx = 15 from 4 pups in 2 independent cultures) and **c)** inhibitory interneurons (n = number of cells, CTRL = 14, αBTx = 9, DhβE = 16, and αCTx = 16 from 4 pups in 2 independent cultures). Average traces of GCaMP7s signals and summary data of normalized peak amplitude in each condition in **d)** PV+ interneurons (n = number of cells, CTRL = 30, αBTx = 38, DhβE = 32, and αBTx + DhβE = 43 from 6 pups in 3 independent cultures) and **e)** SST+ interneurons (n = number of cells, CTRL = 27, αBTx = 21, DhβE = 24, and αBTx + DhβE = 30 from 6 pups in 3 independent cultures). *$p < 0.05$, **$p < 0.01$, ***$p < 0.001$, and ****$p < 0.0001$. one-way ANOVA, Tukey test. An arrow indicates photostimulation. n.s.: not significant.

We next treated 12-14 DIV cultured mouse hippocampal neurons with nAChR subtype-specific antagonists and conducted Ca^{2+} imaging with nicotine uncaging to identify which subtypes of nAChRs played a crucial role in nicotinic cholinergic regulation of hippocampal excitatory and inhibitory cells. In excitatory cells, when compared to controls (CTRL), acute treatment of 3 μM α-Conotoxin AuIB (αCTx), an α3β4-receptor inhibitor, significantly reduced nicotinic cholinergic activity, while 50 nM α-Bungarotoxin (αBTx), an α7-receptor inhibitor, or 1 μM Dihydro-β-erythroidine hydrobromide (DHβE), an α4β2-receptor inhibitor, had no effects (CTRL, 1.000 ± 0.492 $\Delta F/F_0$, αBTx, 0.870 ± 0.328 $\Delta F/F_0$, $p = 0.8881$, DHβE, 1.042 ± 0.644 $\Delta F/F_0$, $p = 0.9932$, and αCTx, 0.325 ± 0.362 $\Delta F/F_0$, $p = 0.0003$) (**Fig. 1b and Table S2**). Conversely, in inhibitory cells, when compared to controls (CTRL), αBTx or DHβE treatment significantly reduced nicotine-induced activity, but the α3β4 antagonist had no effect (CTRL, 1.000 ± 0.525 $\Delta F/F_0$, αBTx, 0.398 ± 0.290 $\Delta F/F_0$, $p = 0.0025$, DHβE, 0.335 ± 0.300 $\Delta F/F_0$, $p < 0.0001$, and αCTx, 0.871 ± 0.330 $\Delta F/F_0$, $p = 0.7866$) (**Fig. 1c and Table S2**). This data show that α7- and α4β2-nAChRs are mainly responsible for nicotinic cholinergic activity in hippocampal inhibitory cells, while α3β4-nAChRs are important for nicotinic cholinergic activity in hippocampal excitatory cells. These findings are consistent with the previous reports demonstrating that postsynaptic α7- and α4β2-nAChRs are mainly localized on GABAergic interneurons in the hippocampus and mediate nicotine currents (*40, 42*), while they are expressed in the presynaptic area of excitatory cells to regulate neurotransmitter release without neuronal activation such as action potentials (*73-77*). This suggests that stimulation of α7- and α4β2-nAChRs has more profound effects on neuronal activation in inhibitory cells than excitatory neurons in the hippocampus.

We next analyzed subtype-specific roles of nAChRs in cultured hippocampal PV+ and SST+ interneurons. Since α3β4-nAChRs are shown to mainly regulate excitatory neurons, we focused on the role of α7- and α4β2-nAChRs in these inhibitory cells. In PV+ interneurons, when compared to controls (CTRL),

acute treatment of αBTx significantly reduced nicotinic cholinergic activity, while DHβE had no effects (CTRL, 1.000 ± 0.590 $\Delta F/F_0$, αBTx, 0.507 ± 0.374 $\Delta F/F_0$, $p = 0.0006$, and DHβE, 1.076 ± 0.613 $\Delta F/F_0$, $p = 0.9340$) (**Fig. 1d and Table S3**). Importantly, co-treatment of αBTx and DHβE had no additional effect (αBTx + DHβE, 0.607 ± 0.448 $\Delta F/F_0$) (**Fig. 1d and Table S3**). Conversely, in SST+ interneurons, when compared to controls (CTRL), acute treatment of DHβE significantly reduced nicotinic cholinergic activity, while αBTx had no effects (CTRL, 1.000 ± 0.426 $\Delta F/F_0$, αBTx, 0.917 ± 0.519 $\Delta F/F_0$, $p = 0.8707$, and DHβE, 0.524 ± 0.262 $\Delta F/F_0$, $p < 0.0001$) (**Fig. 1e and Table S3**). Importantly, co-treatment of αBTx and DHβE had no additional effect (αBTx + DHβE, 0.533 ± 0.272 $\Delta F/F_0$) (**Fig. 1e and Table S3**). These findings show that α7- and α4β2-nAChRs play important roles in nicotinic cholinergic regulation of PV+ and SST+ cells, respectively.

The Aβ-induced decrease in the neuronal activity of PV+ and SST+ interneurons is reversed by stimulation of α7- and α4β2-nAChRs, respectively.

We next examined whether Aβ affected nicotinic cholinergic activity of PV+ and SST+ interneurons using nicotine uncaging as described in **Fig. 1**. We found that 250 nM soluble Aβ42 oligomers (oAβ42) treatment significantly reduced nicotine-induced activity in both PV+ and SST+ interneurons compared to neurons treated with 250 nM scrambled Aβ42 (sAβ42) (PV+ interneurons, sAβ42, 1.000 ± 0.772 $\Delta F/F_0$ and oAβ42, 0.448 ± 0.233 $\Delta F/F_0$, $p = 0.0038$ and SST+ interneurons, sAβ42, 1.000 ± 0.391 $\Delta F/F_0$ and oAβ42, 0.600 ± 0.237 $\Delta F/F_0$, $p = 0.0002$) (**Fig. 2a-b and Table S4**).

Figure 2. The Aβ-induced decrease in the neuronal activity of PV+ and SST+ interneurons is reversed by stimulation of α7- and α4β2-nAChRs, respectively.

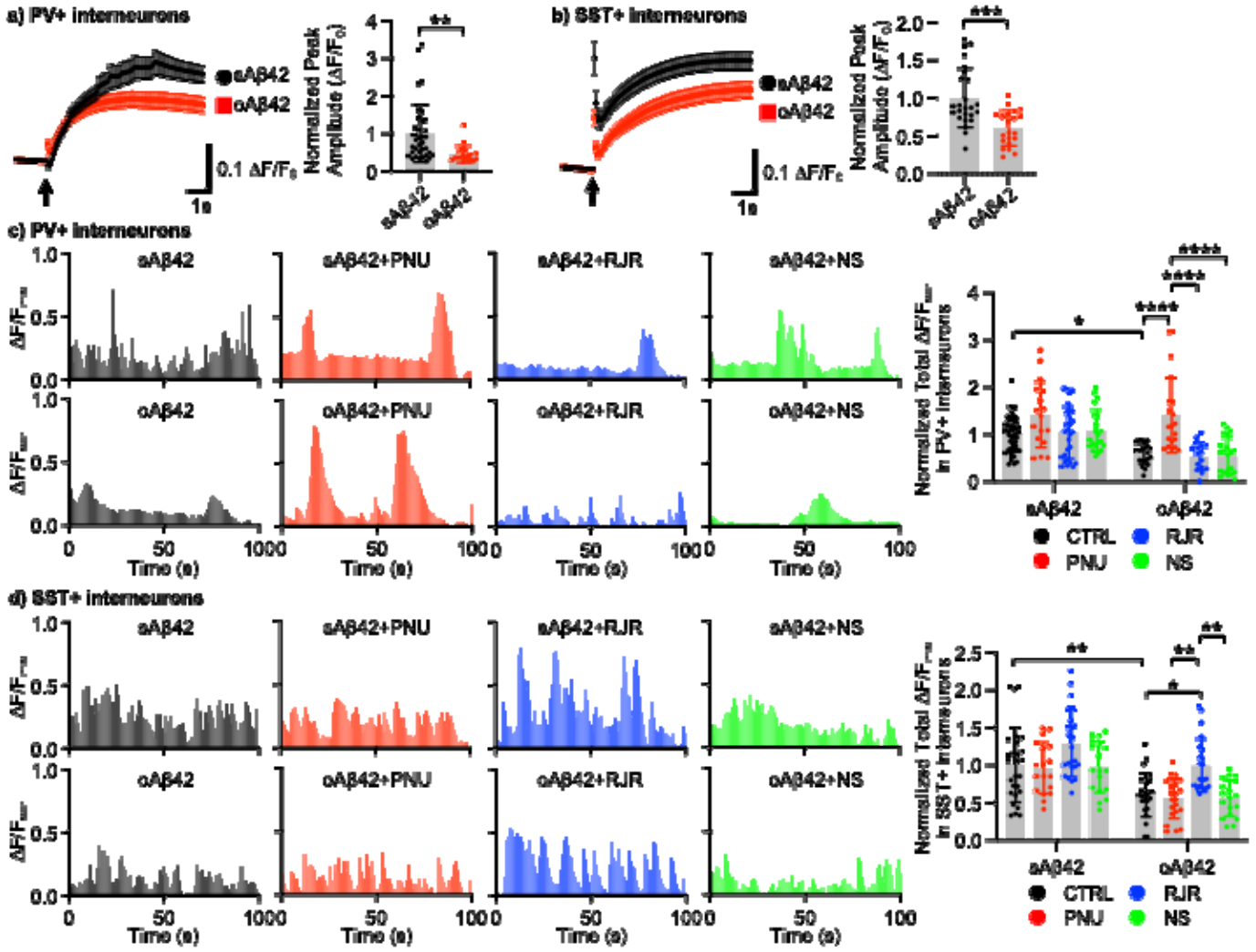

Average traces of GCaMP7s signals and summary data of normalized peak amplitude in each condition in **a)** PV+ interneurons (n = number of cells, sAβ42 = 36 and oAβ42 = 19 from 6 pups in 3 independent cultures) and **b)** SST+ interneurons (n = number of cells, sAβ42 = 25 and oAβ42 = 21 from 6 pups in 3 independent cultures). $^{**}p < 0.01$ and $^{***}p < 0.001$, unpaired two-tailed student's t-test. An arrow indicates photostimulation. Representative traces of GCaMP7s fluorescence intensity and summary graphs of normalized total Ca^{2+} activity in each condition in **c)** PV+ interneurons (n = number of cells, sAβ42 (CTRL) = 47, sAβ42 + PNU = 17, sAβ42 + RJR = 28, sAβ42 + NS = 21, oAβ42 (CTRL) = 21, oAβ42 + PNU = 20, oAβ42 + RJR = 15, and oAβ42 + NS = 21 from 6 pups in 3 independent cultures) and **d)** SST+ interneurons (n = number of cells, sAβ42 (CTRL) = 27, sAβ42 + PNU = 18, sAβ42 + RJR = 24, sAβ42 + NS = 18, oAβ42 (CTRL) = 24, oAβ42 + PNU = 22, oAβ42 + RJR = 22, and oAβ42 +NS = 18 from 6 pups in 3 independent cultures). $^{*}p < 0.05$, $^{**}p < 0.01$, and $^{****}p < 0.0001$, Two-way ANOVA, Tukey test.

We further determined how Aβ affected neuronal activity in PV+ and SST+ interneurons. As somatic Ca^{2+} levels in neurons indicate neuronal activity (*78*), we measured spontaneous somatic Ca^{2+} activity without tetrodotoxin (TTX) in 12-14 DIV cultured hippocampal neurons as carried out previously (*64, 65, 79, 80*). 250 nM oAβ42 treatment significantly decreased neuronal activity in both PV+ and SST+ interneurons (PV+

interneurons, sAβ42, 1.000 ± 0.379 $\Delta F/F_{min}$ and oAβ42, 0.589 ± 0.223 $\Delta F/F_{min}$, $p = 0.0371$, and SST+ interneurons, sAβ42, 1.000 ± 0.499 $\Delta F/F_{min}$ and oAβ42, 0.604 ± 0.295 $\Delta F/F_{min}$, $p = 0.0044$) (**Fig. 2c-d and Table S5 and S6**). To determine subtype-specific roles of nAChRs in the Aβ effect on PV+ and SST+ cells' activity, we treated these cells with 250 nM oAβ42 or 250 nM sAβ42 and subtype-specific nAChR agonists - 1 μM PNU-282987 (PNU), an α7 agonist, 2 μM RJR-2403 Oxalate (RJR), an α4β2 agonist, or 1 μM NS-3861 (NS), an α3β4 agonist, as carried out previously (*65*). In PV+ interneurons, when compared to controls, activation of α7-nAChRs significantly reversed the Aβ effects, while stimulation of other nAChR subtype had no effects (oAβ42 + PNU, 1.408 ± 0.806 $\Delta F/F_{min}$, $p < 0.0001$, oAβ42 + RJR, 0.528 ± 0.299 $\Delta F/F_{min}$, $p > 0.9999$, and oAβ42 + NS, 0.550 ± 0.384 $\Delta F/F_{min}$, $p > 0.9999$) (**Fig. 2c and Table S5**). In SST+ interneurons, when compared to controls, stimulation of α4β2-nAChRs reversed the Aβ effects, but other agonists were unable to reverse the Aβ effects (oAβ42 + PNU, 0.557 ± 0.271 $\Delta F/F_{min}$, $p = 0.9900$, oAβ42 + RJR, 0.994 ± 0.358 $\Delta F/F_{min}$, $p = 0.0103$, and oAβ42 + NS, 0.561 ± 0.249 $\Delta F/F_{min}$, $p > 0.9999$) (**Fig. 2d and Table S6**). We discover that the Aβ-induced decrease in the neuronal activity of PV+ and SST+ interneurons is reversed by stimulation of α7- and α4β2-nAChRs, respectively. Additionally, our findings show that α3β4-nAChRs are important for nicotinic cholinergic activity in excitatory cells. This suggests that stimulation of α7- and α4β2-nAChRs is a novel and ideal way to stimulate PV+ and SST+ interneurons' activity rather than excitatory neurons' activity.

Co-stimulation of PV+ and SST+ interneurons by activating α7- and α4β2-nAChRs together is required to reverse hippocampal hyperexcitability in 5XFAD mice.

Previous studies suggest that a reduction of GABAergic inhibitory interneurons' activity in the hippocampus by Aβ is one of the main causes of neuronal hyperexcitability in AD (*3, 33, 34, 81*). However, cell-type specificity is absent in these studies, thus it is essential to determine cell-type specific changes of neuronal activity in the AD hippocampus. We measured the expression of the activity-regulated gene, c-Fos (*82*), to determine if the activity of PV+ and SST+ cells was reduced while pyramidal neurons were hyperexcitable in the hippocampus in AD pathology animals. We then examined whether co-stimulation of PV+ and SST+ cells via activating α7- and α4β2-nAChRs together is necessary for reducing hyperexcitability in hippocampal excitatory cells in the AD hippocampus in mice. Widely used amyloid pathology model mice, 5XFAD, were used because they show hippocampal hyperexcitability as early as 2.5 months of age (*83*).

Hippocampal sections of 5-month-old 5XFAD and wild-type (WT) female and male were stained with anti-PV, anti-SST, and anti-c-Fos antibodies, and DAPI was used to identify nuclei in pyramidal cells (**Fig. 3a)**.

Figure 3. Co-stimulation of PV+ and SST+ interneurons by activating α7- and α4β2-nAChRs together is required to reverse hippocampal hyperexcitability in 5XFAD mice.

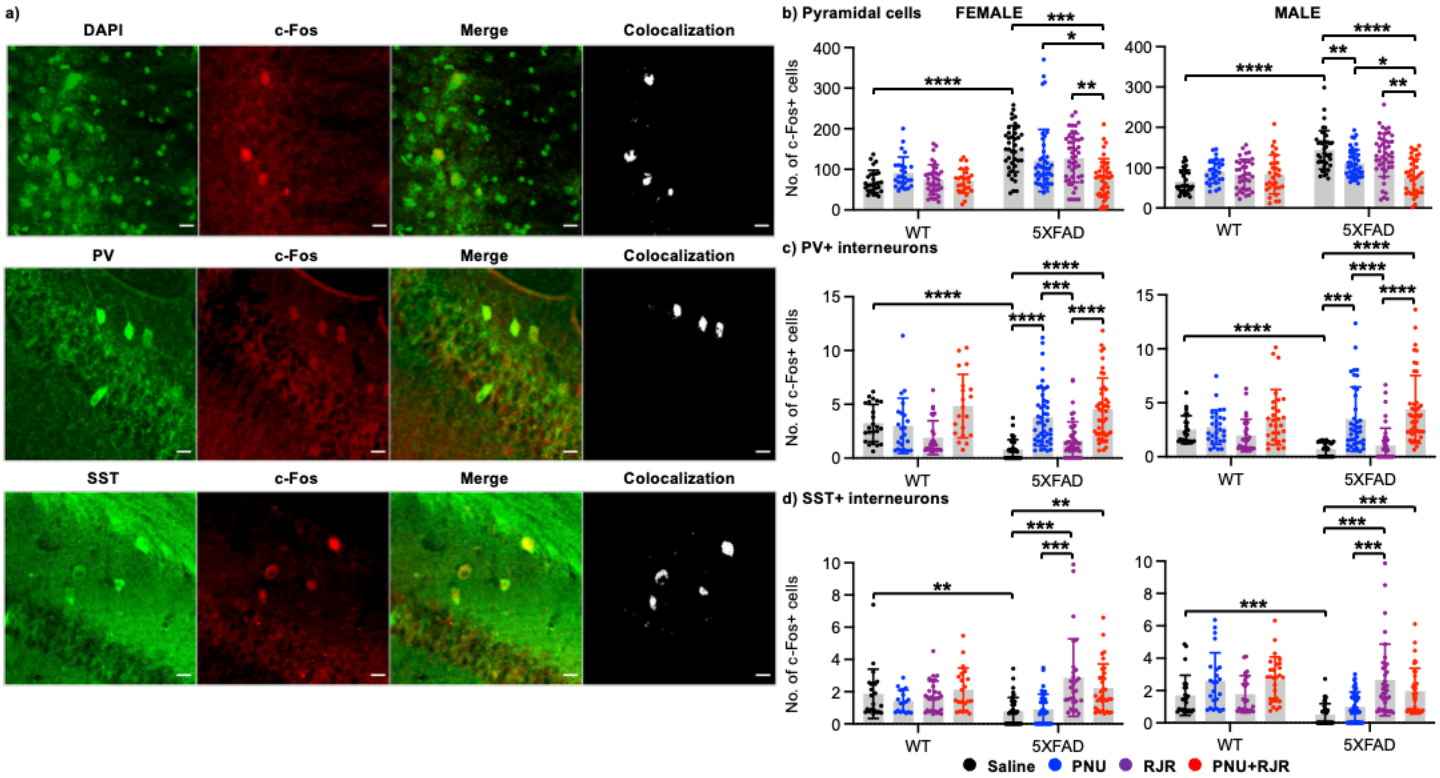

a) Representative images of DAPI, PV, or SST (green), c-Fos (red), merge, and colocalization in the hippocampus. A scale bar represents 10 μm. **b)** Summary data of an average of the total number of c-Fos+ pyramidal neurons in each condition (n = number of sections [number of animals]; Female, WT + Saline = 28 [7], WT + PNU = 26 [7], WT + RJR = 36 [8], WT + PNU + RJR = 26 [6], 5XFAD + saline = 40 [9], 5XFAD + PNU = 44 [11], 5XFAD + RJR = 46 [10], and 5XFAD + PNU + RJR = 42 [10], Male, WT + Saline = 30 [6], WT + PNU = 28 [6], WT + RJR = 36 [7], WT + PNU + RJR = 30 [6], 5XFAD + saline = 40 [9], 5XFAD + PNU = 44 [11], 5XFAD + RJR = 45 [11], and 5XFAD + PNU + RJR = 37 [10]). **c)** Summary data of an average of the total number of c-Fos+ PV+ interneurons in each condition (n = number of sections [number of animals]; Female, WT + Saline = 23 [7], WT + PNU = 22 [7], WT + RJR = 28 [8], WT + PNU + RJR = 20 [6], 5XFAD + saline = 40 [9], 5XFAD + PNU = 45 [11], 5XFAD + RJR = 45 [10], and 5XFAD + PNU + RJR = 44 [10], Male, WT + Saline = 23 [6], WT + PNU = 28 [6], WT + RJR = 31 [7], WT + PNU + RJR = 28 [6], 5XFAD + saline = 35 [9], 5XFAD + PNU = 39 [11], 5XFAD + RJR = 46 [11], and 5XFAD + PNU + RJR = 44 [10]). **d)** Summary data of an average of the total number of c-Fos+ SST+ interneurons in each condition (n = number of sections [number of animals]; Female, WT + Saline = 23 [7], WT + PNU = 18 [7], WT + RJR = 30 [8], WT + PNU + RJR = 21 [6], 5XFAD + saline = 40 [9], 5XFAD + PNU = 43 [11], 5XFAD + RJR = 28 [10], and 5XFAD + PNU + RJR = 33 [10], Male, WT + Saline = 24 [6], WT + PNU = 23 [6], WT + RJR = 22 [7], WT + PNU + RJR = 27 [6], 5XFAD + saline = 39 [9], 5XFAD + PNU = 47 [11], 5XFAD + RJR = 35 [11], and 5XFAD + PNU + RJR = 36 [10]). *$p < 0.05$, **$p < 0.01$, ***$p < 0.001$, and ****$p < 0.0001$. Mixed-effects models / repeated-measures ANOVA, Tukey test.

We then counted hippocampal c-Fos-positive (c-Fos+) cells in pyramidal, PV+, and SST+ cells per 5.0 X 10^6 μm^2 and compared them in each condition. First, we found a significant elevation of the number of c-

Fos+ pyramidal cells in the hippocampus of both female and male 5XFAD mice when compared to WT animals (Female; WT + Saline, 69.845 ± 27.943 and 5XFAD + Saline, 150.818 ± 56.931, $p < 0.0001$, Male; WT + Saline, 65.166 ± 28.820 and 5XFAD + Saline, 143.918 ± 47.784, $p < 0.0001$) (**Fig. 3b, Fig. S1a and S1b, and Table S7**), indicating hyperexcitability. To test whether co-activation α7- and α4β2-nAChRs was required to reverse hippocampal hyperexcitation in 5XFAD mice, we used subtype-specific nAChR agonists, PNU and RJR. We first treated PNU to animals for examining whether stimulating α7-nAChRs was sufficient to reverse hippocampal hyperexcitability. Interestingly, PNU treatment was unable to reverse hyperexcitation in the female 5XFAD hippocampus while it had a slight but significant effect on the activation of hippocampal pyramidal cells in 5XFAD mice (Female; 5XFAD + PNU, 121.873 ± 76.511, $p = 0.6233$ and Male; 5XFAD + PNU, 110.495 ± 34.132, $p = 0.0013$) although these neurons were still hyperexcitable when compared to cells in the WT hippocampus ($p = 0.0104$) (**Fig. 3b, Fig. S1a and S1b, and Table S7**). RJR treatment for activation of α4β2-nAChRs was incapable of reversing hippocampal hyperexcitability in 5XFAD mice (Female; 5XFAD + RJR, 127.829 ± 59.897, $p = 0.2577$ and Male; 5XFAD + RJR, 131.236 ± 53.291, $p = 0.3558$ (**Fig. 3b, Fig. S1a and S1b, and Table S7**). As single receptor activation was unable to reverse hyperexcitation, we next treated PNU and RJR together and found that co-activation of α7- and α4β2-nAChRs was required to reduce hippocampal hyperexcitation in 5XFAD mice (Female; 5XFAD + PNU + RJR, 79.067 ± 47.185, $p = 0.0001$ and Male; 5XFAD + PNU + RJR, 78.509 ± 43.314, $p < 0.0001$) (**Fig. 3b, Fig. S1a and S1b, and Table S7**). Importantly, agonist treatments had no major effect on the activity of hippocampal pyramidal cells in WT mice (**Fig. 3b, Fig. S1a and S1b, and Table S7**). Notably, in the male 5XFAD hippocampus, PNU + RJR treatment had a stronger effect on neuronal hyperexcitation than PNU alone ($p = 0.0175$) (**Table S7**). This thus suggests that Aβ induces neuronal hyperactivation in hippocampal pyramidal neurons in 5XFAD mice, and co-stimulation of α7- and α4β2-nAChRs is required to reverse hippocampal hyperexcitability in 5XFAD mice.

We next examined whether hippocampal disinhibition was linked to hyperexcitation in 5XFAD mice. The number of in c-Fos+ PV+ cells was significantly decreased in the 5XFAD hippocampus (Female; WT + Saline, 3.256 ± 1.730 and 5XFAD + Saline, 0.788 ± 0.929, $p < 0.0001$, Male; WT + Saline, 2.513 ± 1.294 and 5XFAD + Saline, 0.733 ± 0.624, $p < 0.0001$) (**Fig. 3c, Fig. S1c and S1d, and Table S8**). PNU treatment significantly increased the hippocampal PV+ cells' activity in 5XFAD mice (Female; 5XFAD + PNU, 3.827 ±

2.703, $p < 0.0001$ and Male; 5XFAD + PNU, 3.487 ± 2.980, $p = 0.0005$) (**Fig. 3c, Fig. S1c and S1d, and Table S8**). Conversely, RJR had no effect on PV+ cells' activity in the 5XFAD hippocampus (Female; 5XFAD + RJR, 1.627 ± 1.735, $p = 0.0735$ and Male; 5XFAD + RJR, 1.067 ± 1.580, $p = 0.8721$) (**Fig. 3c, Fig. S1c and S1d, and Table S8**). Co-activation of α7- and α4β2-nAChRs markedly elevated the activity of hippocampal PV+ cells to the same degree as PNU treatment itself (Female; 5XFAD + PNU + RJR, 4.554 ± 2.889, $p < 0.0001$ and Male; 5XFAD + PNU + RJR, 4.391 ± 3.143, $p < 0.0001$) (**Fig. 3c, Fig. S1c and S1d, and Table S8**). Agonist treatments had no major effect on PV+ cells' activity in the WT hippocampus (**Fig. 3c, Fig. S1c and S1d, and Table S8**). This suggests that Aβ reduces the activity of hippocampal PV+ cells, but activation of α7-nAChRs by PNU selectively simulates these cells in 5XFAD mice, which is consistent with our findings in cultured neurons (**Fig. 2a and 2c**).

Finally, we examined the contribution of SST+ cells to hyperexcitability. The hippocampal SST+ cells' activity was markedly reduced in 5XFAD mice (Female; WT + Saline, 1.868 ± 1.527 and 5XFAD + Saline, 0.781 ± 0.854, $p = 0.0037$, Male; WT + Saline, 1.699 ± 1.238 and 5XFAD + Saline, 0.511 ± 0.669, $p = 0.0001$) (**Fig. 3d, Fig. S1e and S1f, and Table S9**). Notably, PNU was unable to affect SST+ cells' activity in the 5XFAD hippocampus (Female; 5XFAD + PNU, 0.911 ± 0.934, $p = 0.6740$ and Male; 5XFAD + PNU, 1.001 ± 0.903, $p = 0.2145$) (**Fig. 3d, Fig. S1e and S1f, and Table S9**). However, RJR treatment markedly elevated the activity of hippocampal SST+ cells in 5XFAD mice (Female; 5XFAD + RJR, 2.876 ± 2.408, $p = 0.0006$ and Male; 5XFAD + RJR, 2.650 ± 2.216, $p < 0.0001$) (**Fig. 3d, Fig. S1e and S1f, and Table S9**). Importantly, co-activation of α7- and α4β2-nAChRs significantly elevated the hippocampal SST+ cells' activity to the same degree as RJR treatment itself in 5XFAD mice (Female; 5XFAD + PNU + RJR, 2.219 ± 1.498, $p = 0.0002$ and Male; 5XFAD + PNU + RJR, 1.967 ± 1.413, $p = 0.0004$) (**Fig. 3d, Fig. S1e and S1f, and Table S9**). Notably, agonist treatments had no effect on hippocampal SST+ cells' activity in WT mice (**Fig. 3d, Fig. S1e and S1f, and Table S9**). This suggests that Aβ reduces the hippocampal SST+ cells' activity, but stimulation of α4β2-nAChRs by RJR selectively activates these cells in 5XFAD mice, which is consistent with our findings in cultured neurons (**Fig. 2b and 2d**). These findings all together suggest that Aβ significantly reduces both PV+ and SST+ interneurons' activity to induce hyperexcitation in pyramidal cells in 5XFAD hippocampus, and co-

stimulation of PV+ and SST+ cells via activating α7- and α4β2-nAChRs together is required to reduce disinhibition-induced hippocampal hyperexcitability in 5XFAD mice.

Deficits in hippocampal network activity in 5XFAD mice following fear learning.

Neural network activity in the hippocampus plays important roles in memory processes (*84-88*). Studies have shown that altered hippocampal network activity can impair learning and memory processes, which contributes to the development of AD (*10, 89-92*). In people at high risk of developing AD, abnormal activation and/or deactivation of specific network activities during hippocampal memory processes are detected decades before the onset of clinical disease (*10, 89-93*). This suggests that monitoring hippocampal network activity may be a useful tool for early detection and diagnosis of AD. Especially, hippocampal inhibitory interneurons regulate network oscillations of local field potentials (LFPs), which are thought to play a mechanistic role in various aspects of hippocampus-dependent memory processes (*32, 84-88*). In mice, it has been reported that theta (4-8 Hz) synchrony is increased between the hippocampal CA1 and lateral amygdala during the consolidation and reconsolidation of fear memory (*84, 85*). Research also suggests that gamma rhythms (30-100 Hz) are two functionally distinct oscillatory activities, slow (30-50 Hz) and fast (50-100 Hz) gamma (*94, 95*). Slow gamma oscillations are likely involved in storing memory (*96-98*). Fast gamma rhythms promote the transmission of current sensory information to the hippocampus during new memory encoding (*87, 99*). It has been shown that spatial learning increases theta, slow gamma, and fast gamma powers in the hippocampal CA1 area (*100-102*). We thus first recorded hippocampal LFPs before and following contextual fear conditioning (CFC) to determine if hippocampal network activity was disrupted in 5XFAD mice after fear learning. Prior to learning, basal LFPs were recorded for an hour (PRE) (**Fig. 4a**). Especially, the excitatory/inhibitory (E/I) balance within the hippocampus is critical for neural network stability and is precisely regulated during sleep to facilitate memory consolidation (*103*). Consolidation of hippocampus-dependent fear memory is known to occur between 1 and 3 hours after training (*104, 105*). Therefore, test animals were returned to their home cage for 90 minutes after fear learning, and then we recorded hippocampal LFPs for additional one hour (POST) (**Fig. 4a**).

Figure 4. Deficits in hippocampal network activity in 5XFAD mice following fear learning.

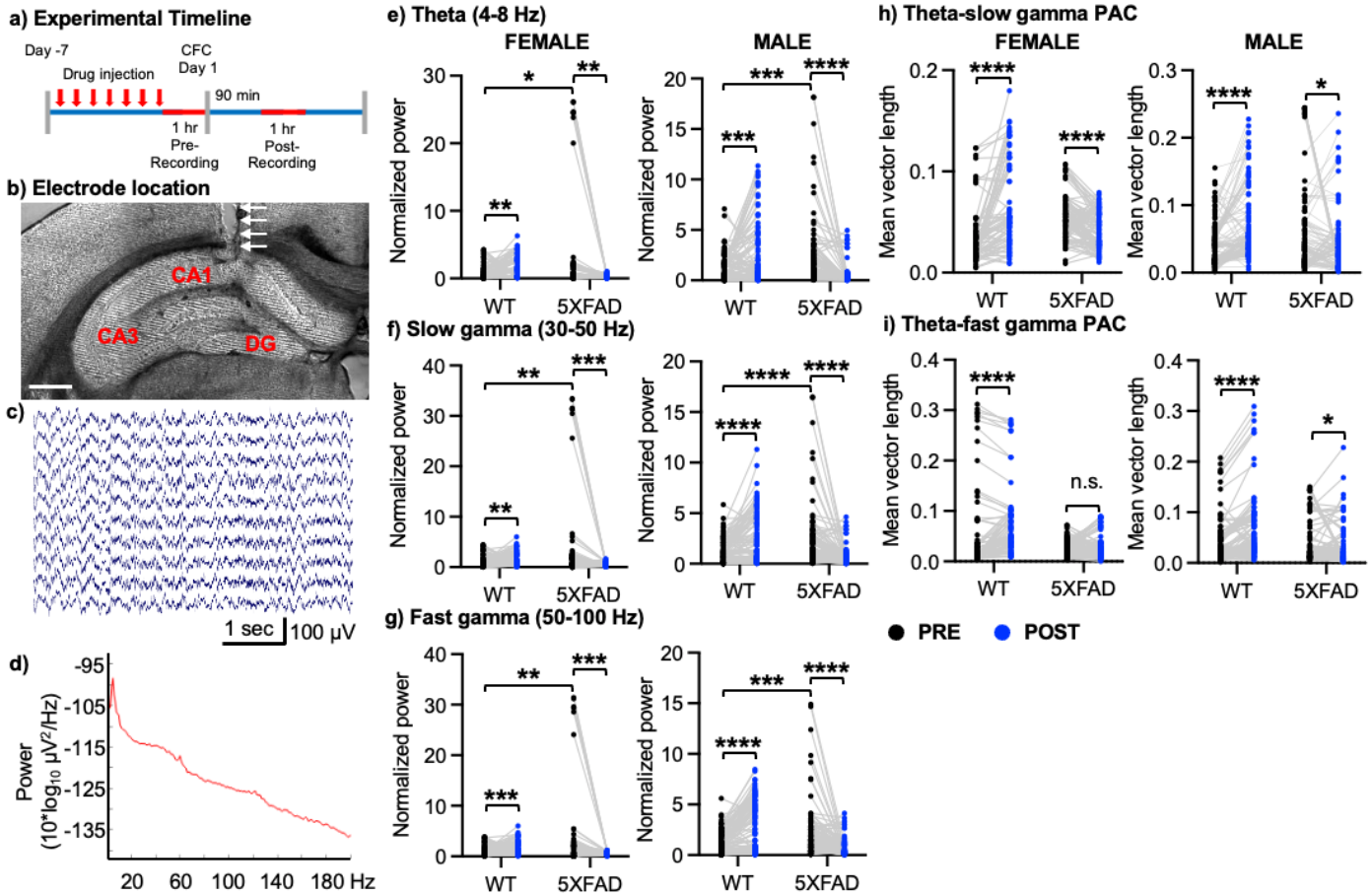

a) Experimental timeline. **b)** A representative image of a brain section after electrolytic lesioning indicates electrode placement (arrows) in the hippocampus CA1 area. A scale bar represents 1 mm. **c)** Representative section of LFP traces in CA1 of a freely behaving mouse. **d)** Representative power spectral density. Summary graphs of normalized powers of **e)** theta, **f)** slow gamma and **g)** fast gamma frequencies in female and male mice in each condition. Summary of **h)** Theta-slow gamma PAC and **i)** Theta-fast gamma PAC in each condition. n = number of channels [number of animals]; Female, WT = 74 [7] and 5XFAD = 101 [9], Male, WT =125 [12] and 5XFAD = 106 [10]). *$p < 0.05$, **$p < 0.01$, ***$p < 0.001$, and ****$p < 0.0001$. n.s. – not significant. Paired two-tailed student's t-test was used to compare between PRE and POST data. Two-way ANOVA, Šídák's test was used to compare between WT PRE and 5XFAD PRE data.

We then compared hippocampal theta, slow gamma, and fast gamma powers between 5XFAD mice and WT littermates. We found that theta (Female; WT PRE, 1.000 ± 1.199 and WT POST, 1.696 ± 1.552, $p = 0.0029$, Male; WT PRE, 1.000 ± 1.270 and WT POST, 1.926 ± 2.849, $p = 0.0001$), slow gamma (Female; WT PRE, 1.000 ± 1.223 and WT POST, 1.624 ± 1.420, $p = 0.0031$, Male; WT PRE, 1.000 ± 1.124 and WT POST, 2.049 ± 2.413, $p < 0.0001$), and fast gamma powers (Female; WT PRE, 1.000 ± 1.086 and WT POST, 1.601 ± 1.372, $p = 0.0009$, Male; WT PRE, 1.000 ± 1.051 and WT POST, 2.467 ± 2.486, $p < 0.0001$) were significantly elevated following CFC in WT female and male mice (**Fig. 4e-g and Table S10**). Conversely, 5XFAD mice

showed significant reduction in powers of theta (Female; 5XFAD PRE, 2.195 ± 6.108 and 5XFAD POST, 0.225 ± 0.210, $p = 0.0015$, Male; 5XFAD PRE, 2.168 ± 3.446 and 5XFAD POST, 0.539 ± 1.019, $p < 0.0001$), slow gamma (Female; 5XFAD PRE, 3.145 ± 7.767 and 5XFAD POST, 0.480 ± 0.342, $p = 0.0007$, Male; 5XFAD PRE, 2.095 ± 3.080 and 5XFAD POST, 0.690 ± 1.940, $p < 0.0001$), and fast gamma bands (Female; 5XFAD PRE, 3.059 ± 7.262 and 5XFAD POST, 0.493 ± 0.284, $p = 0.0005$, Male; 5XFAD PRE, 2.055 ± 2.724 and 5XFAD POST, 0.770 ± 0.855, $p < 0.0001$) (**Fig. 4e-g and Table S10**). Interestingly, we found significant higher basal powers in 5XFAD mice than WT animals in all frequency bands (**Fig. 4e-g and Table S10**), which is likely related to Aβ-induced early hippocampal hyperexcitation. These findings suggest that the learning-induced increase in hippocampal oscillations is impaired in 5XFAD mice.

In healthy rodents and humans, the hippocampus exhibits prominent gamma oscillations that emerge at specific phases of theta oscillations known as theta-gamma coupling (*106*). The strength of theta-gamma coupling in the hippocampus is correlated with the task load of memory in humans (*107*). This coupling is impaired in hippocampal slices in AD model mice (*108*). Appropriate phase-amplitude coupling (PAC) and entrainment to hippocampal oscillations are thought to be essential for cognition and have been directly linked to memory performance in humans (*107, 109, 110*). We thus calculated the mean vector length (MVL) as an entrainment strength. We found that the MVL in both theta-slow gamma and theta-fast gamma was significantly higher following learning than before learning in WT female and male mice (Theta-slow gamma, Female; WT PRE, 0.036 ± 0.027 and WT POST, 0.067 ± 0.044, $p < 0.0001$, Male; WT PRE, 0.041 ± 0.032 and WT POST, 0.070 ± 0.053, $p < 0.0001$. Theta-fast gamma, Female; WT PRE, 0.059 ± 0.087 and WT POST, 0.076 ± 0.070, $p = 0.0004$, Male; WT PRE, 0.036 ± 0.042 and WT POST, 0.061 ± 0.061, $p < 0.0001$) (**Fig. 4h-l and Table S11**). In contrast, the theta-slow gamma MVL in 5XFAD mice was significantly lower following learning when compared to the basal condition (Female; 5XFAD PRE, 0.055 ± 0.021 and 5XFAD POST, 0.042 ± 0.018, $p < 0.0001$, Male; 5XFAD PRE, 0.060 ± 0.067 and 5XFAD POST, 0.043 ± 0.047, $p = 0.0157$) (**Fig. 4h-l and Table S11**). Moreover, fear learning was unable to elevate 5XFAD animals' theta-fast gamma PAC in the hippocampus (Female; 5XFAD PRE, 0.028 ± 0.015 and 5XFAD POST, 0.028 ± 0.022, $p = 0.9556$, Male; 5XFAD PRE, 0.041 ± 0.046 and 5XFAD POST, 0.030 ± 0.039, $p = 0.0180$) (**Fig. 4h-l and Table S11**). This data suggest that fear learning strengthens PAC entrainment in WT mice, consistent with the previous report

(*111*). However, fear leaning is unable to increase theta-gamma coupling in 5XFAD mice. These findings thus show deficits in hippocampal network activity in 5XFAD mice following fear learning.

Co-activation of α7- and α4β2-nAChRs is required to restore normal hippocampal network activity in 5XFAD mice.

We next compared hippocampal oscillatory activity following fear learning between WT and 5XFAD mice. When compared to WT mice, 5XFAD mice exhibited a significant decrease in the powers of theta (Female; WT, 1.000 ± 0.915 and 5XFAD, 0.151 ± 0.148, $p < 0.0001$, Male; WT, 1.000 ± 1.479 and 5XFAD, 0.280 ± 0.529, $p < 0.0001$), slow gamma (Female; WT, 1.000 ± 1.874 and 5XFAD, 0.268 ± 10.167, $p = 0.0015$, Male; WT, 1.000 ± 1.079 and 5XFAD, 0.304 ± 0.414, $p = 0.0007$), and fast gamma bands (Female; WT, 1.000 ± 0.853 and 5XFAD, 0.297 ± 0.162, $p = 0.0024$, Male; WT, 1.000 ± 1.008 and 5XFAD, 0.312 ± 0.347, $p < 0.0001$) (**Fig. 5a-c and Table S12-S14**).

Figure 5. Co-activation of α7- and α4β2-nAChRs is required to restore normal hippocampal network activity in 5XFAD mice.

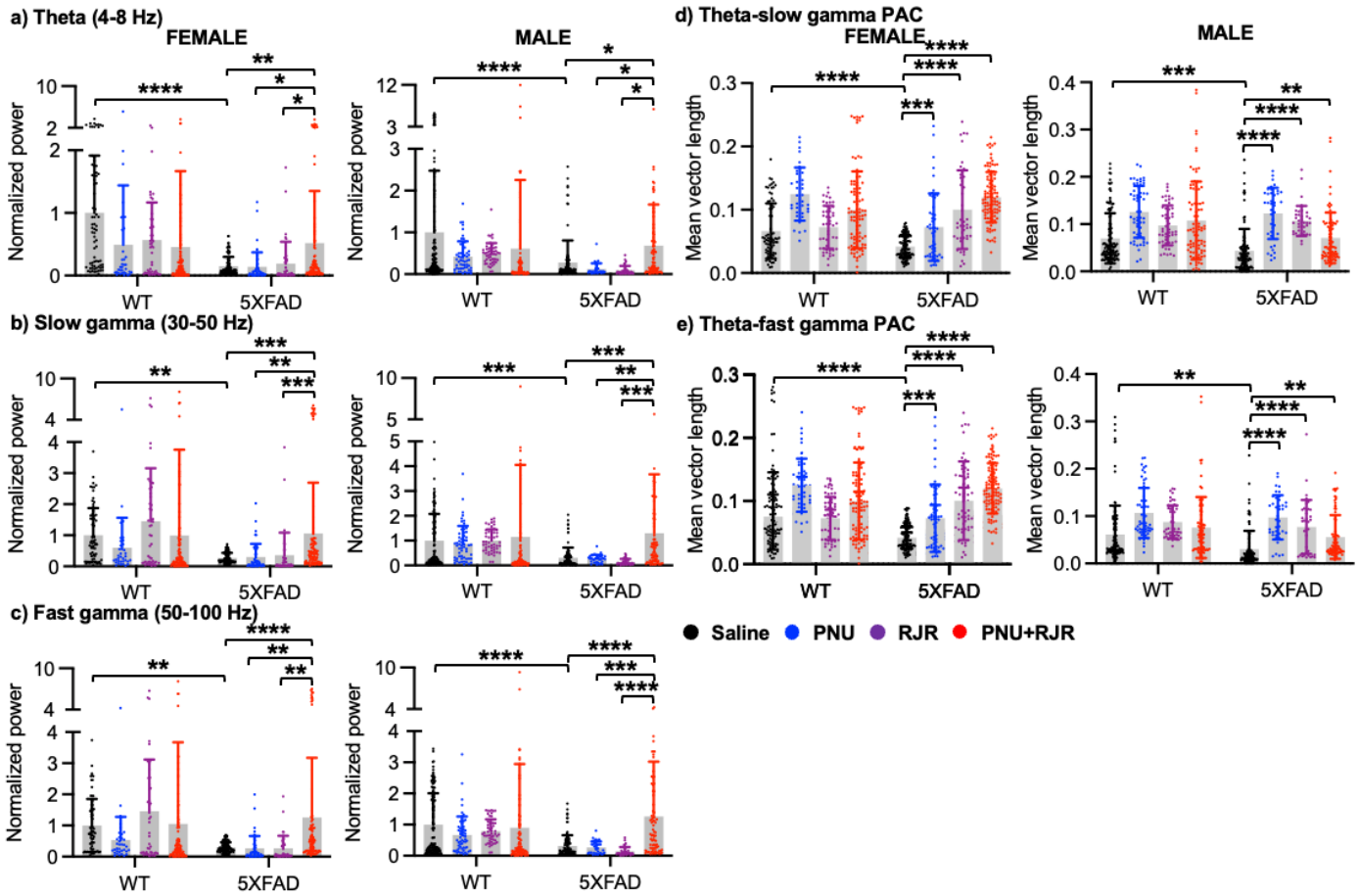

Summary graphs of normalized powers of **a)** theta, **b)** slow gamma and **c)** fast gamma frequencies in female and male mice in each condition. Summary of **d)** Theta-slow gamma PAC and **e)** Theta-fast gamma PAC in each condition. n = number of channels [number of animals]; Female, WT + Saline = 74 [7], WT + PNU = 35 [4], WT + RJR = 48 [4], WT + PNU + RJR = 97 [9], 5XFAD + saline = 101 [9], 5XFAD + PNU = 51 [4], 5XFAD + RJR = 41 [4], and 5XFAD + PNU + RJR = 93 [8], Male, WT + Saline = 125 [12], WT + PNU = 57 [5], WT + RJR = 51 [4], WT + PNU + RJR = 86 [8], 5XFAD + saline = 106 [10], 5XFAD + PNU = 36 [4], 5XFAD + RJR = 38 [4], and 5XFAD + PNU + RJR = 79 [7]. *$p < 0.05$, **$p < 0.01$, ***$p < 0.001$, and ****$p < 0.0001$. Mixed-effects models / repeated-measures ANOVA, Tukey test.

This indicates impaired fear memory processing in 5XFAD mice. Acetylcholine modulates hippocampal oscillations to control memory processes (*112-114*). We thus examined if stimulating α7- and α4β2-nAChRs together was required to reverse hippocampal network deficits in 5XFAD mice after fear conditioning. We found that activation of single receptors by themselves using PNU or RJR had no effect on the powers of theta (Female; 5XFAD + PNU, 0.138 ± 0.234, $p = 0.9997$, and 5XFAD + RJR, 0.127 ± 0.174, $p = 0.9984$, Male; 5XFAD + PNU, 0.123 ± 0.137, $p = 0.8638$, and 5XFAD + RJR, 0.090 ± 0.107, $p = 0.7720$), slow gamma (Female; 5XFAD + PNU, 0.305 ± 0.419, $p = 0.9988$, and 5XFAD + RJR, 0.214 ± 0.297, $p = 0.8501$, Male; 5XFAD + PNU, 0.272 ± 0.157, $p = 0.9995$, and 5XFAD + RJR, 0.142 ± 0.122, $p = 0.9405$), and fast gamma

bands (Female; 5XFAD + PNU, 0.269 ± 0.392, p = 0.9995, and 5XFAD + RJR, 0.198 ± 0.240, p = 0.9849, Male; 5XFAD + PNU, 0.263 ± 0.195, p = 0.9962, and 5XFAD + RJR, 0.142 ± 0.139, p = 0.8634) (**Fig. 5a-c and Table S12-S14**). This data show that stimulation of either α7- or α4β2-nAChRs is insufficient to improve hippocampal network activity in 5XFAD mice. However, co-stimulation of α7- and α4β2-nAChRs significantly elevated the powers of theta (Female; 5XFAD + PNU+RJR, 0.518 ± 0.834, p = 0.0057, Male; 5XFAD + PNU+RJR, 0.684 ± 0.986, p = 0.0460), slow gamma (Female; 5XFAD + PNU + RJR, 1.058 ± 1.633, p = 0.0006, Male; 5XFAD + PNU + RJR, 1.300 ± 2.375, p = 0.0001), and fast gamma bands (Female; 5XFAD + PNU + RJR, 1.253 ± 1.919, p < 0.0001, Male; 5XFAD + PNU + RJR, 1.261 ± 1.763, p < 0.0001) (**Fig. 5a-c and Table S12-S14**). Interestingly, agonist treatment significantly reduced theta power only in WT mice (Female; WT + PNU, 0.490 ± 0.950, p = 0.0077, WT + RJR, 0.566 ± 0.600, p = 0.0138, WT + PNU + RJR, 0.457 ± 1.209, p < 0.0001, Male; WT + PNU, 0.422 ± 0.365, p = 0.0031, WT + RJR, 0.489 ± 0.256, p = 0.0173, WT + PNU + RJR, 0.609 ± 1.648, p = 0.0382) while drugs had no major effect on slow and fast gamma powers in WT animals (**Fig. 5a-c and Table S12-S14**). These findings suggest that a memory consolidation-mediated increase in hippocampal oscillations is disrupted in 5XFAD mice, which is reversed only by co-activation of α7- and α4β2-nAChRs.

We next analyzed the strength of theta-gamma coupling in the hippocampus. We found that the MVL in both theta-slow gamma and theta-fast gamma was significantly lower in 5XFAD mice following learning than WT animals (Theta-slow gamma, Female; WT, 0.067 ± 0.044 and 5XFAD, 0.042 ± 0.018, p = 0.0004, Male; WT, 0.070 ± 0.053 and 5XFAD, 0.043 ± 0.047, p = 0.0003. Theta-fast gamma, Female; WT, 0.076 ± 0.070 and 5XFAD, 0.028 ± 0.022, p < 0.0001, Male; WT, 0.061 ± 0.061 and 5XFAD, 0.030 ± 0.039, p < 0.0001) (**Fig. 5d-e and Table S15 and S16**). Interestingly, we found that activation of single receptors or two receptors together was sufficient to increase MVL in 5XFAD mice (Theta-slow gamma, Female; 5XFAD + PNU, 0.072 ± 0.053, p = 0.0005, 5XFAD + RJR, 0.100 ± 0.062, p < 0.0001, and 5XFAD + PNU + RJR, 0.120 ± 0.040, p < 0.0001, Male; 5XFAD + PNU, 0.122 ± 0.054, p < 0.0001, 5XFAD + RJR, 0.107 ± 0.032, p < 0.0001, and 5XFAD + PNU + RJR, 0.071 ± 0.053, p = 0.0055. Theta-fast gamma, Female; 5XFAD + PNU, 0.055 ± 0.039, p = 0.0008, 5XFAD + RJR, 0.086 ± 0.036, p < 0.0001, and 5XFAD + PNU + RJR, 0.078 ± 0.041, p < 0.0001, Male; 5XFAD + PNU, 0.097 ± 0.047, p < 0.0001, 5XFAD + RJR, 0.077 ± 0.057, p < 0.0001, and 5XFAD + PNU + RJR, 0.056

± 0.046, p = 0.0052) (**Fig. 5d-e and Table S15 and S16**). This data show that activation of α7- and/or α4β2-nAChRs is sufficient to strengthen fear learning-related PAC entrainment in 5XFAD mice. In sum, 5XFAD mice showed significant deficits in hippocampal network activity following fear conditioning. While stimulation of α7- and/or α4β2-nAChRs is sufficient to increase PAC in 5XFAD mice, co-activation of α7- and α4β2-nAChRs, perhaps stimulating PV+ and SST+ cells together, is essential to restore normal powers of AD-related hippocampal oscillations following fear learning.

Co-activation of α7- and α4β2-nAChRs is required to improve contextual fear memory in 5XFAD mice.

Conditioned fear responses have been demonstrated to be impaired in patients with mild to moderate AD (*115, 116*). Fear memory loss in 5XFAD mice starts at the age of 5 months (*117*). We thus carried out contextual fear conditioning (CFC) as described previously (*118, 119*) with 5-month-old 5XFAD and WT female and male mice. In consistent with the previous finding (*117*), 5XFAD female and male mice intraperitoneally given saline displayed significant less freezing in contextual fear conditioning compared to WT controls, indicating impaired hippocampus-dependent fear memory (Female, WT + Saline, 36.785 ± 10.866% and 5XFAD + Saline, 14.188 ± 12.202%, p < 0.0001, and Male, WT + Saline, 38.938 ± 13.066% and 5XFAD + Saline, 16.177 ± 8.761%, p < 0.0001) (**Fig. 6 and Table S17**).

Figure 6. Co-activation of α7- and α4β2-nAChRs is required to improve contextual fear memory in 5XFAD mice.

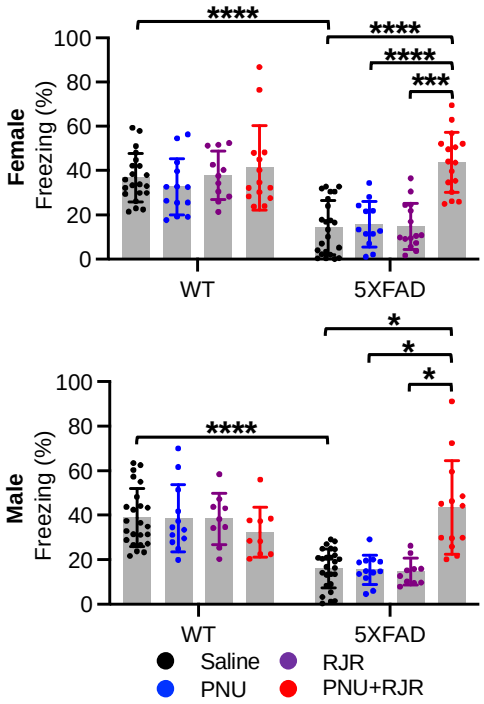

Summary data of freezing behavior of WT and 5XFAD female (n = number of animals, WT + Saline = 21, WT + PNU = 13, WT + RJR = 11, WT + PNU+RJR = 14, 5XFAD + Saline = 23, 5XFAD + PNU = 12, 5XFAD + RJR = 15, 5XFAD + PNU+RJR = 16) and male mice (n = number of animals, WT + Saline = 24, WT + PNU = 12, WT + RJR = 9, WT + PNU + RJR = 9, 5XFAD + Saline = 26, 5XFAD + PNU = 12, 5XFAD + RJR = 10, 5XFAD + PNU + RJR = 13) in each condition. *$p < 0.05$ and ****$p<0.0001$, Two-way ANOVA, Tukey test.

Given that co-activation of α7- and α4β2-nAChRs is required to reverse fear learning-associated hippocampal network activity (**Fig. 5**), we examined the effects of stimulating these receptors on contextual fear memory in 5XFAD mice. We intraperitoneally injected PNU or RJR into 5XFAD and WT mice to see if activation of either α7- or α4β2-nAChRs reversed impaired contextual fear memory in AD model mice. Notably, neither PNU nor RJR single injection reversed fear memory loss in 5XFAD mice (Female, 5XFAD + PNU, 15.751 ± 10.332%, $p > 0.9999$, and 5XFAD + RJR, 14.836 ± 10.400%, $p > 0.9999$, and Male, 5XFAD + PNU, 15.558 ± 6.577%, $p > 0.9999$, and 5XFAD + RJR, 14.648 ± 6.018%, $p > 0.9999$) (**Fig. 6 and Table S17**). This shows that stimulation of either α7- or α4β2-nAChRs is insufficient to improve fear memory in 5XFAD mice. We thus intraperitoneally injected PNU and RJR together into 5XFAD and WT littermates and examined whether co-activation of α7- and α4β2-nAChRs improved contextual fear memory in 5XFAD mice. We found that co-activation of α7- and α4β2-nAChRs significantly enhanced contextual fear memory in 5XFAD male and female mice (Female, 5XFAD + PNU + RJR, 43.664 ± 13.580%, $p < 0.0001$, and Male, 5XFAD + PNU + RJR, 43.434 ± 21.002%, $p = 0.0101$) (**Fig. 6 and Table S17**). These findings suggest that co-activation of α7- and α4β2-nAChRs (potentially stimulates hippocampal PV+ and SST+ cells together) is required to improve hippocampus-dependent fear memory in 5XFAD mice.

Co-activation of α7- and α4β2-nAChRs is required to reduce the Aβ buildup in the 5XFAD hippocampus.

Amyloid plaques are aggregation of Aβ in the extracellular space of the brain, central to the AD pathology. It has been shown that *in vivo* extracellular Aβ levels are dynamically and directly influenced by neuronal activity (*4*). Importantly, neuronal hyperexcitability increases Aβ secretion and accumulation (*4, 5*). Therefore, it is possible that Aβ-induced hippocampal hyperexcitation promotes the *in vivo* rapid growth of amyloid plaques, which can be prevented by reducing neuronal activity through enhancing hippocampal inhibition. To test this idea, we examined if enhancing PV+ and SST+ activity together by co-stimulating α7- and α4β2-nAChRs was required to reduce the Aβ buildup in the 5XFAD hippocampus. Notably, longitudinal *in*

vivo imaging studies in AD pathology model mice have demonstrated that amyloid plaques form and grow quickly over the course of a day and one week (*120, 121*). We thus intraperitoneally injected PNU and RJR on their own or together into 5-month-old 5XFAD mice for 7 days. Saline was given to mice as a control. We then visualized amyloid plaques and measured the total number of amyloid plaques in the hippocampus. We found that stimulation of each receptor had no effect on amyloid pathology in the hippocampus of both female and male 5XFAD mice when compared to the saline-injected controls (Female, Saline, 50.62 ± 13.21, PNU, 49.71 ± 11.17, $p = 0.9978$, and RJR, 47.71 ± 10.28, $p = 0.9359$, and Male, Saline, 38.95 ± 13.53, PNU, 38.66 ± 8.85, $p > 0.9999$, and RJR, 47.88 ± 5.97, $p = 0.2469$) (**Fig. 7 and Table S18**). However, we revealed that co-stimulation of α7- and α4β2-nAChRs significantly reduced the total number of amyloid plaques in the hippocampus of both female and male 5XFAD mice when compared to the saline-injected controls (Female, PNU + RJR, 32.19 ± 7.19, $p = 0.0013$, and Male, PNU+RJR, 24.82 ± 9.89, $p = 0.0042$) (**Fig. 7 and Table S18**). This data show that co-activation of α7- and α4β2-nAChRs is required to reduce the rapid growth of amyloid plaques in 5XFAD mice.

Figure 7. Co-activation of α7- and α4β2-nAChRs prevents the *in vivo* growth of amyloid plaques.

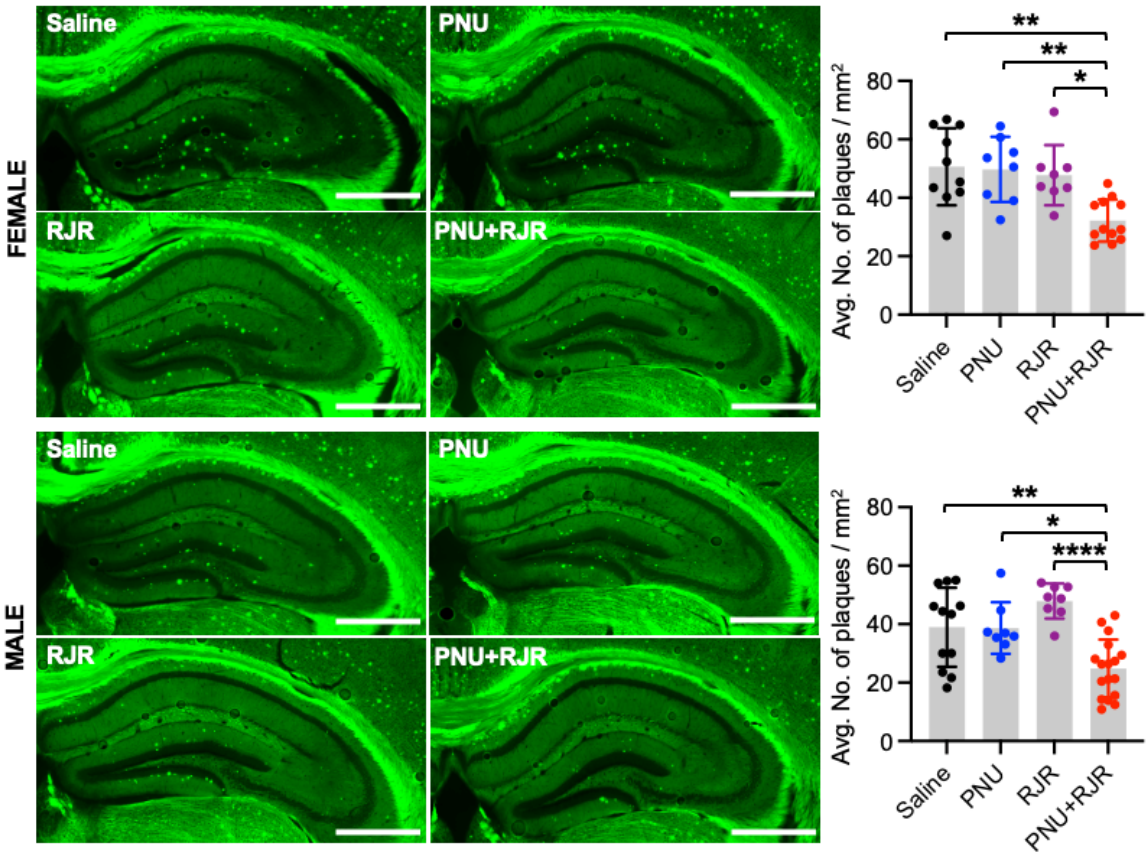

Representative images of Thioflavin S-positive amyloid plaques (Green puncta) in the hippocampus in 5-month-old 5XFAD female (n = number of animals, Saline = 10, PNU = 8, RJR = 8, and PNU + RJR = 12) and

male (n = number of animals, Saline = 12, PNU = 8, RJR = 8, and PNU + RJR = 17) mice in each condition. A scale bar represents 1 mm. Summary graphs of the total number of amyloid plaques per mm^2 in each condition. *$p < 0.05$, **$p < 0.01$, and ****$p < 0.0001$, One-way ANOVA, Tukey test.

Discussion

A large body of research has suggested that Aβ-induced inhibitory dysfunction in the hippocampus can be a crucial trigger for disruptions in neural oscillations and consequent cognitive function in AD (*93, 122-128*). However, the molecular mechanisms underlying Aβ-induced hippocampal interneuron dysfunctions in AD have not been fully understood. Cholinergic dysfunction may be a prime suspect for Aβ-induced inhibitory dysfunction because cholinergic signaling has greater effects on hippocampal inhibitory cells than excitatory neurons (*39-44*), and there are diverse lines of evidence that molecular interactions between Aβ and nAChRs impair receptor functions in the early stage of AD (*53, 129-131*). This suggests that Aβ inhibits nAChR activities in inhibitory interneurons, which reduces hippocampal inhibition and oscillations to trigger cognitive decline in the early stage of AD. However, hippocampal inhibitory cells are highly diverse, and distinct interneuron subtypes differentially contributes to hippocampal oscillations and memory formation (*32*). In addition, various neuronal nAChRs have been found in the human brain (*61-63*), and distinct nAChR subtypes differentially affect hippocampal inhibition and oscillations (*75, 132-135*). Therefore, it is challenging to elucidate the nAChR-mediated mechanisms by which Aβ affects hippocampal neural network and memory processing in AD at the interneuron subtype levels. Our published works have discovered that Aβ selectively binds to two of the three major hippocampal nAChR subtypes, α7- and α4β2-nAChRs, but not α3β4-nAChRs, and inhibits these two receptors in cultured hippocampal inhibitory interneurons to decrease their activity, leading to hyperexcitation in excitatory neurons (*64, 65*). We have also revealed that co-activation of α7- and α4β2-nAChRs is required to reverse the Aβ-induced adverse effects in hippocampal neurons (*64, 65*). In the current study, we further identify that α7-, α4β2-, and α3β4-nAChRs regulate the cholinergic activity mainly in PV+, SST+, and excitatory cells, respectively. Additionally, we discover that co-activation of α7- and α4β2-nAChRs is necessary to reverse hippocampal hyperexcitability, network dysfunction, and fear memory loss and reduce amyloid pathology in 5XFAD mice. In sum, our study provides the mechanistic link between hippocampal disinhibition-induced hyperexcitability via altered cholinergic activity, network dysfunction, pathology, and memory loss in AD.

Based on our findings, we propose the following model. α7-, α4β2-, and α3β4-nAChRs predominantly control the nicotinic cholinergic signaling in PV+ interneurons that provide somatic inhibition, SST+ interneurons that provides dendritic inhibition, and pyramidal excitatory neurons, respectively, in the

hippocampus, which is supported by the previous findings (*40, 42, 43, 75, 135-144*) (**Fig. 8a**). These distinct cholinergic regulations of inhibitory activity contribute to inhibition onto pyramidal cells, which controls hippocampal network activity and memory processes (**Fig. 8a**). Aβ selectively inhibits α7- and α4β2-nAChRs in PV+ and SST+ cells, respectively, but not α3β4-nAChRs in excitatory neurons, which reduces inhibition to induce hyperexcitability and network dysfunction in the hippocampus, leading to amyloid pathology and memory loss in AD (**Fig. 8b**). Stimulation of PV+ or SST+ cells by the activation of each nAChR subtype-specific agonists, PNU-282987 (PNU), an α7 agonist, or RJR-2403 Oxalate (RJR), an α4β2 agonist, is insufficient to reverse the adverse effects of Aβ (**Fig. 8c-d**). Therefore, co-stimulation of hippocampal PV+ and SST+ inhibitory interneurons via activation of α7- and α4β2-nAChRs together is required to be protective against AD (**Fig. 8e**).

Figure 8. A schematic model of nAChR-mediated mechanisms of Aβ-induced dysfunction in hippocampal inhibition, network activities, amyloid pathology, and memory in AD.

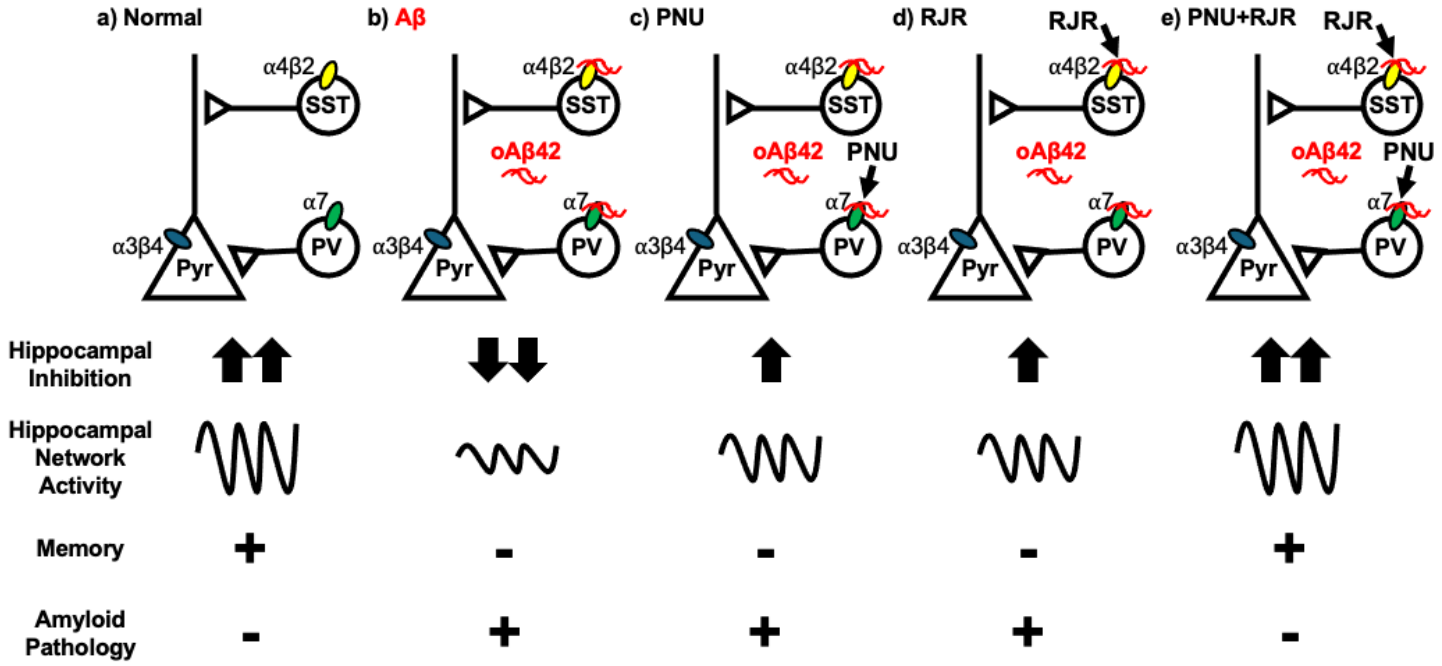

a) α7-, α4β2-, and α3β4-nAChRs predominantly control the nicotinic cholinergic signaling in parvalbumin-positive (PV+), somatostatin-positive (SST+), and pyramidal cells (Pyr), respectively, in the hippocampus. The cholinergic regulation of inhibitory activity contributes to inhibition onto pyramidal cells, which controls hippocampal network activity and memory processes. **b)** Aβ selectively inhibits α7- and α4β2-nAChRs in PV+ and SST+ cells, respectively, but not α3β4-nAChRs in excitatory neurons, which reduces inhibition to induce hyperexcitability and network dysfunction in the hippocampus, leading to memory loss in AD. Additionally, Aβ-induced hippocampal hyperexcitability increases Aβ secretion to enhance the amyloid pathology. Stimulation of PV+ or SST+ cells by the activation of each nAChR subtype-specific agonists, **c)** PNU-282987 (PNU), an α7 agonist, or **d)** RJR-2403 Oxalate (RJR), an α4β2 agonist, is insufficient to reverse the adverse effects of Aβ. **e)** Co-stimulation of hippocampal PV+ and SST+ inhibitory interneurons via activation of α7- and α4β2-nAChRs together is required to be protective against AD.

Given that cholinergic deficiency is associated with AD, strategies aiming to restore normal cholinergic function have been developed as therapeutic drugs for AD, including several acetylcholinesterase inhibitors (*145*). Therefore, all cholinergic synapses can be intensified by these drugs. However, some subtypes of nAChRs that may not be affected by Aβ (e.g. α3β4) can also be activated when attempts are made to use such drugs in the treatment of AD, resulting in unexpected side effects. Moreover, acetylcholinesterase inhibitors have been shown to be only partially effective in reversing experimental deficits in hippocampal-dependent memory in rodents (*146*). Consistently, we have revealed a non-selective cholinergic agonist exacerbates Aβ adverse effects on hippocampal neurons (*64, 65*). Furthermore, overstimulation of the M1 type metabotropic AChRs adversely affect neuronal activity in the prefrontal cortex, related to working memory(*147*). Therefore, acetylcholinesterase inhibitors are not very effective in slowing AD progression due to non-selective stimulation of acetylcholine receptors (*148, 149*). There are also discrepancies involving the use of nicotine treatment to stimulate nAChRs to alter cognitive function. For example, nicotine agonists have been found to improve performance in a variety of memory tasks in rodents and non-human primate studies (*150*), while several other studies have failed to find significant enhancement of learning and memory by nicotine treatment (*151*). Nonetheless, nAChR agonists have consistently suggested promising approaches in the treatment of AD (*152*). However, clinical trials thus far have been challenged by adverse effects or minimal improvement (*153*). Additionally, some studies demonstrate that stimulating one type of nAChRs by using a subtype specific agonist enhances cognitive performance, but other studies find no beneficial effect. For instance, selective α7 nAChR agonists have been reported to improve cognition in a variety of animal models (*154-156*), while another study has found almost no beneficial effect on learning and memory in mice (*157*). An α4β2-nAChR agonist alone can improve working memory only in young rats but not older animals (*158*). It is thus not yet clear whether single activation of specific nAChR subtypes provide optimal efficacy in AD (*152*). Research also shows that co-activation of α7- and α4β2-nAChRs has substantially greater neuroprotective effects against a ketamine-based model of schizophrenia-like cognitive impairments in rats, when compared to single receptor stimulation (*159*). Moreover, pharmacological inhibition of each α7- or α4β2-nAChR subtype has no effect on working memory in nonhuman primates (*160*). Additionally, both α7-nAChR agonists and positive allosteric modulators have largely failed to demonstrate efficacy in placebo-controlled trials in schizophrenia (*161*). These studies suggest that proper cholinergic modulation in hippocampal functions requires both α7- and

α4β2-nAChRs. Our published works (*64, 65*) and current study further support this idea. Therefore, the idea that selective co-activation of nAChRs in the hippocampus can reverse Aβ effects on AD pathology is a new concept, which may lead to innovative and novel therapeutic strategies. In fact, several subtype-specific agonists have been developed for clinical trials, but co-activation of nAChRs has not been applied for clinical trials yet (*152*). The current work thus suggests activation of α7- and α4β2-nAChRs as an innovative and selective way to stimulate hippocampal PV+ and SST+ cells in the hippocampal local circuits, which has potentials for a novel therapeutic strategy in AD.

Aβ is suggested to have profound effects on NMDA and AMPA receptors (NMDARs and AMPARs) via the direct interaction. However, there is insufficient data supporting this idea. First, only immunocytochemistry data supports that Aβ can bind to NMDARs (*162*). There are no confirmed studies demonstrating direct physical binding of Aβ oligomers to AMPAR subunits. Conversely, multiple experimental data using immunocytochemistry (*163*), co-immunoprecipitation (*65, 163*), and a specific and quantitative time-resolved FRET (TR-FRET)-based binding assay (*164*) demonstrate that Aβ binds to nAChRs, particularly the α7- and α4β2-subtypes. In fact, we provide computational and biochemical evidence showing that Aβ directly associates with α7- and α4β2-nAChRs (*65*). Second, it is known that Aβ affects excitatory and inhibitory neurons differently (*35*). Since both excitatory and inhibitory cells express AMPARs and NMDARs, it is unknown how Aβ modifies these receptors to influence excitatory and inhibitory neurons differently. Importantly, we demonstrate that AMPAR dysfunction is downstream of Aβ-induced imbalance of excitation and inhibition by blocking α7- and α4β2-nAChRs in hippocampal neurons (*65*). According to these findings, the effects of Aβ on AMPARs and NMDARs are unlikely to be the main pathogenic mechanism in AD.

Theta oscillations in the hippocampus are generated by cholinergic input from the medial septum (MS) and is highly sensitive to nAChRs. Thus, they can be more responsive to agonist stimulation than other frequencies (*165, 166*). In contrast, the local inhibitory interneuron networks play important roles in both slow and fast gamma oscillations, which makes them less sensitive to cholinergic inputs (*166*). In fact, we find that PNU or RJR treatment reduces theta power but have no major effect on slow and fast gamma powers in WT mice (**Fig. 5a**). This reduction may have been observed due to excessive nAChR activation. Importantly, we do not see this same reduction of theta rhythm in 5XFAD mice because the baseline cholinergic signaling is already impaired, and we are able to see that co-activation of α7 and α4β2 nAChRs is able to restore to the

optimal cholinergic tone. Therefore, agonist treatment likely enhances normal cholinergic activity in the WT hippocampus, resulting in this selective reduction in theta power, whereas local interneuron networks remain stable and resilient apart from this pharmacological activation.

Aβ can inhibit glial nAChRs on astrocytes and microglia rather than neuronal receptors to contribute to AD pathology. Therefore, stimulation of nAChR on glial cells may induce the protective effects. Although roles of astrocytic and microglial nAChRs in AD have not been fully understood to date (*167*), it has been shown that stimulation of astrocytic and microglial α7-nAChRs enhances Aβ phagocytosis in astrocytes and microglia to reduce Aβ levels (*168, 169*). Hippocampal Aβ in AD model mice can thus inhibit glial α7-nAChRs to reduce phagocytic activity in these cells, resulting in an increase in Aβ levels to promote disease progress. nAChR agonist treatment would stimulate glial α7-nAChRs to reduce Aβ levels in the AD hippocampus by enhancing phagocytosis, leading to the protective effects. In addition, activation of astrocytic α7- and α4β2-nAChRs promotes the expression of glial cell-derived neurotrophic factor (GDNF) (*170-172*) that has been shown the protective roles in neurodegenerative disorders characterized mainly by damage of cholinergic neurons, such as AD (*173*). Thus, Aβ can inhibit astrocytic α7- and α4β2-nAChRs to reduce GDNF levels, resulting in the pathology, while activation of these receptors may induce the protective effects by increasing GDNF levels. This is important future research to differentiate between the potential contributions of neuronal and glial nAChRs to AD pathology.

Many α7-nAChR agonists including PNU are known to act as serotonin 5-HT_3 receptor antagonists due to high structural homology between the receptors. However, the previous study has demonstrated that PNU is unable to affect hippocampal network activity in α7-nAChR knockout mice, suggesting that effects of PNU on hippocampal oscillatory activity are exclusively mediated via α7-nAChRs rather than 5-HT_3 receptors (*174*). Therefore, effects of PNU via 5-HT_3 receptor antagonism are unlikely.

Finally, the current work provides an opportunity to revisit the cholinergic hypothesis. Unfortunately, attempts to restore normal cholinergic activity using acetylcholinesterase inhibitors have only been moderately successful. Most of the previous research has focused on single nAChR subtype stimulation or non-selective activation in several brain disorders (*152, 154-157, 159-161*). It is also difficult to identify optimal combinations of nAChR agonists, thus co-activation of selective nAChRs has not been applied for both preclinical studies

and clinical trials yet in AD (*152*). Identifying co-activation of α7- and α4β2-nAChRs as a protective approach on hippocampal functions and memory in AD will thus provide a new perspective on the cholinergic hypothesis.

Materials and Methods

Animals

C57Bl6J (Jax 000664), PV-Cre (Jax 017320), SST-Cre (Jax 018973), B6SJLF1/J (Jax 100012), and 5XFAD (Jax 034840) mice were purchased from Jackson laboratory and bred in the animal facility at Colorado State University (CSU). Clinical studies are observational and limited in the mechanistic information that can be tested in living patients. In contrast, animal studies permit the manipulation of variables and the investigation of effects on an entire organism. The animal model, however, is disadvantaged by species differences. AD is a strictly human disease, and we are aware that rodents do not develop true AD (*175*). Nonetheless, multiple transgenic mouse models develop the pathological hallmarks of the disease as they age, like those found in humans (*175, 176*). We thus employed a widely used amyloid pathology 5XFAD mouse models of AD. 5XFAD mice express human amyloid precursor protein (APP) and human presenilin 1 with the Familial Alzheimer's Disease (FAD) mutations (*71, 177*). Interestingly, biphasic changes in hippocampal circuit excitability are documented along the course of AD, with hyperactivity in the disease's preclinical stages and hypoactivity in its later stages (*178-182*). Importantly, 5XFAD mice show hippocampal hyperexcitability as early as 2.5 months of age (*83*). Additionally, at the age of 5 months, Aβ levels are significantly elevated in 5XFAD mice, which is associated with neuronal dysfunction and memory loss (*71, 117, 183-186*). Moreover, deep proteome profiling of the hippocampus shows no major difference in nAChR expression between 5XFAD mice and wild-type (WT) littermate controls at the age of 5 months (*187*). However, cholinergic neuron loss is found after the age of 9 months in 5XFAD mice (*188, 189*). These findings suggest that in 5-month-old 5XFAD mice, Aβ-induced nAChR dysfunction occurs at the functional levels as opposed to the receptor expression levels. Hippocampal network dysfunction also reported in this model at the age of 3-6 months (*124, 190*). 5-month-old 5XFAD mice are thus the ideal amyloid pathology animal model for the current study. To collect brain tissues from animals, mice were deeply anesthetized and euthanized by CO_2 asphyxiation. Animals were housed under a 12:12 hour light/dark cycle. CSU's Institutional Animal Care and Use Committee (IACUC) reviewed and approved the animal care and protocol (3408). Results were reported following the ARRIVE (Animal Research: Reporting of In Vivo Experiments) guidelines (*191*).

Primary hippocampal neuronal culture

Postnatal day 0 (P0) male and female C57Bl6J, PV-Cre, or SST-Cre pups were used to produce mouse hippocampal neuron cultures as shown previously (*79, 192, 193*). Hippocampi were isolated from P0 mouse brain tissues and digested with 10 U/mL papain (Worthington Biochemical Corp., LK003176). Mouse hippocampal neurons were plated on following poly lysine-coated dishes for glass bottom dishes (500,000 cells) for Ca^{2+} imaging. Neurons were grown in Neurobasal Medium without phenol red (Thermo Fisher Scientific, 12348017) with B27 supplement (Thermo Fisher Scientific, 17504044), 0.5 mM Glutamax (Thermo Fisher Scientific, 35050061), and 1% penicillin/streptomycin (Thermo Fisher Scientific, 15070063). The previous study evaluates maturation, aging, and death of mouse cortical cultured neurons for 60 days *in vitro* (DIV), which demonstrates that synaptogenesis is prominent during the first 15 days and then synaptic markers remained stable through 60 DIV (*194*). In particular, the levels of glutamate receptors increase to a maximum by 10-15 DIV and then remain unchanged through 60 DIV. This indicates that 12-14 DIV neurons that we used here are mature cells, and their maturity is likely comparable to that of older neurons. Additionally, neuronal cultures are shown to contain excitatory and inhibitory cells, cholinergic neurons, as well as glia (*64, 65, 195*).

Reagents

Soluble Aβ42 oligomers (oAβ42) were prepared as previously described (*64, 196*). 1 mg of lyophilized human Aβ42 (Anaspec) was dissolved in 1mL of 1,1,1,3,3,3-hexafluoro-2-propanol (HFIP) (Sigma, St. Louis, MO) to prevent aggregation, portioned into 10 μg aliquots, air-dried and stored at -80 °C. For use in experiments, an aliquot was thawed at room temperature and then dissolved in DMSO to make a 100 μM solution. The solution was incubated for 16 hours at 4°C and then diluted to a final concentration for use in experiments. Scrambled Aβ42 oligomers (sAβ42) were prepared the same way for controls. The following nAChR antagonists were used in this study: α-Bungarotoxin (αBTx) (Alomone labs), an α7 antagonist, Dihydro-β-erythroidine hydrobromide (DHβE) (Tocris Bioscience), an α4β2 antagonist, and α-Conotoxin AuIB (Alomone labs), an α3β4 antagonist. The following nAChR agonists were used in this study: PNU-282987 (PNU) (Tocris Bioscience), an α7 agonist, RJR-2403 Oxalate (RJR) (Tocris Bioscience), an α4β2 agonist, and NS-3861 (NS) (Tocris Bioscience), an α3β4 agonist. Tetrodotoxin (TTX) (Abcam) was used to prevent action potential-dependent spontaneous network activity.

GCaMP Ca^{2+} imaging with nicotine uncaging

For Ca^{2+} imaging with nicotine uncaging, a genetically encoded Ca^{2+} indicator, GCaMP, was used. As the majority of cells in hippocampal cultures are excitatory neurons (*197*), we expressed GCaMP6f (Addgene #40755) (*198*) under the control of the CMV promoter by transfection for imaging excitatory cells, and GCaMP6f under the control of the GABAergic neuron-specific enhancer of the mouse *Dlx* (mDlx) gene (Addgene #83899) (*199*) was transfected for imaging inhibitory interneurons as shown previously (*64*). Glass-bottom dishes were mounted on a temperature-controlled stage on an Olympus IX73 microscope and maintained at 37°C and 5% CO_2 using a Tokai-Hit heating stage and digital temperature and humidity controller. For nicotine uncaging, 1 μM photoactivatable nicotine (PA-Nic) (Tocris Bioscience) was added to the culture media, and epi-illumination photolysis (390 nm, 0.12 mW/mm^2, 1 sec) was used as shown previously (*72*). TTX (1 μM) was added in culture media to prevent action potential-dependent spontaneous network activity. A baseline average (F_0) of 20 frames (50 ms exposure) were captured in the soma prior to nicotine uncaging, and 50 more frames (50 ms exposure) were obtained after photostimulation. The fractional change in fluorescence intensity relative to baseline ($\Delta F/F_0$) was calculated. For **Fig. 1a**, the average peak amplitude in excitatory cells (EX) was used to normalize the peak amplitude in each cell and was compared to the inhibitory cells' average (IN). For **Fig. 1b and 1c**, the images were captured right after each antagonist was added to the media. The average peak amplitude in the control group without drug treatment (CTRL) was used to normalize the peak amplitude in each cell, and the control group's average peak amplitude was compared to the experimental groups' average. For **Fig. 1d and 1e**, PV-Cre and SST-Cre mice were used to culture hippocampal neurons. We infected 4 DIV neurons prepared from PV-Cre or SST-Cre mice with adeno-associated virus (AAV) expressing Cre-dependent GCaMP7s (Addgene# 104495-AAV1) - pGP-AAV-CAG-FLEX-jGCaMP7s-WPRE was a gift from Douglas Kim & GENIE Project (Addgene plasmid #104495; http://n2t.net/addgene:104495 ; RRID:Addgene_104495) (*200*) to determine nicotinic cholinergic activity in PV+ and SST+ cells using nicotine uncaging. For GCaMP7s, the images were captured right after each antagonist was added to the media. A baseline average (F_0) of 20 frames (5 ms exposure) were captured prior to nicotine uncaging, and 100 more frames (5 ms exposure) were obtained after photolysis. The average peak amplitude in the control group (CTRL) was used to normalize the peak amplitude in each cell, and the control

group's average peak amplitude was compared to the experimental groups' average. For Fig. 2, PV-Cre and SST-Cre mice were also used to culture hippocampal neurons. For **Fig 2a and 2b**, Ca^{2+} imaging with nicotine uncaging was conducted as described in **Fig. 1d and 1e**. The images were captured right after 250 nM sAβ42 or 250 nM oAβ42 was added to the media. The average peak amplitude in sAβ42-treated cells was used to normalize the peak amplitude in each cell, and the sAβ42 group's average peak amplitude was compared to the oAβ42-treated cells' average.

GCaMP Ca^{2+} imaging

We measured spontaneous Ca^{2+} activity in cultured hippocampal excitatory neurons because It has been shown that networks of neurons in culture can produce spontaneous synchronized activity (*201*). In fact, network activity emerges at 3-7 DIV independent of either ongoing excitatory or inhibitory synaptic activity and matures over the following several weeks in cultures (*201*). Therefore, the somatic Ca^{2+} signals we observed are from the spontaneous network activity in cultured cells. To do this, we used AAV to express Cre-dependent GCaMP7s (Addgene# 104495-AAV1) (*200*) in cells prepared from PV-Cre or SST-Cre mice. We then measured Ca^{2+} activity in the soma of 14 DIV cultured hippocampal excitatory neurons with a modification of the previously described method (*64, 65, 79, 80, 202-204*). For GCaMP7s, the images were captured right after 250 nM sAβ42 or 250 nM oAβ42 was added to the media in the presence or absence of each agonist. A 10 ms exposure time and a total of 100 images were obtained with a one-second interval. F_{min} was determined as the minimum fluorescence value during the imaging. Total Ca^{2+} activity was obtained by 100 values of $\Delta F/F_{min} = (F_t - F_{min}) / F_{min}$ in each image, and values of $\Delta F/F_{min} < 0.1$ were rejected due to potential photobleaching. The average total Ca^{2+} activity in the control group (CTRL) was used to normalize total Ca^{2+} activity in each cell. The control group's average total Ca^{2+} activity was compared to the experimental groups' average as described previously (*64, 65, 79, 202-204*).

***In vivo* activation of nAChRs**

For *in vivo* activation of nAChRs, we used PNU-282987 (PNU), an α7-nAChR agonist, and RJR-2403 Oxalate (RJR), an α4β2-nAChR agonist. These agonists have a number of advantages that can be used to test our hypothesis; 1) they are blood-brain barrier (BBB) permeable (*156-158, 205, 206*), 2) they do not

require endogenous acetylcholine to stimulate receptors since they are direct agonists rather than positive allosteric modulators (*156, 157, 205, 207-210*), and 3) repeated injection of these agonists is sufficient to show receptor activation in the rodent brains without causing receptor desensitization (*208, 209, 211-213*). PNU and RJR were prepared at concentrations of 1 mg/ml and intraperitoneally injected into 5-month-old 5XFAD and WT female and male mice at a dose of 5 mg/kg by themselves or together once per day for 7 days, a condition that is sufficient to stimulate each nAChR subtype *in vivo* (*156-158, 205*). Saline was given to mice as a control.

Immunohistochemistry

c-Fos labeling was used to measure cell-type specific neuronal activity as shown previously (*214, 215*) because this provides activity patterns across multiple cell types simultaneously. We conducted immunohistochemistry with 5-month-old 5XFAD mice and WT littermates. Brain tissues were isolated and sectioned at 40 μm by using a vibratome. 10 consecutive sections containing the hippocampus (from Bregma: -1.64mm) in each mouse were stained with anti-PV, anti-SST, and anti-c-Fos antibodies. Nuclei were also labeled with DAPI as shown previously (*214, 215*). We imaged these sections using Olympus inverted microscope IX73 with the CellSens software. The colocalization analysis function in the CellSens program was utilized to identify c-Fos-positive (c-Fos+) signals on DAPI-positive (DAPI+) cells but PV and SST-negative cells as the activity of pyramidal cells. Similarly, we measured interneurons' activity by identifying c-Fos+ signals on PV+ or SST+ cells. The total number of c-Fos+ cells on each neuronal subtype in the hippocampus was counted using the particle analysis function in ImageJ (threshold = 100 μm^2). In addition, we measured the size of the hippocampus using ImageJ and normalize the total number of c-Fos+ cells on each neuronal subtype per 5.0 X 10^6 μm^2. As no overt hippocampal neuron loss is found by 12-month-old 5XFAD mice (*216*), cell-type specific neuronal activity was measured as an average of the total number of c-Fos+ cells on each cell subtype/5.0 X 10^6 μm^2 from each section. The average counts per section across all experimental conditions were then compared because multiple immunostainings were performed on the same anatomical sections, analyses were conducted at the section level to assess within-section differences in marker-defined cell populations.

Stereotaxic surgery

5-month-old mice were anaesthetized with an intraperitoneal injection of a mixture of ketamine (100 mg/kg) and xylazine (10 mg/kg) and placed in a stereotactic frame. The target craniotomy site for local field potential (LFP) recordings was marked on the skull, and electrodes were implanted bilaterally into the dorsal hippocampal CA1 area (Bregma coordinates: AP: −1.95 mm, ML: ± 1.12 mm, DV: −1.20 mm). One small screw for the ground anchored at the anterior edges of the surgical site and a wire for a reference in the posterior part of the craniotomy site were bound with dental cement (GC America) to secure the implant in place. The electrodes were constructed by twisting 16 Formvar-insulated NiCh wires (75 μm, California Fine Wire) and attached to a Mill-Max connector. After surgery, animals' health was closely monitored as described in our approved IACUC protocol.

Hippocampal LFP recording

We conducted contextual fear conditioning one week after the surgery as a learning and memory paradigm. Basal LFPs were recorded before learning for one hour (**Fig. 4a**). According to a large body of studies, consolidation of hippocampus-dependent fear memory occurs between 1 and 3 hours after training (*104, 105*). Therefore, after fear learning, test animals were returned to their home cage for 90 minutes, and then we recorded hippocampal LFPs for one hour, a time for fear memory consolidation (**Fig. 4a**). LFP data were collected through electrodes which connect to a 16-channel head-stage (Intan Technologies) that digitizes the raw analog LFP signals via an onboard analog-to-digital converter. We used the Open Ephys Acquisition Board (*217*) to acquire the digitized signal at 2 kHz. The electrode locations were verified histologically at the end of recordings (**Fig. 4b**). If the electrode was placed outside the CA1 area, the animal was excluded in analysis.

LFP data analysis

LFP data were analyzed in MATLAB (The Mathworks Inc.). The data were formatted for importation into the Brainstorm platform (*218*). Recorded traces were downsampled to 2 kHz and then bandpass filtered between 0.1 and 500 Hz (**Fig. 4c**). We applied a notch filter at 60 Hz to reduce powerline artifacts. Power spectral density was calculated using Welch's method in the Brainstorm platform (*218*), which involves segmenting the signals and applies a Fast Fourier Transform (FFT) algorithm to each segment before

averaging the power spectra (**Fig. 4d**). The power spectra were then processed by averaging frequency bins into larger predefined bands, including theta (4-8 Hz), slow gamma (30-50 Hz), and fast gamma (50-100 Hz). The power of each frequency band was normalized to WT controls and then compared before and after fear conditioning in WT and 5XFAD mice. We also compared the powers in each condition between WT and 5XFAD mice following learning. LFP power was quantified for each electrode and frequency band because multiple electrodes were obtained from the same animal. For theta-gamma phase amplitude coupling (PAC) analysis, we measured the high-frequency bands modulated by theta bands in epochs with a matched, filtered LFP amplitude envelope. Data were filtered into theta, slow gamma, and fast gamma using a zero-phase FIR filter implemented with the eegfilt function in the EEGLAB toolbox for MATLAB (*219*). The analytic signal for each was computed using the Hilbert Transform (MATLAB function hilbert.m), resulting in instantaneous theta phase and gamma band amplitude. The peaks of the gamma-band amplitudes were defined as local maxima at or exceeding the mean + 1 standard deviation (SD) of the baseline gamma-band amplitude from the Hilbert Transform envelopes. The instantaneous theta phase for each peak was extracted. The mean vector length (MVL) was calculated as an entrainment strength. We compared the MVL before and after fear conditioning. The MVL in each condition was also compared in WT and 5XFAD mice following fear learning.

Contextual fear conditioning (CFC)

Contextual fear conditioning (Habitest Modular System, Coulbourn Instrument) was carried out as described previously (*118, 119*). In Day 1 (encoding), the test mouse was placed in a novel rectangular chamber with a grid floor. After a 3-min baseline period, the test animal was given one shock (a 2 sec, 0.5 mA shock) and stayed in the chamber for an additional 1 min after the shock before being returned to the home cage for overnight (consolidation). A contextual memory test was conducted the next day (Day 2 - retrieval) in the same conditioning chamber for 3 min. Fear memory was determined by measuring the percentage of the freezing response (immobility excluding respiration and heartbeat) using an automated tracking program (FreezeFrame).

Amyloid plaque analysis

10 hippocampal sections (from Bregma: -1.64mm) in each mouse were obtained and stained with 1%

Thioflavin S. Amyloid plaques were identified as Thioflavin S-positive puncta. The total number of amyloid plaques in the hippocampus was counted using the particle analysis function in ImageJ (threshold = 10 μm^2). We also measured the size of the hippocampus using ImageJ and normalized these measurements per 1 mm^2. Amyloid plaques were measured as an average of these measurements per 1 mm^2 from 10 sections (total 20 hemisphere/animal). The average counts per animal across all experimental conditions were then compared between the conditions.

Statistical analysis

The Franklin A. Graybill Statistical Laboratory at CSU was consulted for statistical analysis in the current study, including sample size determination, randomization, experiment conception and design, data analysis, and interpretation. We used the GraphPad Prism 10 software to determine statistical significance (set at $p < 0.05$). Grouped results of single comparisons were tested for normality with the Shapiro-Wilk normality or Kolmogorov-Smirnov test and analyzed using an unpaired or paired two-tailed Student's t-test when data are normally distributed. Differences between multiple groups were assessed by N-way analysis of variance (ANOVA) with the Tukey test or Šídák's test. Statistical analyses for LFP and immunostaining data were performed using mixed-effects models / repeated-measures ANOVA with Tukey test, and animal identity included as a random effect. Electrodes and sections in LFP and c-Fos analysis, respectively, were treated as repeated measures nested within animals, and animal identity was included as a random effect. This approach accounts for the nested structure of the data, avoids pseudoreplication, and accommodates unequal electrode counts across animals. The graphs were presented as mean ± Standard Deviation (SD).

References

1. W. Wong, Economic burden of Alzheimer disease and managed care considerations. *Am J Manag Care* **26**, S177-S183 (2020).
2. D. M. Walsh, D. J. Selkoe, Amyloid beta-protein and beyond: the path forward in Alzheimer's disease. *Curr Opin Neurobiol* **61**, 116-124 (2020).
3. H. Targa Dias Anastacio, N. Matosin, L. Ooi, Neuronal hyperexcitability in Alzheimer's disease: what are the drivers behind this aberrant phenotype? *Transl Psychiatry* **12**, 257 (2022).
4. J. R. Cirrito, K. A. Yamada, M. B. Finn, R. S. Sloviter, K. R. Bales, P. C. May, D. D. Schoepp, S. M. Paul, S. Mennerick, D. M. Holtzman, Synaptic activity regulates interstitial fluid amyloid-beta levels in vivo. *Neuron* **48**, 913-922 (2005).
5. K. Yamamoto, Z. I. Tanei, T. Hashimoto, T. Wakabayashi, H. Okuno, Y. Naka, O. Yizhar, L. E. Fenno, M. Fukayama, H. Bito, J. R. Cirrito, D. M. Holtzman, K. Deisseroth, T. Iwatsubo, Chronic optogenetic activation augments abeta pathology in a mouse model of Alzheimer disease. *Cell Rep* **11**, 859-865 (2015).
6. A. M. Pooler, E. C. Phillips, D. H. Lau, W. Noble, D. P. Hanger, Physiological release of endogenous tau is stimulated by neuronal activity. *EMBO Rep* **14**, 389-394 (2013).
7. J. W. Wu, S. A. Hussaini, I. M. Bastille, G. A. Rodriguez, A. Mrejeru, K. Rilett, D. W. Sanders, C. Cook, H. Fu, R. A. Boonen, M. Herman, E. Nahmani, S. Emrani, Y. H. Figueroa, M. I. Diamond, C. L. Clelland, S. Wray, K. E. Duff, Neuronal activity enhances tau propagation and tau pathology in vivo. *Nat Neurosci* **19**, 1085-1092 (2016).
8. P. Yuan, J. Grutzendler, Attenuation of beta-Amyloid Deposition and Neurotoxicity by Chemogenetic Modulation of Neural Activity. *J Neurosci* **36**, 632-641 (2016).
9. K. A. Vossel, K. G. Ranasinghe, A. J. Beagle, D. Mizuiri, S. M. Honma, A. F. Dowling, S. M. Darwish, V. Van Berlo, D. E. Barnes, M. Mantle, A. M. Karydas, G. Coppola, E. D. Roberson, B. L. Miller, P. A. Garcia, H. E. Kirsch, L. Mucke, S. S. Nagarajan, Incidence and impact of subclinical epileptiform activity in Alzheimer's disease. *Ann Neurol* **80**, 858-870 (2016).

10. C. R. Mondadori, A. Buchmann, H. Mustovic, C. F. Schmidt, P. Boesiger, R. M. Nitsch, C. Hock, J. Streffer, K. Henke, Enhanced brain activity may precede the diagnosis of Alzheimer's disease by 30 years. *Brain : a journal of neurology* **129**, 2908-2922 (2006).

11. P. E. Sanchez, L. Zhu, L. Verret, K. A. Vossel, A. G. Orr, J. R. Cirrito, N. Devidze, K. Ho, G. Q. Yu, J. J. Palop, L. Mucke, Levetiracetam suppresses neuronal network dysfunction and reverses synaptic and cognitive deficits in an Alzheimer's disease model. *Proc Natl Acad Sci U S A* **109**, E2895-2903 (2012).

12. J. Q. Shi, B. R. Wang, Y. Y. Tian, J. Xu, L. Gao, S. L. Zhao, T. Jiang, H. G. Xie, Y. D. Zhang, Antiepileptics topiramate and levetiracetam alleviate behavioral deficits and reduce neuropathology in APPswe/PS1dE9 transgenic mice. *CNS Neurosci Ther* **19**, 871-881 (2013).

13. X. Y. Zheng, H. C. Zhang, Y. D. Lv, F. Y. Jin, X. J. Wu, J. Zhu, Y. Ruan, Levetiracetam alleviates cognitive decline in Alzheimer's disease animal model by ameliorating the dysfunction of the neuronal network. *Frontiers in aging neuroscience* **14**, 888784 (2022).

14. A. Bakker, G. L. Krauss, M. S. Albert, C. L. Speck, L. R. Jones, C. E. Stark, M. A. Yassa, S. S. Bassett, A. L. Shelton, M. Gallagher, Reduction of hippocampal hyperactivity improves cognition in amnestic mild cognitive impairment. *Neuron* **74**, 467-474 (2012).

15. K. Vossel, K. G. Ranasinghe, A. J. Beagle, A. La, K. Ah Pook, M. Castro, D. Mizuiri, S. M. Honma, N. Venkateswaran, M. Koestler, W. Zhang, L. Mucke, M. J. Howell, K. L. Possin, J. H. Kramer, A. L. Boxer, B. L. Miller, S. S. Nagarajan, H. E. Kirsch, Effect of Levetiracetam on Cognition in Patients With Alzheimer Disease With and Without Epileptiform Activity: A Randomized Clinical Trial. *JAMA Neurol* **78**, 1345-1354 (2021).

16. E. N. Cline, M. A. Bicca, K. L. Viola, W. L. Klein, The Amyloid-beta Oligomer Hypothesis: Beginning of the Third Decade. *Journal of Alzheimer's disease : JAD* **64**, S567-S610 (2018).

17. T. Guo, D. Korman, S. L. Baker, S. M. Landau, W. J. Jagust, I. Alzheimer's Disease Neuroimaging, Longitudinal Cognitive and Biomarker Measurements Support a Unidirectional Pathway in Alzheimer's Disease Pathophysiology. *Biological psychiatry* **89**, 786-794 (2021).

18. C. R. Jack, Jr., D. A. Bennett, K. Blennow, M. C. Carrillo, B. Dunn, S. B. Haeberlein, D. M. Holtzman, W. Jagust, F. Jessen, J. Karlawish, E. Liu, J. L. Molinuevo, T. Montine, C. Phelps, K. P. Rankin, C. C.

Rowe, P. Scheltens, E. Siemers, H. M. Snyder, R. Sperling, Contributors, NIA-AA Research Framework: Toward a biological definition of Alzheimer's disease. *Alzheimers Dement* **14**, 535-562 (2018).

19. S. Budd Haeberlein, P. S. Aisen, F. Barkhof, S. Chalkias, T. Chen, S. Cohen, G. Dent, O. Hansson, K. Harrison, C. von Hehn, T. Iwatsubo, C. Mallinckrodt, C. J. Mummery, K. K. Muralidharan, I. Nestorov, L. Nisenbaum, R. Rajagovindan, L. Skordos, Y. Tian, C. H. van Dyck, B. Vellas, S. Wu, Y. Zhu, A. Sandrock, Two Randomized Phase 3 Studies of Aducanumab in Early Alzheimer's Disease. *J Prev Alzheimers Dis* **9**, 197-210 (2022).
20. C. H. van Dyck, C. J. Swanson, P. Aisen, R. J. Bateman, C. Chen, M. Gee, M. Kanekiyo, D. Li, L. Reyderman, S. Cohen, L. Froelich, S. Katayama, M. Sabbagh, B. Vellas, D. Watson, S. Dhadda, M. Irizarry, L. D. Kramer, T. Iwatsubo, Lecanemab in Early Alzheimer's Disease. *N Engl J Med* **388**, 9-21 (2023).
21. M. P. Cadiz, K. A. Gibson, K. T. Todd, D. G. Nascari, N. Massa, M. T. Lilley, K. C. Olney, M. M. Al-Amin, H. Jiang, D. M. Holtzman, J. D. Fryer, Aducanumab anti-amyloid immunotherapy induces sustained microglial and immune alterations. *J Exp Med* **221**, (2024).
22. M. H. Ebell, H. C. Barry, K. Baduni, G. Grasso, Clinically Important Benefits and Harms of Monoclonal Antibodies Targeting Amyloid for the Treatment of Alzheimer Disease: A Systematic Review and Meta-Analysis. *Ann Fam Med* **22**, 50-62 (2024).
23. E. Fedele, Anti-Amyloid Therapies for Alzheimer's Disease and the Amyloid Cascade Hypothesis. *Int J Mol Sci* **24**, (2023).
24. M. Kurkinen, Lecanemab (Leqembi) is not the right drug for patients with Alzheimer's disease. *Adv Clin Exp Med* **32**, 943-947 (2023).
25. S. J. Loomis, R. Miller, C. Castrillo-Viguera, K. Umans, W. Cheng, J. O'Gorman, R. Hughes, S. Budd Haeberlein, C. D. Whelan, Genome-Wide Association Studies of ARIA From the Aducanumab Phase 3 ENGAGE and EMERGE Studies. *Neurology* **102**, e207919 (2024).
26. E. Solopova, W. Romero-Fernandez, H. Harmsen, L. Ventura-Antunes, E. Wang, A. Shostak, J. Maldonado, M. J. Donahue, D. Schultz, T. M. Coyne, A. Charidimou, M. Schrag, Fatal iatrogenic cerebral beta-amyloid-related arteritis in a woman treated with lecanemab for Alzheimer's disease. *Nat Commun* **14**, 8220 (2023).

27. J. Hardy, D. J. Selkoe, The amyloid hypothesis of Alzheimer's disease: progress and problems on the road to therapeutics. *Science* **297**, 353-356 (2002).

28. M. A. Busche, G. Eichhoff, H. Adelsberger, D. Abramowski, K. H. Wiederhold, C. Haass, M. Staufenbiel, A. Konnerth, O. Garaschuk, Clusters of hyperactive neurons near amyloid plaques in a mouse model of Alzheimer's disease. *Science* **321**, 1686-1689 (2008).

29. M. A. Busche, X. Chen, H. A. Henning, J. Reichwald, M. Staufenbiel, B. Sakmann, A. Konnerth, Critical role of soluble amyloid-beta for early hippocampal hyperactivity in a mouse model of Alzheimer's disease. *Proc Natl Acad Sci U S A* **109**, 8740-8745 (2012).

30. B. T. Hyman, J. Q. Trojanowski, Consensus recommendations for the postmortem diagnosis of Alzheimer disease from the National Institute on Aging and the Reagan Institute Working Group on diagnostic criteria for the neuropathological assessment of Alzheimer disease. *J Neuropathol Exp Neurol* **56**, 1095-1097 (1997).

31. T. F. Freund, G. Buzsaki, Interneurons of the hippocampus. *Hippocampus* **6**, 347-470 (1996).

32. K. A. Pelkey, R. Chittajallu, M. T. Craig, L. Tricoire, J. C. Wester, C. J. McBain, Hippocampal GABAergic Inhibitory Interneurons. *Physiological reviews* **97**, 1619-1747 (2017).

33. J. J. Palop, L. Mucke, Amyloid-beta-induced neuronal dysfunction in Alzheimer's disease: from synapses toward neural networks. *Nat Neurosci* **13**, 812-818 (2010).

34. S. F. Kazim, J. H. Seo, R. Bianchi, C. S. Larson, A. Sharma, R. K. S. Wong, K. Y. Gorbachev, A. C. Pereira, Neuronal Network Excitability in Alzheimer's Disease: The Puzzle of Similar versus Divergent Roles of Amyloid beta and Tau. *eNeuro* **8**, (2021).

35. J. J. Palop, L. Mucke, Network abnormalities and interneuron dysfunction in Alzheimer disease. *Nat Rev Neurosci* **17**, 777-792 (2016).

36. S. Q. Ren, W. Yao, J. Z. Yan, C. Jin, J. J. Yin, J. Yuan, S. Yu, Z. Cheng, Amyloid beta causes excitation/inhibition imbalance through dopamine receptor 1-dependent disruption of fast-spiking GABAergic input in anterior cingulate cortex. *Sci Rep* **8**, 302 (2018).

37. A. Caccavano, P. L. Bozzelli, P. A. Forcelli, D. T. S. Pak, J. Y. Wu, K. Conant, S. Vicini, Inhibitory Parvalbumin Basket Cell Activity is Selectively Reduced during Hippocampal Sharp Wave Ripples in a Mouse Model of Familial Alzheimer's Disease. *J Neurosci* **40**, 5116-5136 (2020).

38. Y. Xu, M. Zhao, Y. Han, H. Zhang, GABAergic Inhibitory Interneuron Deficits in Alzheimer's Disease: Implications for Treatment. *Front Neurosci* **14**, 660 (2020).

39. D. Ji, R. Lape, J. A. Dani, Timing and location of nicotinic activity enhances or depresses hippocampal synaptic plasticity. *Neuron* **31**, 131-141 (2001).

40. C. J. Frazier, Y. D. Rollins, C. R. Breese, S. Leonard, R. Freedman, T. V. Dunwiddie, Acetylcholine activates an alpha-bungarotoxin-sensitive nicotinic current in rat hippocampal interneurons, but not pyramidal cells. *J Neurosci* **18**, 1187-1195 (1998).

41. S. Hefft, S. Hulo, D. Bertrand, D. Muller, Synaptic transmission at nicotinic acetylcholine receptors in rat hippocampal organotypic cultures and slices. *The Journal of physiology* **515 (Pt 3)**, 769-776 (1999).

42. S. Jones, J. L. Yakel, Functional nicotinic ACh receptors on interneurones in the rat hippocampus. *The Journal of physiology* **504 (Pt 3)**, 603-610 (1997).

43. A. R. McQuiston, D. V. Madison, Nicotinic receptor activation excites distinct subtypes of interneurons in the rat hippocampus. *J Neurosci* **19**, 2887-2896 (1999).

44. D. Ji, J. A. Dani, Inhibition and disinhibition of pyramidal neurons by activation of nicotinic receptors on hippocampal interneurons. *Journal of neurophysiology* **83**, 2682-2690 (2000).

45. A. Nordberg, Nicotinic receptor abnormalities of Alzheimer's disease: therapeutic implications. *Biological psychiatry* **49**, 200-210 (2001).

46. A. Kadir, O. Almkvist, A. Wall, B. Langstrom, A. Nordberg, PET imaging of cortical 11C-nicotine binding correlates with the cognitive function of attention in Alzheimer's disease. *Psychopharmacology* **188**, 509-520 (2006).

47. T. H. Ferreira-Vieira, I. M. Guimaraes, F. R. Silva, F. M. Ribeiro, Alzheimer's disease: Targeting the Cholinergic System. *Current neuropharmacology* **14**, 101-115 (2016).

48. A. Pensalfini, S. Kim, S. Subbanna, C. Bleiwas, C. N. Goulbourne, P. H. Stavrides, Y. Jiang, J. H. Lee, S. Darji, M. Pawlik, C. Huo, J. Peddy, M. J. Berg, J. F. Smiley, B. S. Basavarajappa, R. A. Nixon, Endosomal Dysfunction Induced by Directly Overactivating Rab5 Recapitulates Prodromal and Neurodegenerative Features of Alzheimer's Disease. *Cell Rep* **33**, 108420 (2020).

49. J. J. Alam, R. A. Nixon, Disease-modifying pharmacological approaches to correcting basal forebrain cholinergic neuronal (BFCN) dysfunction and degeneration. *Neuropsychopharmacology : official publication of the American College of Neuropsychopharmacology*, (2021).

50. Y. Jiang, A. Rigoglioso, C. M. Peterhoff, M. Pawlik, Y. Sato, C. Bleiwas, P. Stavrides, J. F. Smiley, S. D. Ginsberg, P. M. Mathews, E. Levy, R. A. Nixon, Partial BACE1 reduction in a Down syndrome mouse model blocks Alzheimer-related endosomal anomalies and cholinergic neurodegeneration: role of APP-CTF. *Neurobiol Aging* **39**, 90-98 (2016).

51. Y. Chen, V. V. Dyakin, C. A. Branch, B. Ardekani, D. Yang, D. N. Guilfoyle, J. Peterson, C. Peterhoff, S. D. Ginsberg, A. M. Cataldo, R. A. Nixon, In vivo MRI identifies cholinergic circuitry deficits in a Down syndrome model. *Neurobiol Aging* **30**, 1453-1465 (2009).

52. S. D. Ginsberg, E. J. Mufson, M. J. Alldred, S. E. Counts, J. Wuu, R. A. Nixon, S. Che, Upregulation of select rab GTPases in cholinergic basal forebrain neurons in mild cognitive impairment and Alzheimer's disease. *J Chem Neuroanat* **42**, 102-110 (2011).

53. S. Jurgensen, S. T. Ferreira, Nicotinic receptors, amyloid-beta, and synaptic failure in Alzheimer's disease. *J Mol Neurosci* **40**, 221-229 (2010).

54. Q. Liu, H. Kawai, D. K. Berg, beta -Amyloid peptide blocks the response of alpha 7-containing nicotinic receptors on hippocampal neurons. *Proc Natl Acad Sci U S A* **98**, 4734-4739 (2001).

55. D. L. Pettit, Z. Shao, J. L. Yakel, beta-Amyloid(1-42) peptide directly modulates nicotinic receptors in the rat hippocampal slice. *J Neurosci* **21**, RC120 (2001).

56. L. Pym, M. Kemp, V. Raymond-Delpech, S. Buckingham, C. A. Boyd, D. Sattelle, Subtype-specific actions of beta-amyloid peptides on recombinant human neuronal nicotinic acetylcholine receptors (alpha7, alpha4beta2, alpha3beta4) expressed in Xenopus laevis oocytes. *British journal of pharmacology* **146**, 964-971 (2005).

57. A. A. George, J. M. Vieira, C. Xavier-Jackson, M. T. Gee, J. R. Cirrito, H. A. Bimonte-Nelson, M. R. Picciotto, R. J. Lukas, P. Whiteaker, Implications of Oligomeric Amyloid-Beta (oAbeta(42)) Signaling through alpha7beta2-Nicotinic Acetylcholine Receptors (nAChRs) on Basal Forebrain Cholinergic Neuronal Intrinsic Excitability and Cognitive Decline. *J Neurosci* **41**, 555-575 (2021).

58. A. Akaike, Y. Izumi, "Overview" in *Nicotinic Acetylcholine Receptor Signaling in Neuroprotection,* A. Akaike, S. Shimohama, Y. Misu, Eds. (Singapore, 2018), pp. 1-15.

59. S. Thompson, K. L. Lanctot, N. Herrmann, The benefits and risks associated with cholinesterase inhibitor therapy in Alzheimer's disease. *Expert Opin Drug Saf* **3**, 425-440 (2004).

60. F. Mangialasche, A. Solomon, B. Winblad, P. Mecocci, M. Kivipelto, Alzheimer's disease: clinical trials and drug development. *Lancet Neurol* **9**, 702-716 (2010).

61. E. X. Albuquerque, E. F. Pereira, M. Alkondon, S. W. Rogers, Mammalian nicotinic acetylcholine receptors: from structure to function. *Physiological reviews* **89**, 73-120 (2009).

62. J. M. Lindstrom, Nicotinic acetylcholine receptors of muscles and nerves: comparison of their structures, functional roles, and vulnerability to pathology. *Annals of the New York Academy of Sciences* **998**, 41-52 (2003).

63. F. Clementi, D. Fornasari, C. Gotti, Neuronal nicotinic receptors, important new players in brain function. *European journal of pharmacology* **393**, 3-10 (2000).

64. J. L. Sun, S. A. Stokoe, J. P. Roberts, M. F. Sathler, K. A. Nip, J. Shou, K. Ko, S. Tsunoda, S. Kim, Co-activation of selective nicotinic acetylcholine receptors is required to reverse beta amyloid-induced Ca(2+) hyperexcitation. *Neurobiol Aging* **84**, 166-177 (2019).

65. J. P. Roberts, S. A. Stokoe, M. F. Sathler, R. A. Nichols, S. Kim, Selective co-activation of alpha7- and alpha4beta2-nicotinic acetylcholine receptors reverses beta-amyloid-induced synaptic dysfunction. *The Journal of biological chemistry*, 100402 (2021).

66. F. Grassi, E. Palma, R. Tonini, M. Amici, M. Ballivet, F. Eusebi, Amyloid beta(1-42) peptide alters the gating of human and mouse alpha-bungarotoxin-sensitive nicotinic receptors. *The Journal of physiology* **547**, 147-157 (2003).

67. J. Wu, Y. P. Kuo, A. A. George, L. Xu, J. Hu, R. J. Lukas, beta-Amyloid directly inhibits human alpha4beta2-nicotinic acetylcholine receptors heterologously expressed in human SH-EP1 cells. *The Journal of biological chemistry* **279**, 37842-37851 (2004).

68. M. H. Magdesian, A. A. Nery, A. H. Martins, M. A. Juliano, L. Juliano, H. Ulrich, S. T. Ferreira, Peptide blockers of the inhibition of neuronal nicotinic acetylcholine receptors by amyloid beta. *The Journal of biological chemistry* **280**, 31085-31090 (2005).

69. G. Olivero, M. Grilli, J. Chen, S. Preda, E. Mura, S. Govoni, M. Marchi, Effects of soluble beta-amyloid on the release of neurotransmitters from rat brain synaptosomes. *Frontiers in aging neuroscience* **6**, 166 (2014).

70. Z. Z. Guan, X. Zhang, R. Ravid, A. Nordberg, Decreased protein levels of nicotinic receptor subunits in the hippocampus and temporal cortex of patients with Alzheimer's disease. *Journal of neurochemistry* **74**, 237-243 (2000).

71. H. Oakley, S. L. Cole, S. Logan, E. Maus, P. Shao, J. Craft, A. Guillozet-Bongaarts, M. Ohno, J. Disterhoft, L. Van Eldik, R. Berry, R. Vassar, Intraneuronal beta-amyloid aggregates, neurodegeneration, and neuron loss in transgenic mice with five familial Alzheimer's disease mutations: potential factors in amyloid plaque formation. *J Neurosci* **26**, 10129-10140 (2006).

72. S. Banala, M. C. Arvin, N. M. Bannon, X. T. Jin, J. J. Macklin, Y. Wang, C. Peng, G. Zhao, J. J. Marshall, K. R. Gee, D. L. Wokosin, V. J. Kim, J. M. McIntosh, A. Contractor, H. A. Lester, Y. Kozorovitskiy, R. M. Drenan, L. D. Lavis, Photoactivatable drugs for nicotinic optopharmacology. *Nature methods* **15**, 347-350 (2018).

73. K. A. Radcliffe, J. A. Dani, Nicotinic stimulation produces multiple forms of increased glutamatergic synaptic transmission. *J Neurosci* **18**, 7075-7083 (1998).

74. M. Alkondon, E. F. Pereira, H. M. Eisenberg, E. X. Albuquerque, Choline and selective antagonists identify two subtypes of nicotinic acetylcholine receptors that modulate GABA release from CA1 interneurons in rat hippocampal slices. *J Neurosci* **19**, 2693-2705 (1999).

75. M. Alkondon, E. X. Albuquerque, Nicotinic acetylcholine receptor alpha7 and alpha4beta2 subtypes differentially control GABAergic input to CA1 neurons in rat hippocampus. *Journal of neurophysiology* **86**, 3043-3055 (2001).

76. L. Maggi, E. Sher, E. Cherubini, Regulation of GABA release by nicotinic acetylcholine receptors in the neonatal rat hippocampus. *The Journal of physiology* **536**, 89-100 (2001).

77. L. T. Huang, J. L. Sherwood, Y. J. Sun, D. Lodge, Y. Wang, Activation of presynaptic alpha7 nicotinic receptors evokes an excitatory response in hippocampal CA3 neurones in anaesthetized rats: an in vivo iontophoretic study. *British journal of pharmacology* **159**, 554-565 (2010).

78. M. Gleichmann, M. P. Mattson, Neuronal calcium homeostasis and dysregulation. *Antioxid Redox Signal* **14**, 1261-1273 (2011).

79. K. Sztukowski, K. Nip, P. N. Ostwald, M. F. Sathler, J. L. Sun, J. Shou, E. T. Jorgensen, T. E. Brown, J. H. Elder, C. Miller, F. Hofmann, S. VandeWoude, S. Kim, HIV induces synaptic hyperexcitation via cGMP-dependent protein kinase II activation in the FIV infection model. *PLoS biology* **16**, e2005315 (2018).

80. A. Zaytseva, E. Bouckova, M. J. Wiles, M. H. Wustrau, I. G. Schmidt, H. Mendez-Vazquez, L. Khatri, S. Kim, Ketamine's rapid antidepressant effects are mediated by Ca(2+)-permeable AMPA receptors. *Elife* **12**, (2023).

81. J. Gallego-Rudolf, A. I. Wiesman, A. Pichet Binette, S. Villeneuve, S. Baillet, P.-A. R. Group, Synergistic association of Abeta and tau pathology with cortical neurophysiology and cognitive decline in asymptomatic older adults. *Nat Neurosci* **27**, 2130-2137 (2024).

82. M. E. Greenberg, E. B. Ziff, Stimulation of 3T3 cells induces transcription of the c-fos proto-oncogene. *Nature* **311**, 433-438 (1984).

83. Y. Li, K. Zhu, N. Li, X. Wang, X. Xiao, L. Li, L. Li, Y. He, J. Zhang, J. Wo, Y. Cui, H. Huang, J. Zhang, W. Wang, X. Wang, Y. Zheng, Reversible GABAergic dysfunction involved in hippocampal hyperactivity predicts early-stage Alzheimer disease in a mouse model. *Alzheimers Res Ther* **13**, 114 (2021).

84. T. Seidenbecher, T. R. Laxmi, O. Stork, H. C. Pape, Amygdalar and hippocampal theta rhythm synchronization during fear memory retrieval. *Science* **301**, 846-850 (2003).

85. R. T. Narayanan, T. Seidenbecher, S. Sangha, O. Stork, H. C. Pape, Theta resynchronization during reconsolidation of remote contextual fear memory. *Neuroreport* **18**, 1107-1111 (2007).

86. H. Markram, J. Lubke, M. Frotscher, B. Sakmann, Regulation of synaptic efficacy by coincidence of postsynaptic APs and EPSPs. *Science* **275**, 213-215 (1997).

87. L. L. Colgin, Rhythms of the hippocampal network. *Nat Rev Neurosci* **17**, 239-249 (2016).

88. E. Duzel, W. D. Penny, N. Burgess, Brain oscillations and memory. *Curr Opin Neurobiol* **20**, 143-149 (2010).

89. N. Filippini, B. J. MacIntosh, M. G. Hough, G. M. Goodwin, G. B. Frisoni, S. M. Smith, P. M. Matthews, C. F. Beckmann, C. E. Mackay, Distinct patterns of brain activity in young carriers of the APOE-epsilon4 allele. *Proc Natl Acad Sci U S A* **106**, 7209-7214 (2009).

90. R. J. Bateman, C. Xiong, T. L. Benzinger, A. M. Fagan, A. Goate, N. C. Fox, D. S. Marcus, N. J. Cairns, X. Xie, T. M. Blazey, D. M. Holtzman, A. Santacruz, V. Buckles, A. Oliver, K. Moulder, P. S. Aisen, B. Ghetti, W. E. Klunk, E. McDade, R. N. Martins, C. L. Masters, R. Mayeux, J. M. Ringman, M. N. Rossor, P. R. Schofield, R. A. Sperling, S. Salloway, J. C. Morris, N. Dominantly Inherited Alzheimer, Clinical and biomarker changes in dominantly inherited Alzheimer's disease. *N Engl J Med* **367**, 795-804 (2012).

91. E. M. Reiman, Y. T. Quiroz, A. S. Fleisher, K. Chen, C. Velez-Pardo, M. Jimenez-Del-Rio, A. M. Fagan, A. R. Shah, S. Alvarez, A. Arbelaez, M. Giraldo, N. Acosta-Baena, R. A. Sperling, B. Dickerson, C. E. Stern, V. Tirado, C. Munoz, R. A. Reiman, M. J. Huentelman, G. E. Alexander, J. B. Langbaum, K. S. Kosik, P. N. Tariot, F. Lopera, Brain imaging and fluid biomarker analysis in young adults at genetic risk for autosomal dominant Alzheimer's disease in the presenilin 1 E280A kindred: a case-control study. *Lancet Neurol* **11**, 1048-1056 (2012).

92. C. S. Herrmann, T. Demiralp, Human EEG gamma oscillations in neuropsychiatric disorders. *Clin Neurophysiol* **116**, 2719-2733 (2005).

93. J. Gallego-Rudolf, A. I. Wiesman, A. Pichet Binette, S. Villeneuve, S. Baillet, P.-A. R. Group, Synergistic association of Abeta and tau pathology with cortical neurophysiology and cognitive decline in asymptomatic older adults. *Nat Neurosci*, (2024).

94. K. W. Bieri, K. N. Bobbitt, L. L. Colgin, Slow and fast gamma rhythms coordinate different spatial coding modes in hippocampal place cells. *Neuron* **82**, 670-681 (2014).

95. B. J. Griffiths, G. Parish, F. Roux, S. Michelmann, M. van der Plas, L. D. Kolibius, R. Chelvarajah, D. T. Rollings, V. Sawlani, H. Hamer, S. Gollwitzer, G. Kreiselmeyer, B. Staresina, M. Wimber, S. Hanslmayr, Directional coupling of slow and fast hippocampal gamma with neocortical alpha/beta oscillations in human episodic memory. *Proc Natl Acad Sci U S A* **116**, 21834-21842 (2019).

96. K. Nakazawa, M. C. Quirk, R. A. Chitwood, M. Watanabe, M. F. Yeckel, L. D. Sun, A. Kato, C. A. Carr, D. Johnston, M. A. Wilson, S. Tonegawa, Requirement for hippocampal CA3 NMDA receptors in associative memory recall. *Science* **297**, 211-218 (2002).

97. H. A. Steffenach, R. S. Sloviter, E. I. Moser, M. B. Moser, Impaired retention of spatial memory after transection of longitudinally oriented axons of hippocampal CA3 pyramidal cells. *Proc Natl Acad Sci U S A* **99**, 3194-3198 (2002).

98. A. Treves, E. T. Rolls, Computational constraints suggest the need for two distinct input systems to the hippocampal CA3 network. *Hippocampus* **2**, 189-199 (1992).

99. A. J. Mably, L. L. Colgin, Gamma oscillations in cognitive disorders. *Curr Opin Neurobiol* **52**, 182-187 (2018).

100. J. I. Rossato, M. C. Gonzalez, A. Radiske, G. Apolinario, S. Conde-Ocazionez, L. R. Bevilaqua, M. Cammarota, PKMzeta Inhibition Disrupts Reconsolidation and Erases Object Recognition Memory. *J Neurosci* **39**, 1828-1841 (2019).

101. C. Zheng, K. W. Bieri, E. Hwaun, L. L. Colgin, Fast Gamma Rhythms in the Hippocampus Promote Encoding of Novel Object-Place Pairings. *eNeuro* **3**, (2016).

102. J. B. Trimper, R. A. Stefanescu, J. R. Manns, Recognition memory and theta-gamma interactions in the hippocampus. *Hippocampus* **24**, 341-353 (2014).

103. B. O. Watson, G. Buzsaki, Sleep, Memory & Brain Rhythms. *Daedalus* **144**, 67-82 (2015).

104. J. L. Kwapis, M. A. Wood, Epigenetic mechanisms in fear conditioning: implications for treating post-traumatic stress disorder. *Trends Neurosci* **37**, 706-720 (2014).

105. R. Bourtchouladze, T. Abel, N. Berman, R. Gordon, K. Lapidus, E. R. Kandel, Different training procedures recruit either one or two critical periods for contextual memory consolidation, each of which requires protein synthesis and PKA. *Learning & memory* **5**, 365-374 (1998).

106. T. Nakazono, H. Jun, M. Blurton-Jones, K. N. Green, K. M. Igarashi, Gamma oscillations in the entorhinal-hippocampal circuit underlying memory and dementia. *Neurosci Res* **129**, 40-46 (2018).

107. N. Axmacher, M. M. Henseler, O. Jensen, I. Weinreich, C. E. Elger, J. Fell, Cross-frequency coupling supports multi-item working memory in the human hippocampus. *Proc Natl Acad Sci U S A* **107**, 3228-3233 (2010).

108. R. Goutagny, N. Gu, C. Cavanagh, J. Jackson, J. G. Chabot, R. Quirion, S. Krantic, S. Williams, Alterations in hippocampal network oscillations and theta-gamma coupling arise before Abeta

overproduction in a mouse model of Alzheimer's disease. *The European journal of neuroscience* **37**, 1896-1902 (2013).

109. J. Daume, J. Kaminski, A. G. P. Schjetnan, Y. Salimpour, U. Khan, M. Kyzar, C. M. Reed, W. S. Anderson, T. A. Valiante, A. N. Mamelak, U. Rutishauser, Control of working memory by phase-amplitude coupling of human hippocampal neurons. *Nature* **629**, 393-401 (2024).

110. B. Lega, J. Burke, J. Jacobs, M. J. Kahana, Slow-Theta-to-Gamma Phase-Amplitude Coupling in Human Hippocampus Supports the Formation of New Episodic Memories. *Cereb Cortex* **26**, 268-278 (2016).

111. A. Radiske, M. C. Gonzalez, S. Conde-Ocazionez, J. I. Rossato, C. A. Kohler, M. Cammarota, Cross-Frequency Phase-Amplitude Coupling between Hippocampal Theta and Gamma Oscillations during Recall Destabilizes Memory and Renders It Susceptible to Reconsolidation Disruption. *J Neurosci* **40**, 6398-6408 (2020).

112. M. A. Wilson, J. R. Fadel, Cholinergic regulation of fear learning and extinction. *Journal of neuroscience research* **95**, 836-852 (2017).

113. J. Haam, J. L. Yakel, Cholinergic modulation of the hippocampal region and memory function. *Journal of neurochemistry* **142 Suppl 2**, 111-121 (2017).

114. D. B. Headley, D. Pare, Common oscillatory mechanisms across multiple memory systems. *NPJ Sci Learn* **2**, (2017).

115. S. Hamann, E. S. Monarch, F. C. Goldstein, Impaired fear conditioning in Alzheimer's disease. *Neuropsychologia* **40**, 1187-1195 (2002).

116. M. Hoefer, S. C. Allison, G. F. Schauer, J. M. Neuhaus, J. Hall, J. N. Dang, M. W. Weiner, B. L. Miller, H. J. Rosen, Fear conditioning in frontotemporal lobar degeneration and Alzheimer's disease. *Brain : a journal of neurology* **131**, 1646-1657 (2008).

117. R. Kimura, M. Ohno, Impairments in remote memory stabilization precede hippocampal synaptic and cognitive failures in 5XFAD Alzheimer mouse model. *Neurobiology of disease* **33**, 229-235 (2009).

118. S. Kim, J. E. Pick, S. Abera, L. Khatri, D. D. Ferreira, M. F. Sathler, S. L. Morison, F. Hofmann, E. B. Ziff, Brain region-specific effects of cGMP-dependent kinase II knockout on AMPA receptor trafficking and animal behavior. *Learning & memory* **23**, 435-441 (2016).

119. J. Shou, A. Tran, N. Snyder, E. Bleem, S. Kim, Distinct Roles of GluA2-lacking AMPA Receptor Expression in Dopamine D1 or D2 Receptor Neurons in Animal Behavior. *Neuroscience* **398**, 102-112 (2018).

120. P. Yan, A. W. Bero, J. R. Cirrito, Q. Xiao, X. Hu, Y. Wang, E. Gonzales, D. M. Holtzman, J. M. Lee, Characterizing the appearance and growth of amyloid plaques in APP/PS1 mice. *J Neurosci* **29**, 10706-10714 (2009).

121. M. Meyer-Luehmann, T. L. Spires-Jones, C. Prada, M. Garcia-Alloza, A. de Calignon, A. Rozkalne, J. Koenigsknecht-Talboo, D. M. Holtzman, B. J. Bacskai, B. T. Hyman, Rapid appearance and local toxicity of amyloid-beta plaques in a mouse model of Alzheimer's disease. *Nature* **451**, 720-724 (2008).

122. L. Verret, E. O. Mann, G. B. Hang, A. M. Barth, I. Cobos, K. Ho, N. Devidze, E. Masliah, A. C. Kreitzer, I. Mody, L. Mucke, J. J. Palop, Inhibitory interneuron deficit links altered network activity and cognitive dysfunction in Alzheimer model. *Cell* **149**, 708-721 (2012).

123. K. Park, J. Lee, H. J. Jang, B. A. Richards, M. M. Kohl, J. Kwag, Optogenetic activation of parvalbumin and somatostatin interneurons selectively restores theta-nested gamma oscillations and oscillation-induced spike timing-dependent long-term potentiation impaired by amyloid beta oligomers. *BMC Biol* **18**, 7 (2020).

124. H. F. Iaccarino, A. C. Singer, A. J. Martorell, A. Rudenko, F. Gao, T. Z. Gillingham, H. Mathys, J. Seo, O. Kritskiy, F. Abdurrob, C. Adaikkan, R. G. Canter, R. Rueda, E. N. Brown, E. S. Boyden, L. H. Tsai, Gamma frequency entrainment attenuates amyloid load and modifies microglia. *Nature* **540**, 230-235 (2016).

125. H. Chung, K. Park, H. J. Jang, M. M. Kohl, J. Kwag, Dissociation of somatostatin and parvalbumin interneurons circuit dysfunctions underlying hippocampal theta and gamma oscillations impaired by amyloid beta oligomers in vivo. *Brain structure & function* **225**, 935-954 (2020).

126. F. R. Kurudenkandy, M. Zilberter, H. Biverstal, J. Presto, D. Honcharenko, R. Stromberg, J. Johansson, B. Winblad, A. Fisahn, Amyloid-beta-induced action potential desynchronization and degradation of hippocampal gamma oscillations is prevented by interference with peptide conformation change and aggregation. *J Neurosci* **34**, 11416-11425 (2014).

127. V. Villette, F. Poindessous-Jazat, A. Simon, C. Lena, E. Roullot, B. Bellessort, J. Epelbaum, P. Dutar, A. Stephan, Decreased rhythmic GABAergic septal activity and memory-associated theta oscillations after hippocampal amyloid-beta pathology in the rat. *J Neurosci* **30**, 10991-11003 (2010).

128. M. Martinez-Losa, T. E. Tracy, K. Ma, L. Verret, A. Clemente-Perez, A. S. Khan, I. Cobos, K. Ho, L. Gan, L. Mucke, M. Alvarez-Dolado, J. J. Palop, Nav1.1-Overexpressing Interneuron Transplants Restore Brain Rhythms and Cognition in a Mouse Model of Alzheimer's Disease. *Neuron* **98**, 75-89 e75 (2018).

129. M. P. Lambert, A. K. Barlow, B. A. Chromy, C. Edwards, R. Freed, M. Liosatos, T. E. Morgan, I. Rozovsky, B. Trommer, K. L. Viola, P. Wals, C. Zhang, C. E. Finch, G. A. Krafft, W. L. Klein, Diffusible, nonfibrillar ligands derived from Abeta1-42 are potent central nervous system neurotoxins. *Proc Natl Acad Sci U S A* **95**, 6448-6453 (1998).

130. C. A. McLean, R. A. Cherny, F. W. Fraser, S. J. Fuller, M. J. Smith, K. Beyreuther, A. I. Bush, C. L. Masters, Soluble pool of Abeta amyloid as a determinant of severity of neurodegeneration in Alzheimer's disease. *Ann Neurol* **46**, 860-866 (1999).

131. D. S. Auld, S. Kar, R. Quirion, Beta-amyloid peptides as direct cholinergic neuromodulators: a missing link? *Trends Neurosci* **21**, 43-49 (1998).

132. C. B. Lu, C. Z. Li, D. L. Li, Z. Henderson, Nicotine induction of theta frequency oscillations in rodent medial septal diagonal band in vitro. *Acta Pharmacol Sin* **34**, 819-829 (2013).

133. M. Griguoli, E. Cherubini, Regulation of hippocampal inhibitory circuits by nicotinic acetylcholine receptors. *The Journal of physiology* **590**, 655-666 (2012).

134. C. Song, T. A. Murray, R. Kimura, M. Wakui, K. Ellsworth, S. P. Javedan, S. Marxer-Miller, R. J. Lukas, J. Wu, Role of alpha7-nicotinic acetylcholine receptors in tetanic stimulation-induced gamma oscillations in rat hippocampal slices. *Neuropharmacology* **48**, 869-880 (2005).

135. Z. Gu, K. G. Smith, G. M. Alexander, I. Guerreiro, S. M. Dudek, B. Gutkin, P. Jensen, J. L. Yakel, Hippocampal Interneuronal alpha7 nAChRs Modulate Theta Oscillations in Freely Moving Mice. *Cell Rep* **31**, 107740 (2020).

136. M. Alkondon, E. F. Pereira, E. X. Albuquerque, alpha-bungarotoxin- and methyllycaconitine-sensitive nicotinic receptors mediate fast synaptic transmission in interneurons of rat hippocampal slices. *Brain research* **810**, 257-263 (1998).

137. M. Alkondon, E. F. Pereira, E. X. Albuquerque, NMDA and AMPA receptors contribute to the nicotinic cholinergic excitation of CA1 interneurons in the rat hippocampus. *Journal of neurophysiology* **90**, 1613-1625 (2003).

138. A. V. Buhler, T. V. Dunwiddie, Regulation of the activity of hippocampal stratum oriens interneurons by alpha7 nicotinic acetylcholine receptors. *Neuroscience* **106**, 55-67 (2001).

139. A. V. Buhler, T. V. Dunwiddie, alpha7 nicotinic acetylcholine receptors on GABAergic interneurons evoke dendritic and somatic inhibition of hippocampal neurons. *Journal of neurophysiology* **87**, 548-557 (2002).

140. C. J. Frazier, A. V. Buhler, J. L. Weiner, T. V. Dunwiddie, Synaptic potentials mediated via alpha-bungarotoxin-sensitive nicotinic acetylcholine receptors in rat hippocampal interneurons. *J Neurosci* **18**, 8228-8235 (1998).

141. R. J. Lukas, J. P. Changeux, N. Le Novere, E. X. Albuquerque, D. J. Balfour, D. K. Berg, D. Bertrand, V. A. Chiappinelli, P. B. Clarke, A. C. Collins, J. A. Dani, S. R. Grady, K. J. Kellar, J. M. Lindstrom, M. J. Marks, M. Quik, P. W. Taylor, S. Wonnacott, International Union of Pharmacology. XX. Current status of the nomenclature for nicotinic acetylcholine receptors and their subunits. *Pharmacological reviews* **51**, 397-401 (1999).

142. T. D. McClure-Begley, N. M. King, A. C. Collins, J. A. Stitzel, J. M. Wehner, C. M. Butt, Acetylcholine-stimulated [3H]GABA release from mouse brain synaptosomes is modulated by alpha4beta2 and alpha4alpha5beta2 nicotinic receptor subtypes. *Mol Pharmacol* **75**, 918-926 (2009).

143. G. Sharma, S. Vijayaraghavan, Modulation of presynaptic store calcium induces release of glutamate and postsynaptic firing. *Neuron* **38**, 929-939 (2003).

144. S. N. Sudweeks, J. L. Yakel, Functional and molecular characterization of neuronal nicotinic ACh receptors in rat CA1 hippocampal neurons. *The Journal of physiology* **527 Pt 3**, 515-528 (2000).

145. L. Frolich, The cholinergic pathology in Alzheimer's disease--discrepancies between clinical experience and pathophysiological findings. *J Neural Transm (Vienna)* **109**, 1003-1013 (2002).

146. C. M. Yuede, H. Dong, J. G. Csernansky, Anti-dementia drugs and hippocampal-dependent memory in rodents. *Behavioural pharmacology* **18**, 347-363 (2007).

147. S. Vijayraghavan, A. J. Major, S. Everling, Muscarinic M1 Receptor Overstimulation Disrupts Working Memory Activity for Rules in Primate Prefrontal Cortex. *Neuron* **98**, 1256-1268 e1254 (2018).

148. P. Raina, P. Santaguida, A. Ismaila, C. Patterson, D. Cowan, M. Levine, L. Booker, M. Oremus, Effectiveness of cholinesterase inhibitors and memantine for treating dementia: evidence review for a clinical practice guideline. *Ann Intern Med* **148**, 379-397 (2008).

149. Y. Sun, M. S. Lai, C. J. Lu, R. C. Chen, How long can patients with mild or moderate Alzheimer's dementia maintain both the cognition and the therapy of cholinesterase inhibitors: a national population-based study. *Eur J Neurol* **15**, 278-283 (2008).

150. E. D. Levin, B. B. Simon, Nicotinic acetylcholine involvement in cognitive function in animals. *Psychopharmacology* **138**, 217-230 (1998).

151. P. Vicens, M. C. Carrasco, R. Redolat, Effects of early training and nicotine treatment on the performance of male NMRI mice in the water maze. *Neural Plast* **10**, 303-317 (2003).

152. J. J. Buccafusco, Neuronal nicotinic receptor subtypes: defining therapeutic targets. *Mol Interv* **4**, 285-295 (2004).

153. J. L. Hoskin, Y. Al-Hasan, M. N. Sabbagh, Nicotinic Acetylcholine Receptor Agonists for the Treatment of Alzheimer's Dementia: An Update. *Nicotine Tob Res* **21**, 370-376 (2019).

154. R. S. Bitner, W. H. Bunnelle, D. J. Anderson, C. A. Briggs, J. Buccafusco, P. Curzon, M. W. Decker, J. M. Frost, J. H. Gronlien, E. Gubbins, J. Li, J. Malysz, S. Markosyan, K. Marsh, M. D. Meyer, A. L. Nikkel, R. J. Radek, H. M. Robb, D. Timmermann, J. P. Sullivan, M. Gopalakrishnan, Broad-spectrum efficacy across cognitive domains by alpha7 nicotinic acetylcholine receptor agonism correlates with activation of ERK1/2 and CREB phosphorylation pathways. *J Neurosci* **27**, 10578-10587 (2007).

155. S. L. Cincotta, M. S. Yorek, T. M. Moschak, S. R. Lewis, J. S. Rodefer, Selective nicotinic acetylcholine receptor agonists: potential therapies for neuropsychiatric disorders with cognitive dysfunction. *Curr Opin Investig Drugs* **9**, 47-56 (2008).

156. J. P. Redrobe, E. O. Nielsen, J. K. Christensen, D. Peters, D. B. Timmermann, G. M. Olsen, Alpha7 nicotinic acetylcholine receptor activation ameliorates scopolamine-induced behavioural changes in a modified continuous Y-maze task in mice. *European journal of pharmacology* **602**, 58-65 (2009).

157. P. Vicens, D. Ribes, M. Torrente, J. L. Domingo, Behavioral effects of PNU-282987, an alpha7 nicotinic receptor agonist, in mice. *Behavioural brain research* **216**, 341-348 (2011).

158. E. D. Levin, N. C. Christopher, Persistence of nicotinic agonist RJR 2403-induced working memory improvement in rats. *Drug Develop Res* **55**, 97-103 (2002).

159. A. Potasiewicz, J. Golebiowska, P. Popik, A. Nikiforuk, Procognitive effects of varenicline in the animal model of schizophrenia depend on alpha4beta2- and alpha 7-nicotinic acetylcholine receptors. *J Psychopharmacol* **33**, 269881118812097 (2018).

160. N. A. Upright, M. G. Baxter, Effects of nicotinic antagonists on working memory performance in young rhesus monkeys. *Neurobiology of learning and memory* **184**, 107505 (2021).

161. J. T. Kantrowitz, D. C. Javitt, R. Freedman, P. Sehatpour, L. S. Kegeles, M. Carlson, T. Sobeih, M. M. Wall, T. H. Choo, B. Vail, J. Grinband, J. A. Lieberman, Double blind, two dose, randomized, placebo-controlled, cross-over clinical trial of the positive allosteric modulator at the alpha7 nicotinic cholinergic receptor AVL-3288 in schizophrenia patients. *Neuropsychopharmacology : official publication of the American College of Neuropsychopharmacology* **45**, 1339-1345 (2020).

162. K. Taniguchi, F. Yamamoto, A. Amano, A. Tamaoka, N. Sanjo, T. Yokota, F. Kametani, W. Araki, Amyloid-beta oligomers interact with NMDA receptors containing GluN2B subunits and metabotropic glutamate receptor 1 in primary cortical neurons: Relevance to the synapse pathology of Alzheimer's disease. *Neurosci Res* **180**, 90-98 (2022).

163. H. Y. Wang, D. H. Lee, M. R. D'Andrea, P. A. Peterson, R. P. Shank, A. B. Reitz, beta-Amyloid(1-42) binds to alpha7 nicotinic acetylcholine receptor with high affinity. Implications for Alzheimer's disease pathology. *The Journal of biological chemistry* **275**, 5626-5632 (2000).

164. E. Cecon, J. Dam, M. Luka, C. Gautier, A. M. Chollet, P. Delagrange, L. Danober, R. Jockers, Quantitative assessment of oligomeric amyloid beta peptide binding to alpha7 nicotinic receptor. *British journal of pharmacology* **176**, 3475-3488 (2019).

165. S. R. Cobb, D. O. Bulters, S. Suchak, G. Riedel, R. G. Morris, C. H. Davies, Activation of nicotinic acetylcholine receptors patterns network activity in the rodent hippocampus. *The Journal of physiology* **518**, 131-140 (1999).

166. H. Dannenberg, K. Young, M. Hasselmo, Modulation of Hippocampal Circuits by Muscarinic and Nicotinic Receptors. *Frontiers in neural circuits* **11**, 102 (2017).

167. S. Sadigh-Eteghad, A. Majdi, J. Mahmoudi, S. E. J. Golzari, M. Talebi, Astrocytic and microglial nicotinic acetylcholine receptors: an overlooked issue in Alzheimer's disease. *J Neural Transm (Vienna)* **123**, 1359-1367 (2016).

168. K. Takata, Y. Kitamura, M. Saeki, M. Terada, S. Kagitani, R. Kitamura, Y. Fujikawa, A. Maelicke, H. Tomimoto, T. Taniguchi, S. Shimohama, Galantamine-induced amyloid-{beta} clearance mediated via stimulation of microglial nicotinic acetylcholine receptors. *The Journal of biological chemistry* **285**, 40180-40191 (2010).

169. W. Yu, N. Mechawar, S. Krantic, J.-G. Chabot, R. Quirion, Upregulation of astrocytic α7 nicotinic receptors in Alzheimer's disease brain- possible relevant to amyloid pathology. *Molecular Neurodegeneration* **7**, O7 (2012).

170. Y. Liu, X. Zeng, Y. Hui, C. Zhu, J. Wu, D. H. Taylor, J. Ji, W. Fan, Z. Huang, J. Hu, Activation of alpha7 nicotinic acetylcholine receptors protects astrocytes against oxidative stress-induced apoptosis: implications for Parkinson's disease. *Neuropharmacology* **91**, 87-96 (2015).

171. H. Oikawa, N. Nakamichi, Y. Kambe, M. Ogura, Y. Yoneda, An increase in intracellular free calcium ions by nicotinic acetylcholine receptors in a single cultured rat cortical astrocyte. *Journal of neuroscience research* **79**, 535-544 (2005).

172. T. Takarada, N. Nakamichi, H. Kawagoe, M. Ogura, R. Fukumori, R. Nakazato, K. Fujikawa, M. Kou, Y. Yoneda, Possible neuroprotective property of nicotinic acetylcholine receptors in association with predominant upregulation of glial cell line-derived neurotrophic factor in astrocytes. *Journal of neuroscience research* **90**, 2074-2085 (2012).

173. G. Straten, G. W. Eschweiler, W. Maetzler, C. Laske, T. Leyhe, Glial cell-line derived neurotrophic factor (GDNF) concentrations in cerebrospinal fluid and serum of patients with early Alzheimer's disease and normal controls. *Journal of Alzheimer's disease : JAD* **18**, 331-337 (2009).

174. M. Stoiljkovic, C. Kelley, D. Nagy, L. Leventhal, M. Hajos, Selective activation of alpha7 nicotinic acetylcholine receptors augments hippocampal oscillations. *Neuropharmacology* **110**, 102-108 (2016).

175. G. A. Elder, M. A. Gama Sosa, R. De Gasperi, Transgenic mouse models of Alzheimer's disease. *Mt Sinai J Med* **77**, 69-81 (2010).

176. K. Hsiao, P. Chapman, S. Nilsen, C. Eckman, Y. Harigaya, S. Younkin, F. Yang, G. Cole, Correlative memory deficits, Abeta elevation, and amyloid plaques in transgenic mice. *Science* **274**, 99-102 (1996).

177. A. L. Oblak, P. B. Lin, K. P. Kotredes, R. S. Pandey, D. Garceau, H. M. Williams, A. Uyar, R. O'Rourke, S. O'Rourke, C. Ingraham, D. Bednarczyk, M. Belanger, Z. A. Cope, G. J. Little, S. G. Williams, C. Ash, A. Bleckert, T. Ragan, B. A. Logsdon, L. M. Mangravite, S. J. Sukoff Rizzo, P. R. Territo, G. W. Carter, G. R. Howell, M. Sasner, B. T. Lamb, Comprehensive Evaluation of the 5XFAD Mouse Model for Preclinical Testing Applications: A MODEL-AD Study. *Frontiers in aging neuroscience* **13**, 713726 (2021).

178. G. E. Alexander, K. Chen, P. Pietrini, S. I. Rapoport, E. M. Reiman, Longitudinal PET Evaluation of Cerebral Metabolic Decline in Dementia: A Potential Outcome Measure in Alzheimer's Disease Treatment Studies. *Am J Psychiatry* **159**, 738-745 (2002).

179. M. A. Busche, A. Konnerth, Impairments of neural circuit function in Alzheimer's disease. *Philos Trans R Soc Lond B Biol Sci* **371**, (2016).

180. B. C. Dickerson, D. H. Salat, D. N. Greve, E. F. Chua, E. Rand-Giovannetti, D. M. Rentz, L. Bertram, K. Mullin, R. E. Tanzi, D. Blacker, M. S. Albert, R. A. Sperling, Increased hippocampal activation in mild cognitive impairment compared to normal aging and AD. *Neurology* **65**, 404-411 (2005).

181. S. S. Harris, F. Wolf, B. De Strooper, M. A. Busche, Tipping the Scales: Peptide-Dependent Dysregulation of Neural Circuit Dynamics in Alzheimer's Disease. *Neuron* **107**, 417-435 (2020).

182. S. Toniolo, A. Sen, M. Husain, Modulation of Brain Hyperexcitability: Potential New Therapeutic Approaches in Alzheimer's Disease. *Int J Mol Sci* **21**, (2020).

183. J. Seo, P. Giusti-Rodriguez, Y. Zhou, A. Rudenko, S. Cho, K. T. Ota, C. Park, H. Patzke, R. Madabhushi, L. Pan, A. E. Mungenast, J. S. Guan, I. Delalle, L. H. Tsai, Activity-dependent p25 generation regulates synaptic plasticity and Abeta-induced cognitive impairment. *Cell* **157**, 486-498 (2014).

184. M. Wang, J. Jo, J. Song, Adiponectin improves long-term potentiation in the 5XFAD mouse brain. *Sci Rep* **9**, 8918 (2019).

185. L. Devi, M. Ohno, Phospho-eIF2alpha level is important for determining abilities of BACE1 reduction to rescue cholinergic neurodegeneration and memory defects in 5XFAD mice. *PLoS One* **5**, e12974 (2010).

186. N. A. Xiao, J. Zhang, M. Zhou, Z. Wei, X. L. Wu, X. M. Dai, Y. G. Zhu, X. C. Chen, Reduction of Glucose Metabolism in Olfactory Bulb is an Earlier Alzheimer's Disease-related Biomarker in 5XFAD Mice. *Chin Med J (Engl)* **128**, 2220-2227 (2015).

187. D. K. Kim, D. Han, J. Park, H. Choi, J. C. Park, M. Y. Cha, J. Woo, M. S. Byun, D. Y. Lee, Y. Kim, I. Mook-Jung, Deep proteome profiling of the hippocampus in the 5XFAD mouse model reveals biological process alterations and a novel biomarker of Alzheimer's disease. *Exp Mol Med* **51**, 1-17 (2019).

188. H. Yan, P. Pang, W. Chen, H. Zhu, K. A. Henok, H. Li, Z. Wu, X. Ke, J. Wu, T. Zhang, K. Pan, L. Pei, Y. Han, Y. Lu, The Lesion Analysis of Cholinergic Neurons in 5XFAD Mouse Model in the Three-Dimensional Level of Whole Brain. *Mol Neurobiol* **55**, 4115-4125 (2018).

189. L. Devi, M. Ohno, A combination Alzheimer's therapy targeting BACE1 and neprilysin in 5XFAD transgenic mice. *Mol Brain* **8**, 19 (2015).

190. A. J. Martorell, A. L. Paulson, H. J. Suk, F. Abdurrob, G. T. Drummond, W. Guan, J. Z. Young, D. N. Kim, O. Kritskiy, S. J. Barker, V. Mangena, S. M. Prince, E. N. Brown, K. Chung, E. S. Boyden, A. C. Singer, L. H. Tsai, Multi-sensory Gamma Stimulation Ameliorates Alzheimer's-Associated Pathology and Improves Cognition. *Cell* **177**, 256-271 e222 (2019).

191. C. Kilkenny, W. Browne, I. C. Cuthill, M. Emerson, D. G. Altman, N. C. R. R. G. W. Group, Animal research: reporting in vivo experiments: the ARRIVE guidelines. *British journal of pharmacology* **160**, 1577-1579 (2010).

192. M. F. Sathler, L. Khatri, J. P. Roberts, I. G. Schmidt, A. Zaytseva, R. C. C. Kubrusly, E. B. Ziff, S. Kim, Phosphorylation of the AMPA receptor subunit GluA1 regulates clathrin-mediated receptor internalization. *Journal of cell science* **134**, (2021).

193. M. F. Sathler, M. J. Doolittle, J. A. Cockrell, I. R. Nadalin, F. Hofmann, S. VandeWoude, S. Kim, HIV and FIV glycoproteins increase cellular tau pathology via cGMP-dependent kinase II activation. *Journal of cell science* **135**, (2022).

194. C. Lesuisse, L. J. Martin, Long-term culture of mouse cortical neurons as a model for neuronal development, aging, and death. *J Neurobiol* **51**, 9-23 (2002).

195. S. Kaech, G. Banker, Culturing hippocampal neurons. *Nat Protoc* **1**, 2406-2415 (2006).

196. W. B. Stine, Jr., K. N. Dahlgren, G. A. Krafft, M. J. LaDu, In vitro characterization of conditions for amyloid-beta peptide oligomerization and fibrillogenesis. *The Journal of biological chemistry* **278**, 11612-11622 (2003).

197. D. L. Benson, P. A. Cohen, Activity-independent segregation of excitatory and inhibitory synaptic terminals in cultured hippocampal neurons. *J Neurosci* **16**, 6424-6432 (1996).

198. T. W. Chen, T. J. Wardill, Y. Sun, S. R. Pulver, S. L. Renninger, A. Baohan, E. R. Schreiter, R. A. Kerr, M. B. Orger, V. Jayaraman, L. L. Looger, K. Svoboda, D. S. Kim, Ultrasensitive fluorescent proteins for imaging neuronal activity. *Nature* **499**, 295-300 (2013).

199. J. Dimidschstein, Q. Chen, R. Tremblay, S. L. Rogers, G. A. Saldi, L. Guo, Q. Xu, R. Liu, C. Lu, J. Chu, J. S. Grimley, A. R. Krostag, A. Kaykas, M. C. Avery, M. S. Rashid, M. Baek, A. L. Jacob, G. B. Smith, D. E. Wilson, G. Kosche, I. Kruglikov, T. Rusielewicz, V. C. Kotak, T. M. Mowery, S. A. Anderson, E. M. Callaway, J. S. Dasen, D. Fitzpatrick, V. Fossati, M. A. Long, S. Noggle, J. H. Reynolds, D. H. Sanes, B. Rudy, G. Feng, G. Fishell, A viral strategy for targeting and manipulating interneurons across vertebrate species. *Nat Neurosci* **19**, 1743-1749 (2016).

200. H. Dana, Y. Sun, B. Mohar, B. K. Hulse, A. M. Kerlin, J. P. Hasseman, G. Tsegaye, A. Tsang, A. Wong, R. Patel, J. J. Macklin, Y. Chen, A. Konnerth, V. Jayaraman, L. L. Looger, E. R. Schreiter, K. Svoboda, D. S. Kim, High-performance calcium sensors for imaging activity in neuronal populations and microcompartments. *Nature methods* **16**, 649-657 (2019).

201. E. Cohen, M. Ivenshitz, V. Amor-Baroukh, V. Greenberger, M. Segal, Determinants of spontaneous activity in networks of cultured hippocampus. *Brain research* **1235**, 21-30 (2008).

202. S. Kim, R. F. Titcombe, H. Zhang, L. Khatri, H. K. Girma, F. Hofmann, O. Arancio, E. B. Ziff, Network compensation of cyclic GMP-dependent protein kinase II knockout in the hippocampus by Ca2+-permeable AMPA receptors. *Proc Natl Acad Sci U S A* **112**, 3122-3127 (2015).

203. S. Kim, C. J. Violette, E. B. Ziff, Reduction of increased calcineurin activity rescues impaired homeostatic synaptic plasticity in presenilin 1 M146V mutant. *Neurobiol Aging* **36**, 3239-3246 (2015).

204. S. Kim, E. B. Ziff, Calcineurin mediates synaptic scaling via synaptic trafficking of Ca2+-permeable AMPA receptors. *PLoS biology* **12**, e1001900 (2014).

205. M. Hijioka, H. Matsushita, H. Ishibashi, A. Hisatsune, Y. Isohama, H. Katsuki, alpha7 Nicotinic acetylcholine receptor agonist attenuates neuropathological changes associated with intracerebral hemorrhage in mice. *Neuroscience* **222**, 10-19 (2012).

206. M. Bencherif, M. E. Lovette, K. W. Fowler, S. Arrington, L. Reeves, W. S. Caldwell, P. M. Lippiello, RJR-2403: a nicotinic agonist with CNS selectivity I. In vitro characterization. *J Pharmacol Exp Ther* **279**, 1413-1421 (1996).

207. K. Niimi, C. Nishioka, T. Miyamoto, E. Takahashi, I. Miyoshi, C. Itakura, T. Yamashita, Improvement of spontaneous alternation behavior deficit by activation of alpha4beta2 nicotinic acetylcholine receptor signaling in the ganglioside GM3-deficient mice. *Biomed Res* **34**, 189-195 (2013).

208. K. Duris, A. Manaenko, H. Suzuki, W. B. Rolland, P. R. Krafft, J. H. Zhang, alpha7 nicotinic acetylcholine receptor agonist PNU-282987 attenuates early brain injury in a perforation model of subarachnoid hemorrhage in rats. *Stroke; a journal of cerebral circulation* **42**, 3530-3536 (2011).

209. N. Kawamura, E. Novianti, N. Yamada-Goto, R. Nakama, A. Asakawa, G. Katsuura, A. Inui, Activation of alpha7 nicotinic receptors suppresses sucrose addiction in mice. *Progress in neuro-psychopharmacology & biological psychiatry* **113**, 110439 (2022).

210. M. Hajos, R. S. Hurst, W. E. Hoffmann, M. Krause, T. M. Wall, N. R. Higdon, V. E. Groppi, The selective alpha7 nicotinic acetylcholine receptor agonist PNU-282987 [N-[(3R)-1-Azabicyclo[2.2.2]oct-3-yl]-4-chlorobenzamide hydrochloride] enhances GABAergic synaptic activity in brain slices and restores auditory gating deficits in anesthetized rats. *J Pharmacol Exp Ther* **312**, 1213-1222 (2005).

211. A. D. Smith, M. S. Dar, Behavioral cross-tolerance between repeated intracerebellar nicotine and acute Delta(9)-tetrahydrocannabinol-induced cerebellar ataxia: role of cerebellar nitric oxide. *J Pharmacol Exp Ther* **322**, 243-253 (2007).

212. P. M. Lippiello, M. Bencherif, J. A. Gray, S. Peters, G. Grigoryan, H. Hodges, A. C. Collins, RJR-2403: a nicotinic agonist with CNS selectivity II. In vivo characterization. *J Pharmacol Exp Ther* **279**, 1422-1429 (1996).

213. N. S. Sapronov, Y. O. Fedotova, N. N. Kuznetsova, Antiamnestic effect of alpha7-nicotinic receptor agonist RJR-2403 in middle-aged ovariectomized rats with Alzheimer type dementia. *Bull Exp Biol Med* **142**, 700-702 (2006).

214. T. M. Tran, J. K. Sherwood, M. J. Doolittle, M. F. Sathler, F. Hofmann, L. M. Stone-Roy, S. Kim, Loss of cGMP-dependent protein kinase II alters ultrasonic vocalizations in mice, a model for speech impairment in human microdeletion 4q21 syndrome. *Neuroscience letters* **759**, 136048 (2021).

215. S. H. Roh, H. Mendez-Vazquez, M. F. Sathler, M. J. Doolittle, A. Zaytseva, H. Brown, M. Sainsbury, S. Kim, Prenatal exposure to valproic acid reduces synaptic delta-catenin levels and disrupts ultrasonic vocalization in neonates. *Neuropharmacology* **253**, 109963 (2024).

216. S. Jawhar, A. Trawicka, C. Jenneckens, T. A. Bayer, O. Wirths, Motor deficits, neuron loss, and reduced anxiety coinciding with axonal degeneration and intraneuronal Abeta aggregation in the 5XFAD mouse model of Alzheimer's disease. *Neurobiol Aging* **33**, 196 e129-140 (2012).

217. J. H. Siegle, A. C. Lopez, Y. A. Patel, K. Abramov, S. Ohayon, J. Voigts, Open Ephys: an open-source, plugin-based platform for multichannel electrophysiology. *J Neural Eng* **14**, 045003 (2017).

218. F. Tadel, S. Baillet, J. C. Mosher, D. Pantazis, R. M. Leahy, Brainstorm: A User-Friendly Application for MEG/EEG Analysis. *Computational Intelligence and Neuroscience* **2011**, 879716 (2011).

219. A. Delorme, S. Makeig, EEGLAB: an open source toolbox for analysis of single-trial EEG dynamics including independent component analysis. *J Neurosci Methods* **134**, 9-21 (2004).

Acknowledgments

We thank members of the Kim laboratory for their generous support. We appreciate Dr. Eunhye Park for the technical guidance and Dr. Don Rojas to support data analysis. This work is supported by the NIH/NCATS Colorado CTSA Grant (UL1 TR002535), the Boettcher Foundation's Webb-Waring Biomedical Research Program, BrightFocus Foundation, and the NIH grant (1R03AG072102), and Colorado State University College of Veterinary Medicine and Biomedical Sciences. Conceptualization: S.K. Methodology: S.K. Validation: R.L. G.K. and S.K. Formal analysis: R.L. G.K. and S.K. Investigation: R.L. G.K. E.R.B. and S.K. Writing - Original Draft: R.L and S.K. Writing - Review & Editing: R.L and S.K. Visualization: R.L. G.K. and S.K. Supervision: S.K. Project administration: S.K. Funding acquisition: E.R.B. and S.K. The authors declare that they have no competing interests. All data needed to evaluate the conclusions in the paper are present in the paper and the Supplementary Materials.

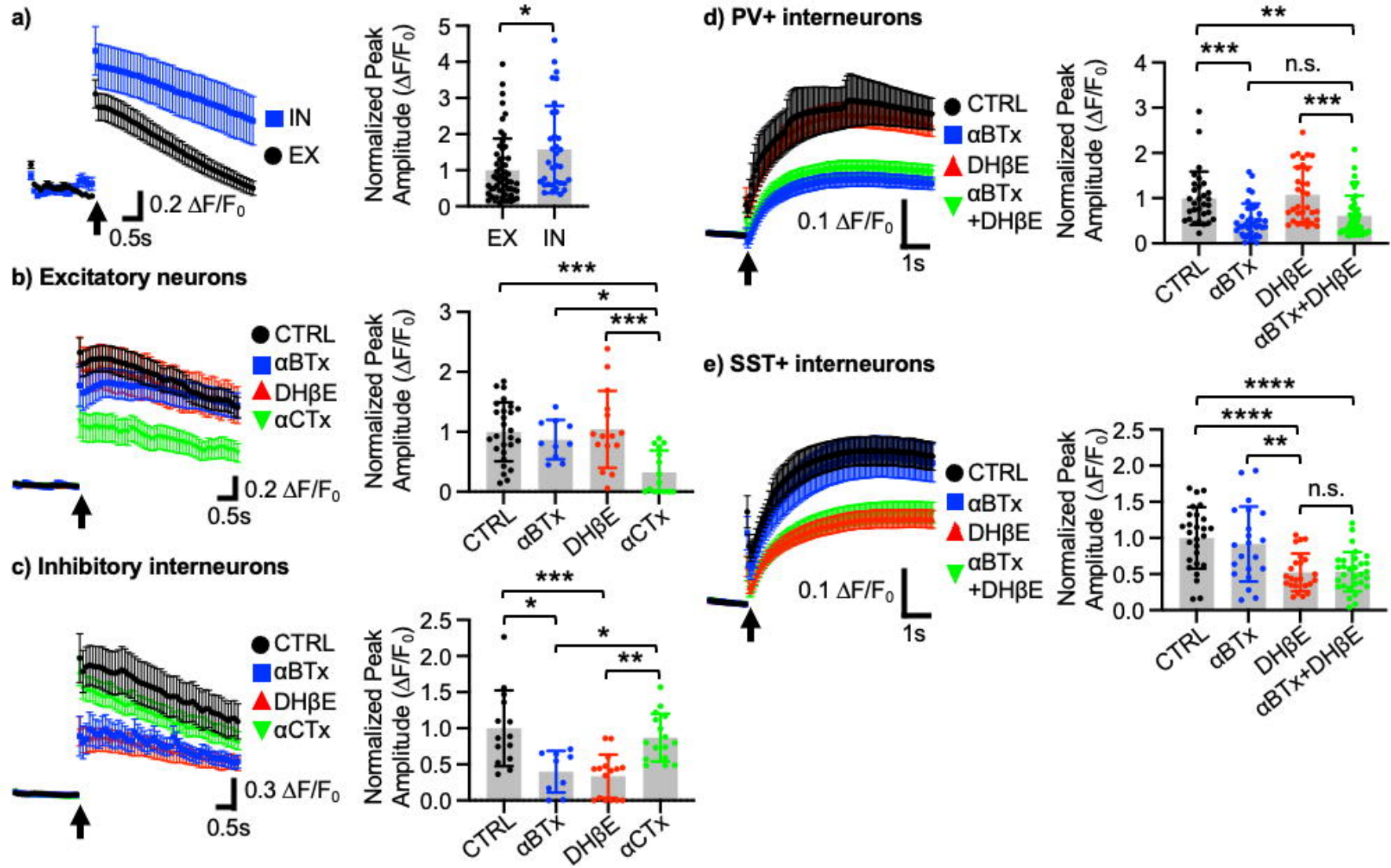
a)
IN
EX
0.2 ΔF/F0
0.5s
Normalized Peak Amplitude (ΔF/F0)
EX
IN
b) Excitatory neurons
CTRL
αBTx
DHβE
αCTx
0.2 ΔF/F0
0.5s
CTRL
αBTx
DHβE
αCTx
c) Inhibitory interneurons
CTRL
αBTx
DHβE
αCTx
0.3 ΔF/F0
0.5s
d) PV+ interneurons
CTRL
αBTx
DHβE
αBTx +DHβE
0.1 ΔF/F0
1s
n.s.
CTRL
αBTx
DHβE
αBTx+DHβE
e) SST+ interneurons
CTRL
αBTx
DHβE
αBTx +DHβE
0.1 ΔF/F0
1s
n.s.
CTRL
αBTx
DHβE
αBTx+DHβE

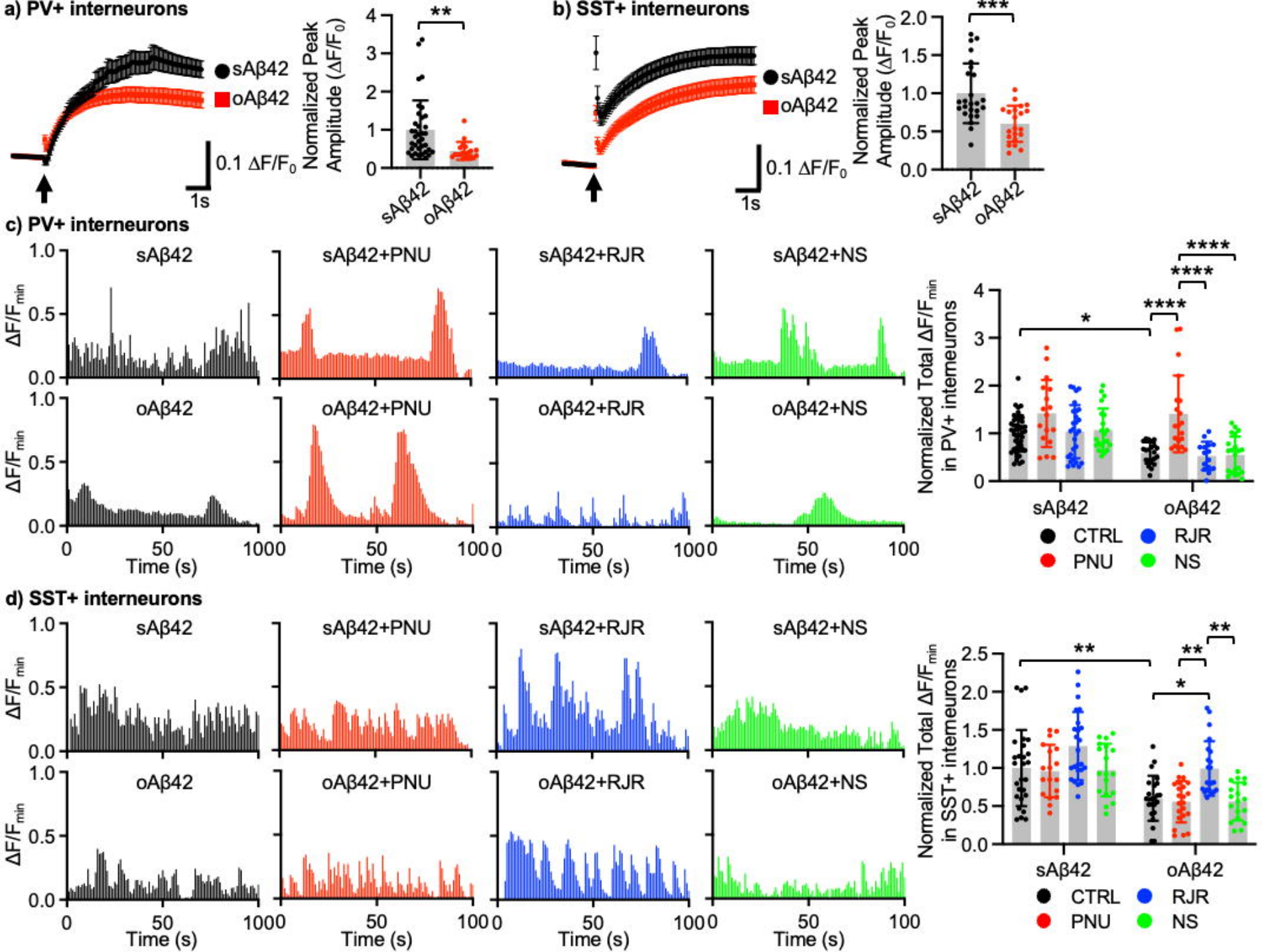
a) PV+ interneurons
sAβ42
oAβ42
0.1 ΔF/F0
1s
Normalized Peak Amplitude (ΔF/F0)
**
sAβ42
oAβ42
b) SST+ interneurons
sAβ42
oAβ42
0.1 ΔF/F0
1s
Normalized Peak Amplitude (ΔF/F0)
***
sAβ42
oAβ42
c) PV+ interneurons
sAβ42
sAβ42+PNU
sAβ42+RJR
sAβ42+NS
oAβ42
oAβ42+PNU
oAβ42+RJR
oAβ42+NS
ΔF/Fmin
Time (s)
Normalized Total ΔF/Fmin in PV+ interneurons
*
****
****
****
sAβ42
oAβ42
CTRL
PNU
RJR
NS
d) SST+ interneurons
sAβ42
sAβ42+PNU
sAβ42+RJR
sAβ42+NS
oAβ42
oAβ42+PNU
oAβ42+RJR
oAβ42+NS
ΔF/Fmin
Time (s)
Normalized Total ΔF/Fmin in SST+ interneurons
**
*
**
**
sAβ42
oAβ42
CTRL
PNU
RJR
NS

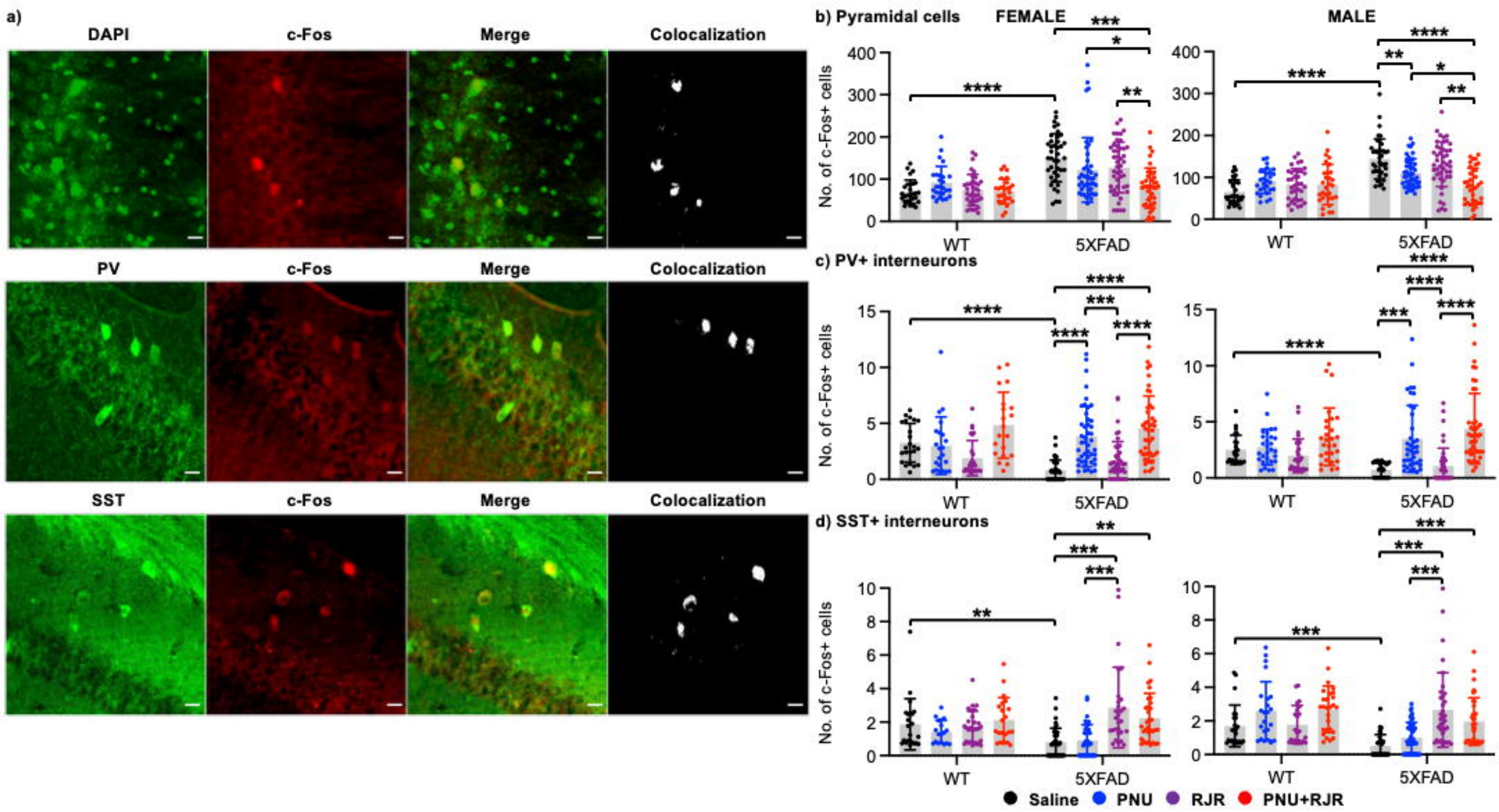
a)
DAPI
c-Fos
Merge
Colocalization
PV
c-Fos
Merge
Colocalization
SST
c-Fos
Merge
Colocalization
b) Pyramidal cells
FEMALE
MALE
No. of c-Fos+ cells
WT
5XFAD
c) PV+ interneurons
No. of c-Fos+ cells
WT
5XFAD
d) SST+ interneurons
No. of c-Fos+ cells
WT
5XFAD
Saline
PNU
RJR
PNU+RJR

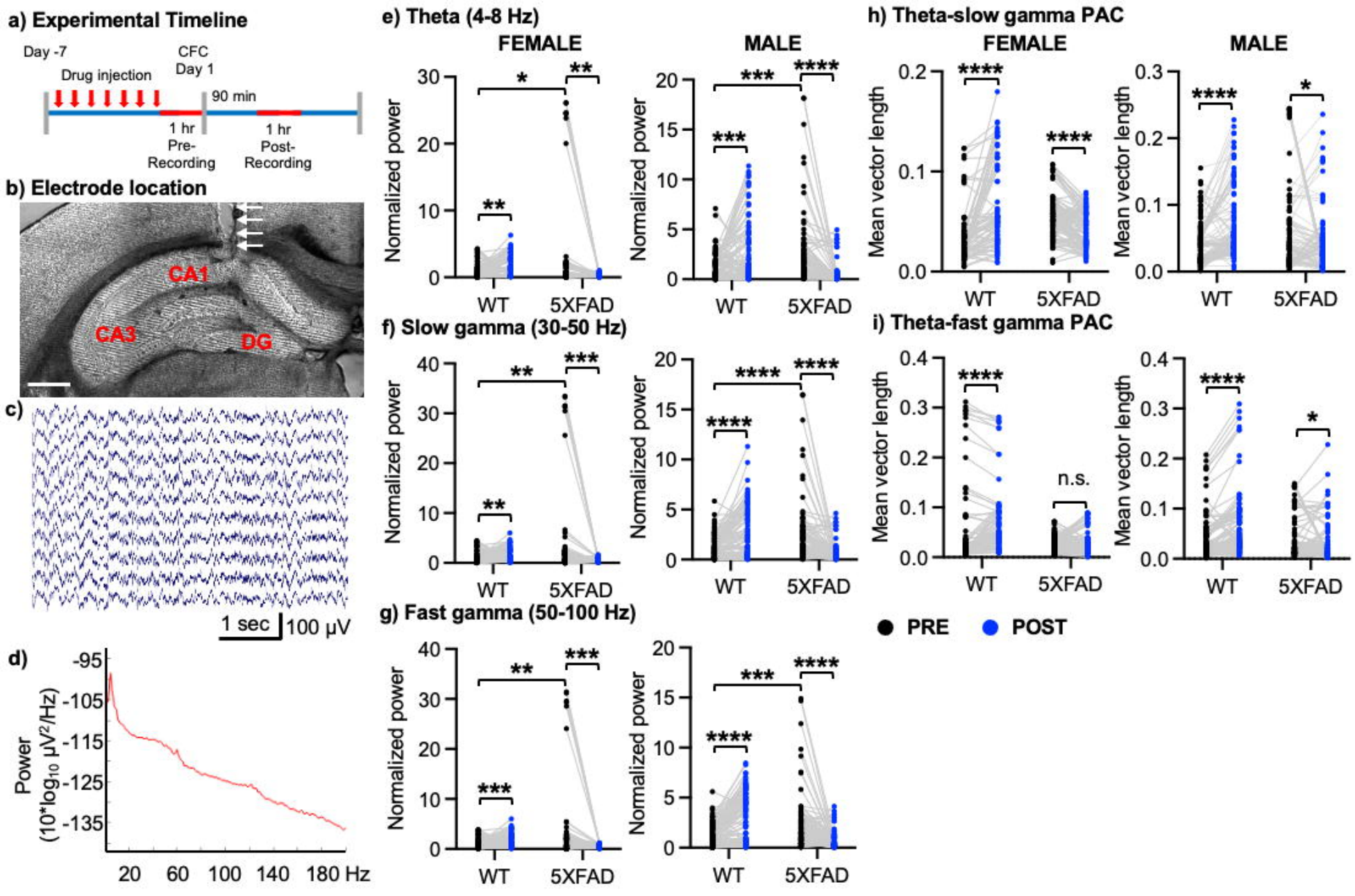
a) Experimental Timeline
Day -7
Drug injection
CFC
Day 1
90 min
1 hr
Pre-
Recording
1 hr
Post-
Recording
b) Electrode location
CA1
CA3
DG
c)
1 sec
100 µV
d)
Power
(10*log10 µV²/Hz)
-95
-105
-115
-125
-135
20
60
100
140
180 Hz
e) Theta (4-8 Hz)
FEMALE
MALE
Normalized power
WT
5XFAD
f) Slow gamma (30-50 Hz)
g) Fast gamma (50-100 Hz)
h) Theta-slow gamma PAC
Mean vector length
i) Theta-fast gamma PAC
n.s.
PRE
POST

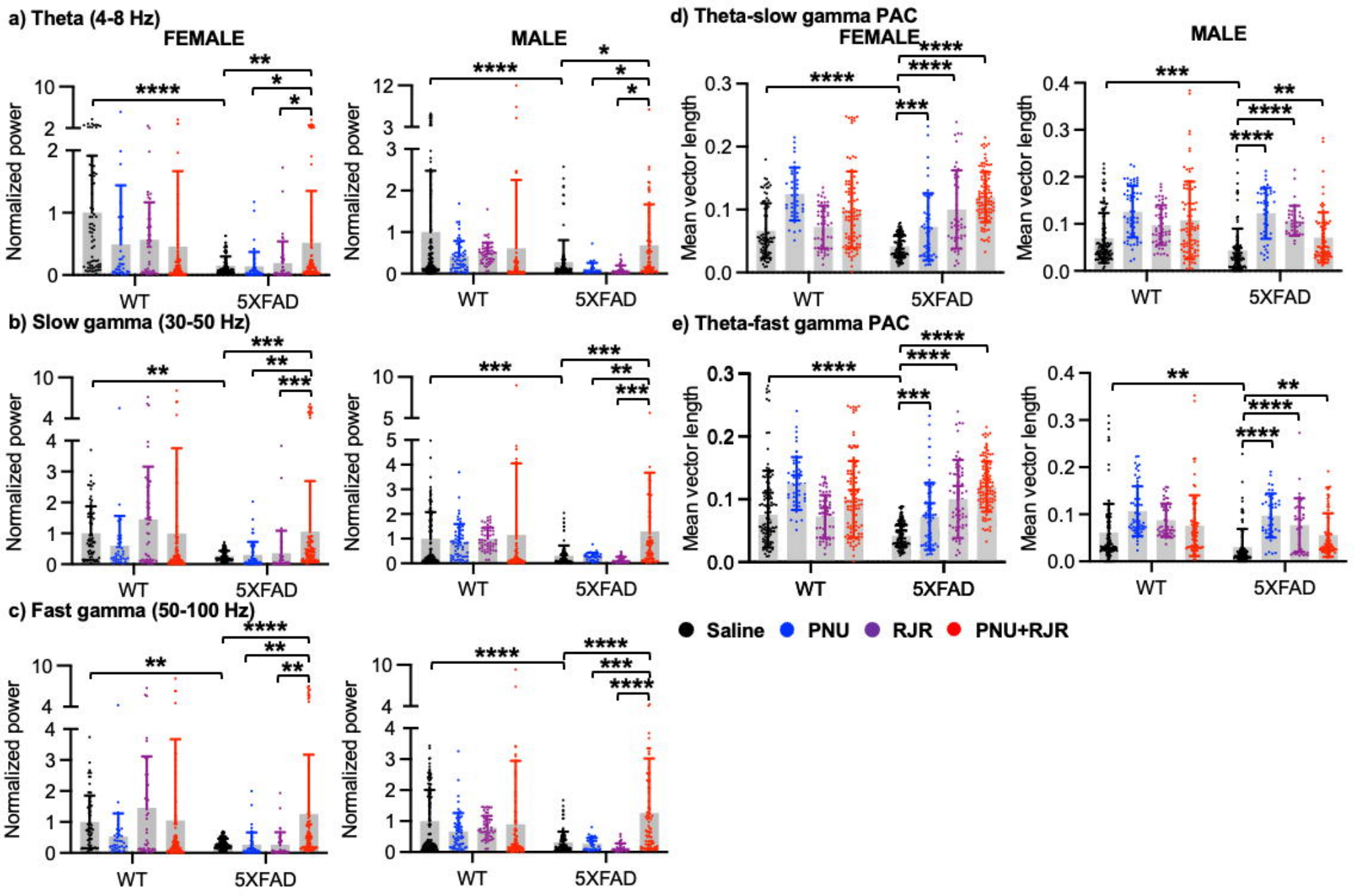
a) Theta (4-8 Hz)
FEMALE
MALE
Normalized power
WT
5XFAD
b) Slow gamma (30-50 Hz)
c) Fast gamma (50-100 Hz)
d) Theta-slow gamma PAC
e) Theta-fast gamma PAC
Mean vector length
Saline
PNU
RJR
PNU+RJR

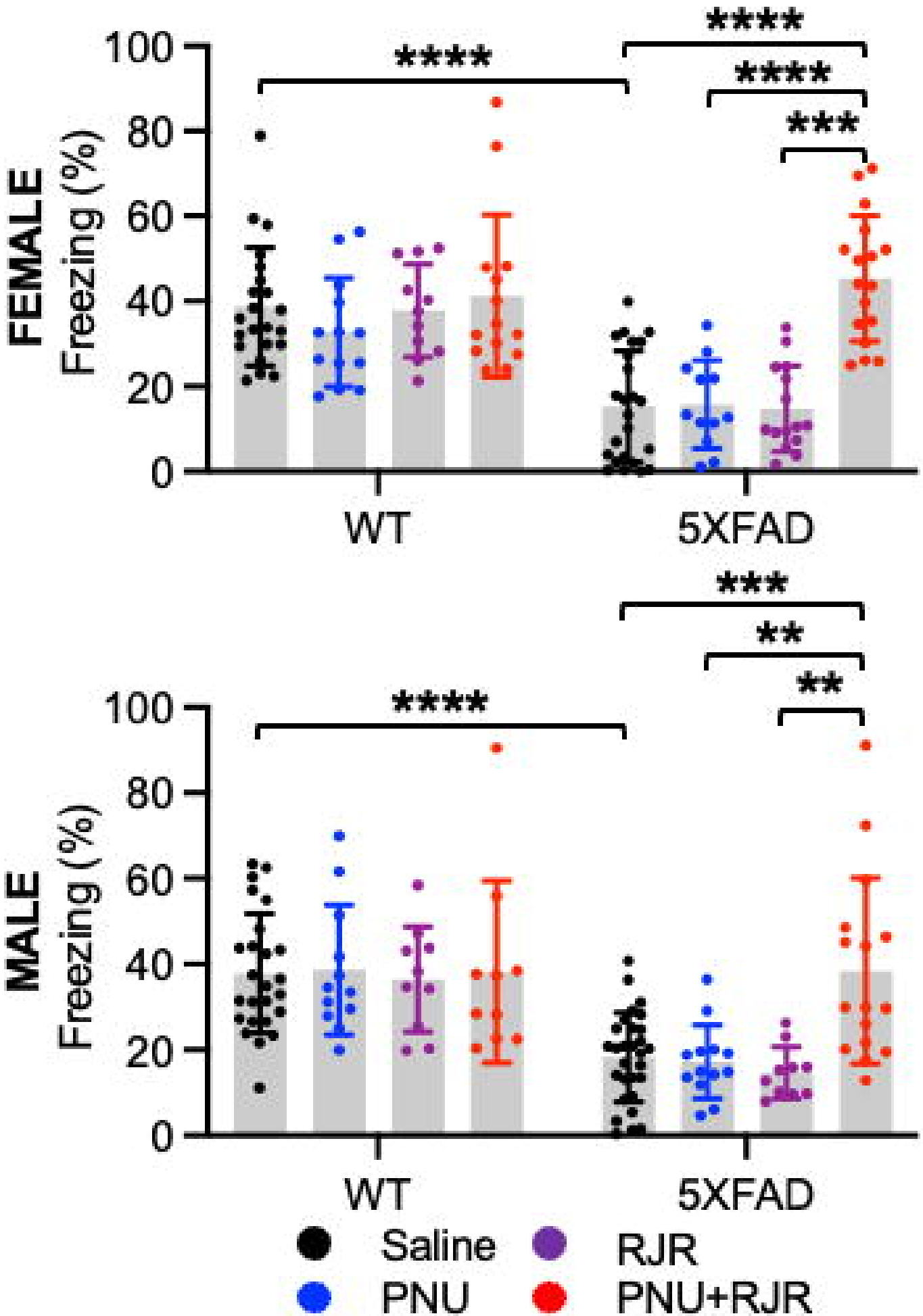
FEMALE
Freezing (%)
100
80
60
40
20
0
****
****
****
***
WT
5XFAD
MALE
Freezing (%)
100
80
60
40
20
0
****
***
**
**
WT
5XFAD
Saline
PNU
RJR
PNU+RJR

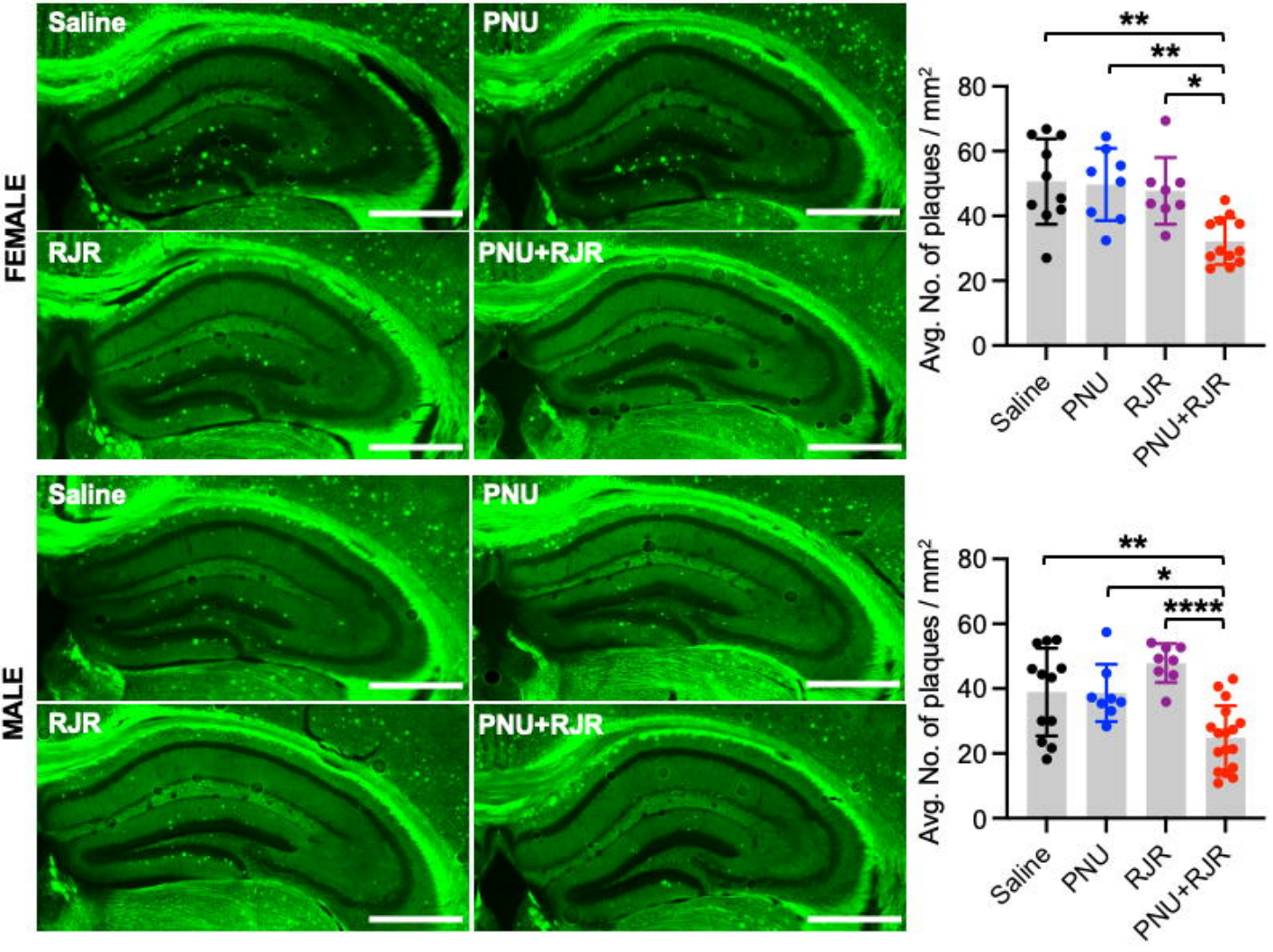
FEMALE
Saline
PNU
RJR
PNU+RJR
MALE
Saline
PNU
RJR
PNU+RJR
Avg. No. of plaques / mm²
0
20
40
60
80
Saline
PNU
RJR
PNU+RJR
**
**
*
Avg. No. of plaques / mm²
0
20
40
60
80
Saline
PNU
RJR
PNU+RJR
**
*
****

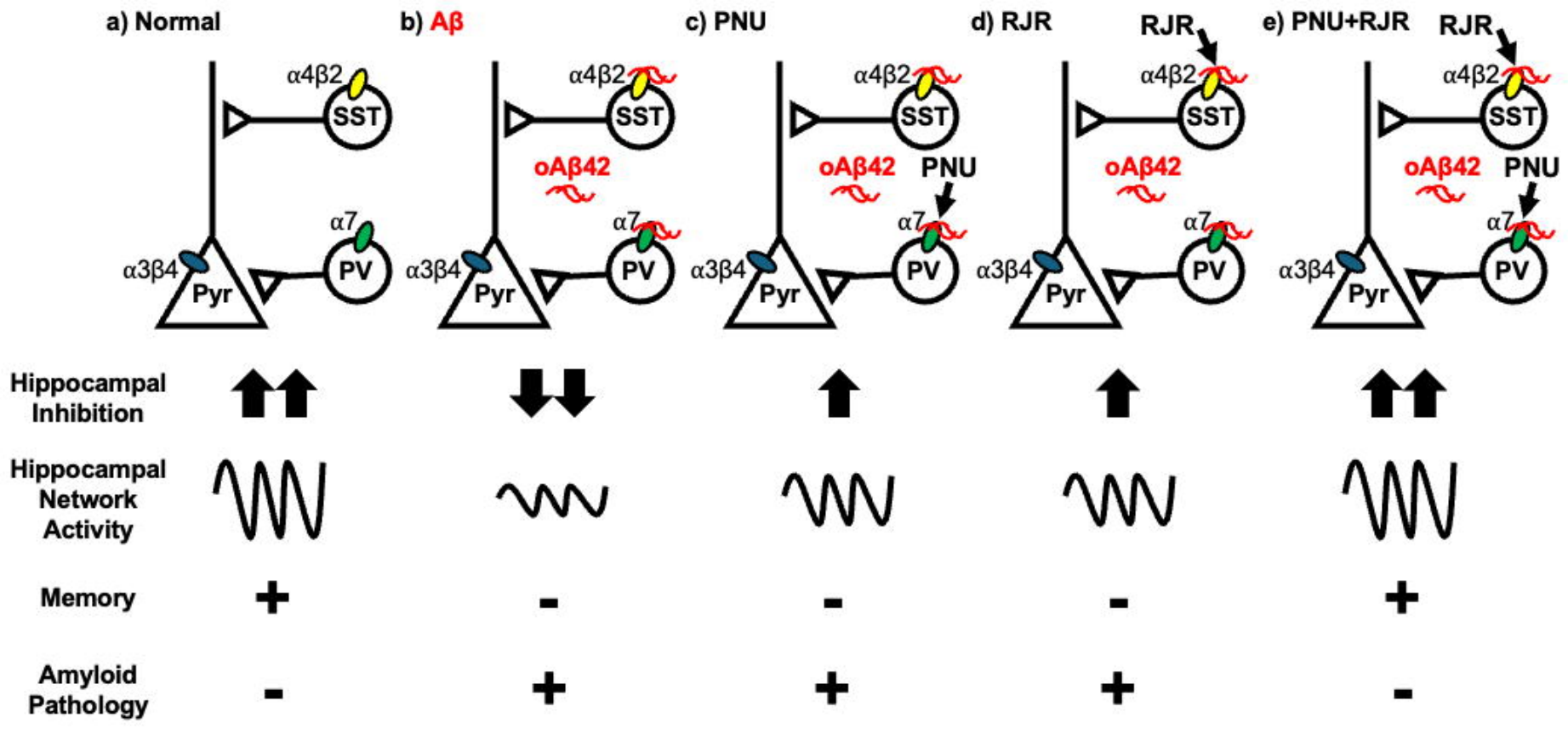
a) Normal
b) Aβ
c) PNU
d) RJR
e) PNU+RJR
RJR
RJR
α4β2
SST
oAβ42
PNU
α7
PV
α3β4
Pyr
Hippocampal Inhibition
Hippocampal Network Activity
Memory
Amyloid Pathology
+
-
-
-
+
-
+
+
+
-